M E C H A N I S T I C S T U D I E S

O F

M E T A L C A R B O N Y L S

A THESIS

Submitted for the Degree of

DOCTOR OF PHILOSOPHY

in the

University of London

by

DAVID HOPGOOD

Chemistry Department,
Imperial College of
Science and Technology,
London, S.W. 7.

September, 1966.

A B S T R A C T

The decomposition of $Mn_2(CO)_{10}$, both in the presence and absence of O_2, and its reactions with PPh_3, to give $Mn_2(CO)_9PPh_3$ and $Mn_2(CO)_8(PPh_3)_2$, and with I_2, to give $Mn(CO)_5I$, were studied in hydrocarbon solvents in the temperature range 60 to 125°C. The data were interpreted as showing that these reactions all proceed via a reactive intermediate which consisted of two $Mn(CO)_5$ radicals, trapped in a solvent "cage", formed by reversible thermal dissociation of $Mn_2(CO)_{10}$ with activation energy of 37 Kcal/mole. This reactive radical pair can then undergo one of four reactions: (a) recombination, (b) diffusion apart of the radicals followed by irreversible decomposition, (c) reaction with oxidising agents e.g. O_2 and I_2, and (d) reaction with Lewis bases to give substitution products. The recombination of the two radicals proceeds with an activation energy of very approximately 20 Kcal/mole.

A parallel second order reaction also occurs in the reaction with I_2 of activation energy of 28 Kcal/mole.

The $Mn_2(CO)_{10}$ reaction with Br_2, in cyclohexane and CCl_4, was much faster than the above reactions and is considered to be of radical chain type propagated by the steps:

$$Mn(CO)_5 + Br_2 \longrightarrow Mn(CO)_5Br + Br$$
$$Br + Mn_2(CO)_{10} \longrightarrow Mn(CO)_5Br + Mn(CO)_5$$

The reaction which appears to be initiated by the $2Mn(CO)_5$ radical pair, has a chain length of about 10^5.

Some results are reported for this reaction catalysed by benzoyl peroxide and light, and inhibited by ethanol.

ACKNOWLEDGEMENT

I wish to thank my supervisor, Dr. A.J. POË for his invaluable guidance and encouragement throughout the course of this work.

CONTENTS

INTRODUCTION

The chemistry of the metal carbonyls has been a subject of interest for over seventy years, and many recent articles review the wide range of compounds known. (1 - 13)

The importance of bond formation between metals, in polynuclear complexes, was realised during the past decade, and much recent work has been concerned with the synthesis and properties of such systems. A recent article (14) reviews metal-metal interaction in transition metal complexes.

This discussion is limited to a description of polynuclear carbonyls and derivatives, of the transition metals, with the exception of members of the copper group.

All the transition metals, with the exception of zirconium and hafnium, form carbonyl derivatives, and the vast majority of these adhere to the noble-gas or effective atomic number (E.A.N.) rule. (1,2) This rule formalises the tendency of a metal atom in a complex to attain the electronic configuration of the succeeding noble-gas.

In almost all complexes, carbon monoxide either forms a linear M-C-O bond, or symmetrically bridges two metal atoms, with M-C-M angle of about 85°, although unsymmetric bridges are known for $[CpFe(CO)_2]_2$ (15). X-ray studies show that carbon monoxide bonds symmetrically to three metal atoms in $Cp_3Ni_3(CO)_2$ (2) and $Rh_6(CO)_{16}$ (16), and similar structures are

postulated for the ions $[Cp_3Co_3(CO)_2]^+$ (2) and $[Fe_3(CO)_{11}]^{2-}$ (2).

Although today, the Valence Bond theory of bonding in metal complexes is conceptually outmoded by the Molecular Orbital theory, it still forms a useful basis for discussion of the stereochemistry and magnetic properties of carbonyl complexes.

(A) VALENCE BOND APPROACH TO METAL - METAL BONDING IN CARBONYL COMPLEXES

The method used here is that developed by Pauling (17) and is so well known as to need little comment.

Bonding between two metals, in a complex, is considered solely in terms of the formation of a σ - bond, by the overlap of singly occupied, hybrid orbitals on each metal.

(1) UNBRIDGED METAL-METAL BONDS.

(a) Normal σ - Bonding

This type of bonding is exemplified by, and is well authenticated for, the $M_2(CO)_{10}$ carbonyls of the manganese group, by X-ray structural determinations (18, 19). Their structures are of two octahedra joined at apices by the overlap of two singly occupied d^2sp^3 hybrid orbitals (Fig. 1). This type of bonding is postulated for the compounds listed in Table 1.

TABLE 1.

Normal σ- Bonded Compounds and Metal-Metal Bond Lengths (A).

Electron Configuration (Hybridisation.)	OXIDATION NUMBER		
	-1	0	1
$d^5 - d^5$ (d^3sp^3)			$[CpCr(CO)_3]_2$ $[CpMo(CO)_3]_2$ 3.22 $[CpW(CO)_3]_2$ $Cp_2MoW(CO)_6$
$d^7 - d^7$ (d^2sp^3)	$[Cr_2(CO)_{10}]^{2-}$ $[Mo_2(CO)_{10}]^{2-}$ $[W_2(CO)_{10}]^{2-}$	$Mn_2(CO)_{10}$ 2.93 $Tc_2(CO)_{10}$ 3.04(19) $Re_2(CO)_{10}$ 3.02 $MnRe(CO)_{10}$ 2.96(92)	$Fe_2(CO)_8I_2$ $[CpOs(CO)_2]_2$
$d^9 - d^9$ (dsp^3)	$[Fe_2(CO)_8]^{2-}$ 2.88	$Co_2(CO)_8$(Soln.) $Rh_2(CO)_8$ $Ir_2(CO)_8$	$[CpPt(CO)]_2$

Literature references to the compounds are given in Section 1 (B).

Bond lengths are from reference (14) or as referenced above.

The mixed metal compounds $C_7H_7(CO)_2MoMn(CO)_5$(20), $Cp(CO)_3MoFe(CO)_2Cp$(2), $(CO)_5MnFe(CO)_2Cp$(2), $(CO)_5ReFe(CO)_2Cp$(21), $(CO)_5MnCo(CO)_4$(2), $(CO)_5ReCo(CO)_4$(22), and $Mn_2Fe(CO)_{14}$(23), and the mono and disubstituted compounds of $Mn_2(CO)_{10}$ and $Co_2(CO)_8$, also bond in this way. (See sections 1 (B) (3) and (5.)

The metal-metal bond lengths, recorded in Table 1, are from 0.2 to 0.3A longer than those determined for the fractional order bonds of the metals themselves (24), and were initially considered to be abnormally long (18). However, a Mn-Mn bond energy, for $Mn_2(CO)_{10}$, of 34 $\pm$ 13 Kcal/mole was calculated from thermochemical data (25), and this, together with chemical and physical data, leaves no doubt as to the strength of the bond. Repulsion, between the non-bonding sub-shells of the two metal atoms, has been proposed as the prime factor in determining metal-metal bond lengths in the manganese group carbonyls.(25)

(b) Bent σ - Bonding

The structures of $Ru_3(CO)_{12}$ and $Os_3(CO)_{12}$ consist of three octahedra joined at apices to give an equilateral triangular arrangement of metal atoms (27, 28). The $M(CO)_4$ fragments are bonded to each other by overlap of singly occupied d^2sp^3 hybrid orbitals (Fig. 2) to form three bent or "banana" bonds (29).

A preliminary investigation of the structure of $Ir_4(CO)_{12}$ suggests a similar type of bonding between four $Ir(CO)_3$ fragments

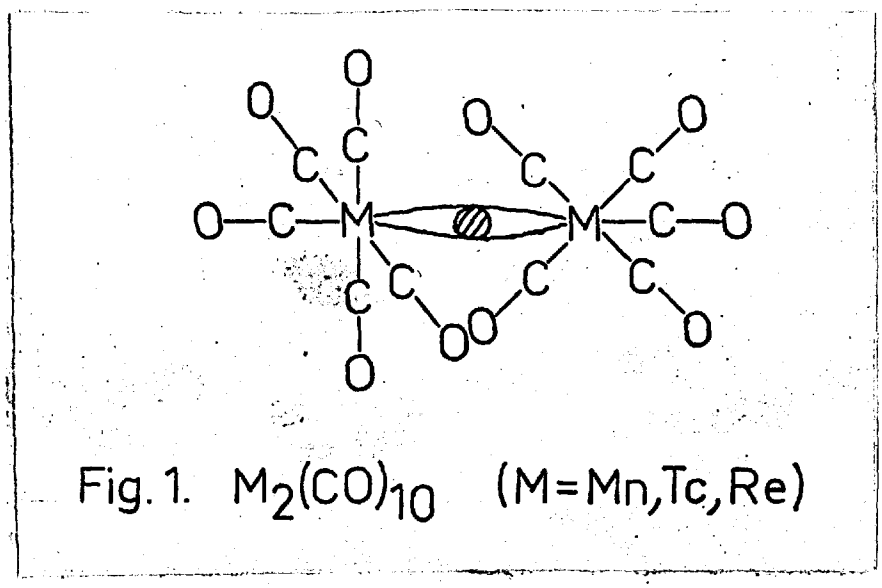

Fig. 1. $M_2(CO)_{10}$ (M=Mn,Tc,Re)

situated at the apices of a regular tetrahedron (30).

Shorter metal-metal distances are expected for bent as compared to normal σ- bonds for the same extent of orbital overlap. However correlations cannot be made due to the paucity of data, but the Os - Os distances in $Os_3(CO)_{12}$ are 0.2A longer than in the metal (24), which is similar to values found for normal σ- bonds.

(2) BRIDGED METAL-METAL BONDS

(a) Carbonyl Bridging Groups

The structure of $Fe_2(CO)_9$(31) is approximately that of two octahedra joined at a face (Fig. 3), but if d^2sp^3 hybridisation

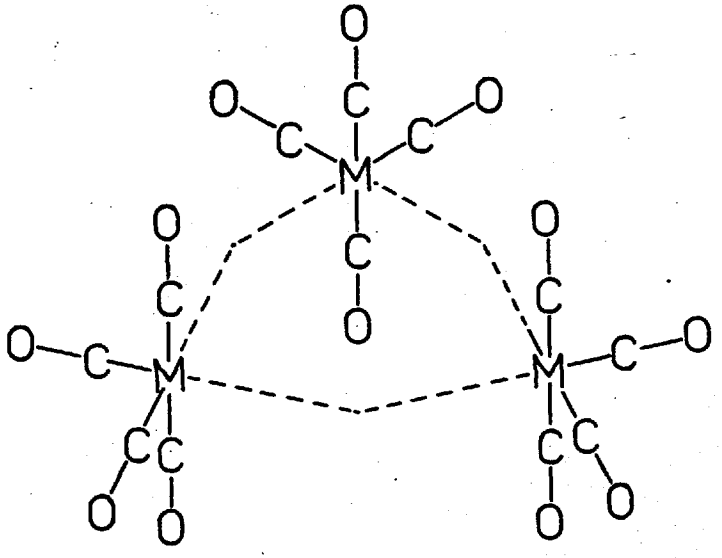

Fig. 2. $M_3(CO)_{12}$ (M=Ru,Os).

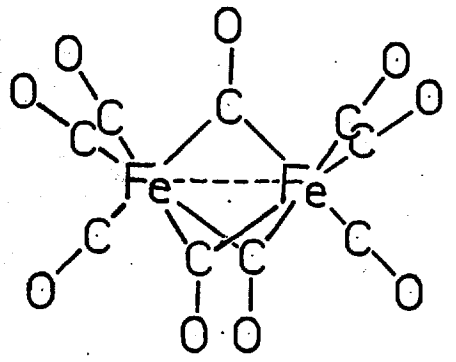

Fig. 3. $Fe_2(CO)_9$.

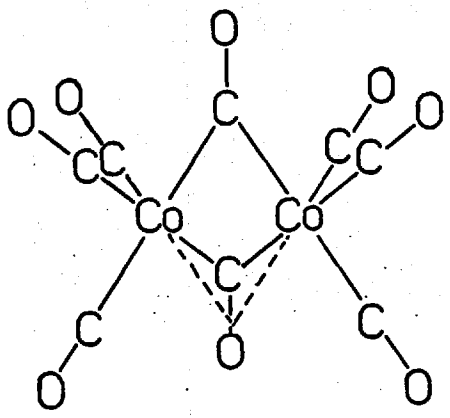

Fig. 4. $Co_2(CO)_8$.

Fig. 5. $M_4(CO)_{12}$

(M=Co,Rh).

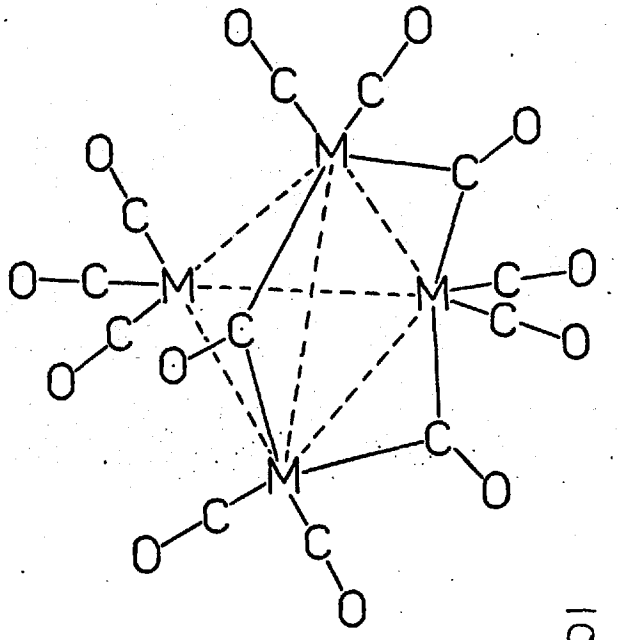

is used then a paramagnetic compound is predicted. A metal-metal bond was proposed to explain the compounds diamagnetism, but it was pointed out that relatively weak coupling of the unpaired spins through the bridging carbonyls would lead to spin pairing (2). The V.B. picture of the metal-metal bonded structure is by d^3sp^3 hybridisation which is valid for seven coordinate bonding, as found in the A - La_2O_3 structure (32), in which a bond is added at the centre of an octahedron face.

The isoelectronic compounds, $Fe_3(CO)_{12}$ (30) and $[MnFe_2(CO)_{12}]^-$ (33), have structures which are derived from that of $Fe_2(CO)_9$ by replacing a bridging carbonyl with a cis $M(CO)_4$ group. This is bonded to the $Fe_2(CO)_8$ fragment by two bent σ- bonds. The structure of the anion, $[HFe_3(CO)_{11}]^-$, is related to that of $Fe_3(CO)_{12}$ by substituting a proton for a bridging carbonyl group.(34)

The structure of $Co_2(CO)_8$ (35) is essentially the same as that of $Fe_2(CO)_9$, with the vacant bridging carbonyl position taken by a bent σ- bond (29) (Fig. 4). It is theoretically possible for a carbonyl group to replace the bent σ- bond and the compound, $Co_2(CO)_9$, may be formed at high carbon monoxide pressures (2). A nonbridged form of $Co_2(CO)_8$ exists, in equilibrium with the bridged form, in solution (36), and the compounds, $Co_4(CO)_{12}$ and $Rh_4(CO)_{12}$, have identical structures containing both bridged and unbridged metals (30) (Fig. 5). The unbridged fragment, $M(CO)_3$, is bonded by three bent σ- bonds

to the $Co_3(CO)_9$ fragment, which is bridged in contrast with the groups found in the many compounds of type $Co_3(CO)_9L$ (See section (A) (2) (b)).

The factors, which influence the formation of bridged species, are not understood, but it is noteworthy that these structures are confined to complexes of vanadium, iron, cobalt, nickel, ruthenium and rhodium. The mixed metal compounds, $Cp(CO)Fe(CO)_2Co(CO)_3$ and $Cp(CO)Fe(CO)_2NiCp$, are bridged (2), in accord with the structures of the parent compounds, $[CpFe(CO)_2]_2$, $Co_2(CO)_8$ and $[CpNi(CO)]_2$ (37), but on the other hand the compounds, $Cp(CO)_2Fe\text{-}M(CO)_5$ and $(CO)_4Co\text{-}M(CO)_5$(M=Mn,Re), do not contain bridging groups.

The metal-metal distances (Table 2) are much shorter than those of nonbridged compounds, and are very similar to those found in the metals (24). A comparison of the complexes $Fe_2(CO)_9$, $Fe_3(CO)_{12}$ and $[HFe_3(CO)_{11}]^-$, shows an inverse relationship between Fe - Fe distance and the number of bridging carbonyl groups. It thus appears that the stereochemical requirements of the bridging groups are the predominant factors in determining the metal-metal distance.

A major defect of the V.B. theory is that it is unable to account for or to predict even the relative energies of different structures, so that elucidation of the factors causing the above trends must await detailed M.O. treatment.

TABLE 2.

Carbonyl Bridged Compounds and Metal-Metal Distances (A).

Electron Configuration	OXIDATION NUMBER	
	0	1
$d^5 - d^5$	$[V(CO)_4(P(C_6H_{11})_3)_2]_2$	
$d^7 - d^7$		$[CpFe(CO)_2]_2$ 2.46 $[CpRu(CO)_2]_2$
$d^8 - d^8$	$Fe_2(CO)_9$ 2.46 $Fe_3(CO)_{12}$ 2.55, 2.69 (30) $[HFe(CO)_{11}]^-$ 2.58, 2.69 (34) $[MnFe_2(CO)_{12}]^-$	
$d^9 - d^9$	$Co_2(CO)_8$ 2.52 $Co_4(CO)_{12}$ 2.49 (30) $Rh_4(CO)_{12}$	$[CpNi(CO)]_2$

Literature references to the compounds are given in Section 1 (B). Metal-metal distances are from reference (14) or as referenced above.

(b) Other bridging groups

Some bridged structures containing metal-metal bonds are well characterised by X-ray structural studies.

The diamagnetic compounds, $[Mn(CO)_4Br]_2$ and $[Rh(CO)_2Cl]_2$, contain bridging halogen atoms. Metal-metal bonding is required by the E.A.N. rule for the latter compound but not for the former, and the determined structures and interatomic distances are in accord with this (38,39) (Fig. 6). Each rhodium atom is formally two electrons short of a xenon configuration, and is considered to form an intermolecular Re-Re bond and an intramolecular bent σ- bond, by using d^2sp^3 hybrid orbitals (39).

The structure of three, chalcogen bridged, diamagnetic iron complexes are known for which metal-metal bonds are predicted. $[EtSFe(CO)_3]_2$ (40) and $[SFe(CO)_3]_2$ (41) consist of two $Fe(CO)_3$ fragments bridged by sulphur atoms. The local environment of each iron atom suggested d^2sp^3 hybridisation and the formation of a bent σ bond (Fig. 7(a) and (b)). Four bent σ bonds are postulated for the complex $Se_2Fe_3(CO)_9$ (42), of which two are Fe-Fe and two are Fe-Se. Two of the iron atoms form d^2sp^3 hybrid orbitals and the third is considered to be seven coordinate with d^3sp^3 hybridisation (Fig. 7(c)).

Many complexes of type $[M(CO)_nER_2]_2$ (E=P,As), which contain bridging phosphorus or arsenic atoms, are known (6), with metal-metal bonding assummed if required by the E.A.N. rule.

Fig. 6.

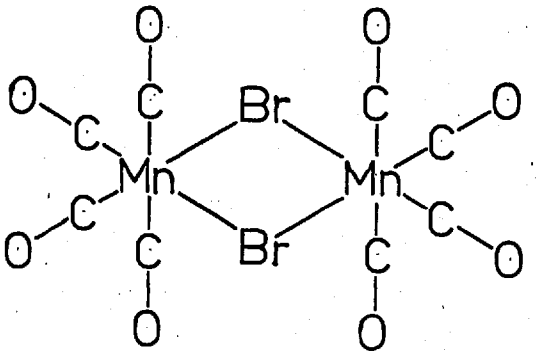

(a) $[Mn(CO)_4Br]_2$.

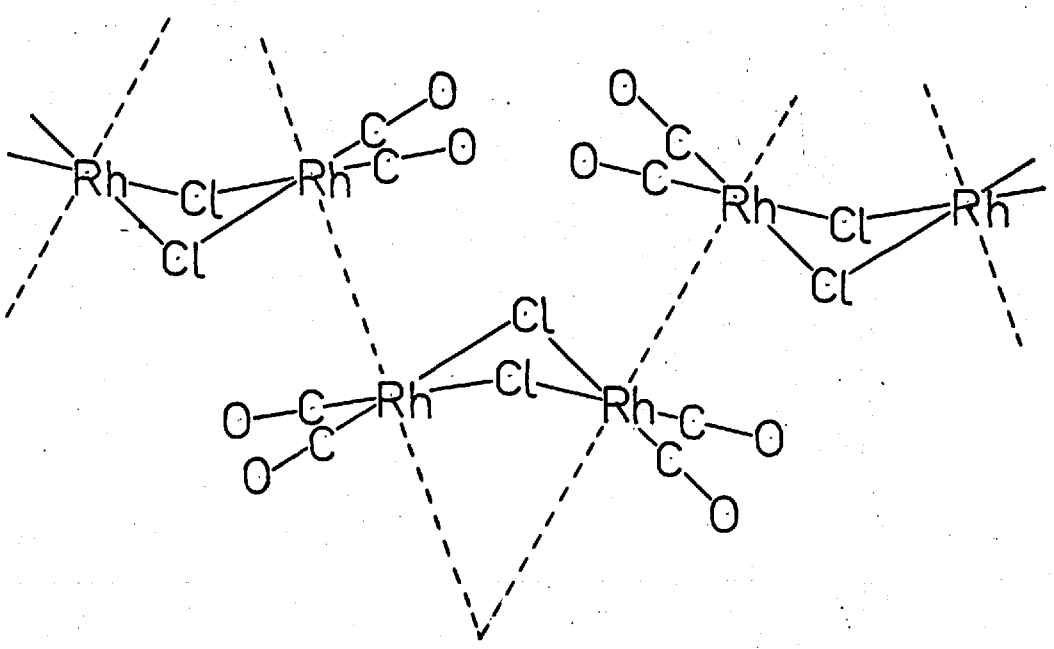

(b) $[Rh(CO)_2Cl]_2$.

Fig. 7.

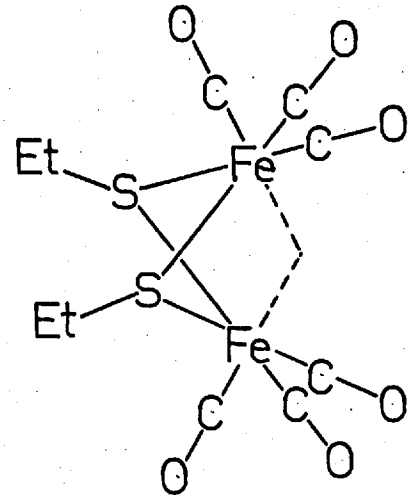

(a) $[EtSFe(CO)_3]_2$.

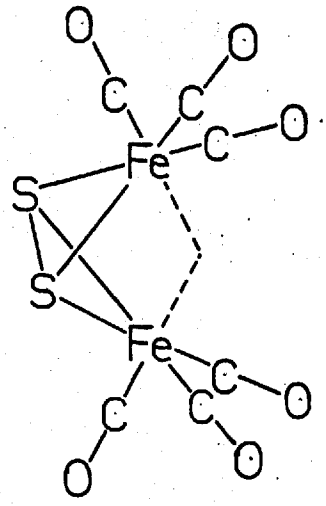

(b) $[SFe(CO)_3]_2$.

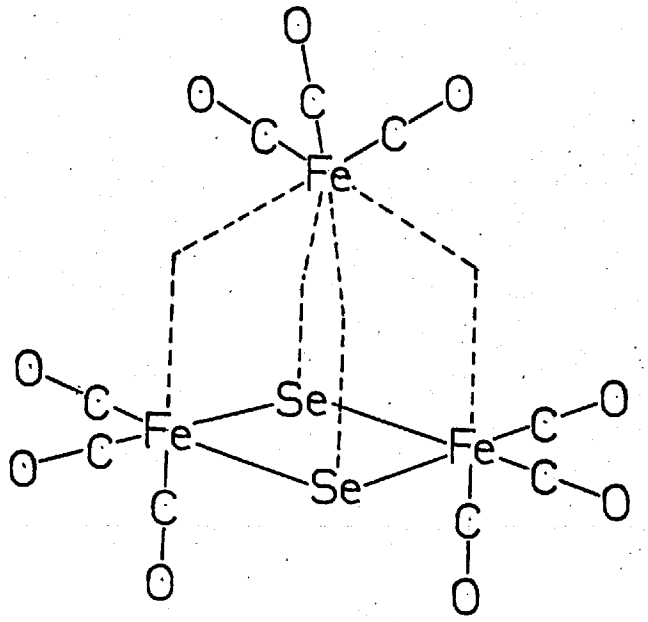

(c) $Se_2Fe_3(CO)_9$.

Iron, osmium and cobalt carbonyls react with acetylenes to give a variety of interesting bridged, metal-metal bonded products (1,9), and structures of many of these have been determined by X-ray diffraction studies.

The simplest structures occur in the compounds, $Fe_3(CO)_9PhCCPh$(43), $Fe_3(CO)_8(PhCCPh)_2$ (violet isomer) (44), $Co_2(CO)_6PhCCPh$ (45), $Co_2(CO)_6C_6F_6$ (46), and $Co_4(CO)_{10}EtCCEt$ (47), in which the acetylene fragments remain intact, and bonding can be considered to be by either σ- bonds or μ- olyfinic bonds. σ- bonded models can be constructed by using hybrid orbitals, as for example in $Co_2(CO)_6PhCCPh$, in which diphenylacetylene replaces the bridging carbonyl groups of $Co_2(CO)_8$ (Fig. 8(a)).

More complex structures occur when the acetylenes lose their identity to form ring systems in the molecule. The simplest compound of this type is $Co_2(CO)_7C_4H_2O_2$, whose structure is derived from that of $Co_2(CO)_8$ by the replacement of a bridging carbonyl group by a lactone ring (48) (Fig. 8(b)).

On the other hand, acetylenes fuse to form metalocyclopentadiene rings in the compounds $Fe_2(CO)_6C_6H_8O_2$ (49), $Fe_3(CO)_8(PhCCPh)_2$ (black isomer) (44), $Fe_2(CO)_6(PhC_2H)_3$ (50) and $Os_2(CO)_6C_6H_8$ (51). The bonding in these compounds is exemplified by the black isomer of $Fe_3(CO)_8(PhCCPh)_2$ (Fig. 9) in which the iron atoms on either side of the ferracyclopentadiene ring bond to it, and also to the iron atom of the ring. The V.B. approach is not useful in the analysis of bond formation

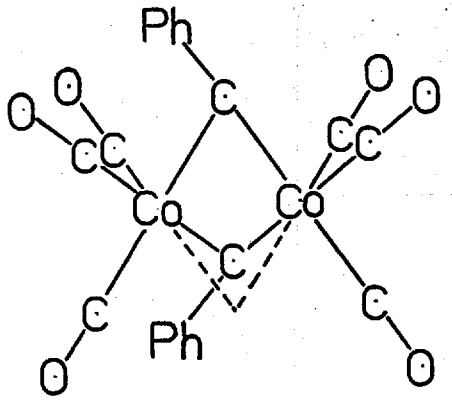

(a) $Co_2(CO)_6PhCCPh$.

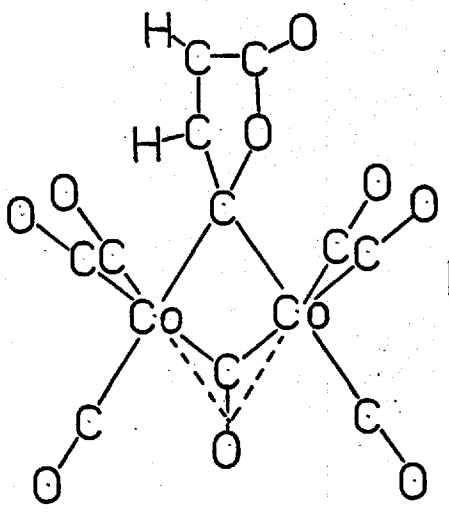

(b) $Co_2(CO)_7C_4H_2O_2$.

Fig. 8.

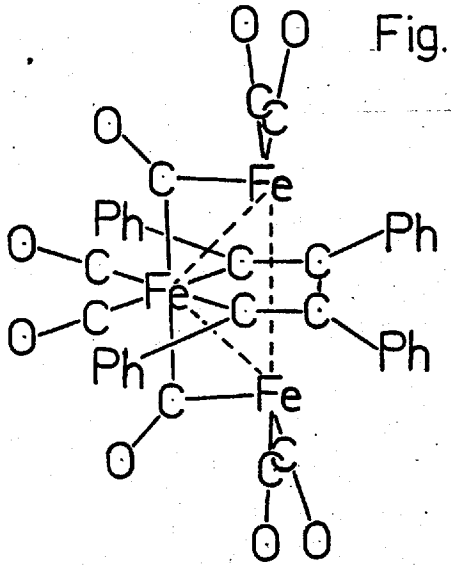

Fig. 9. $Fe_3(CO)_8(PhCCPh)_2$.

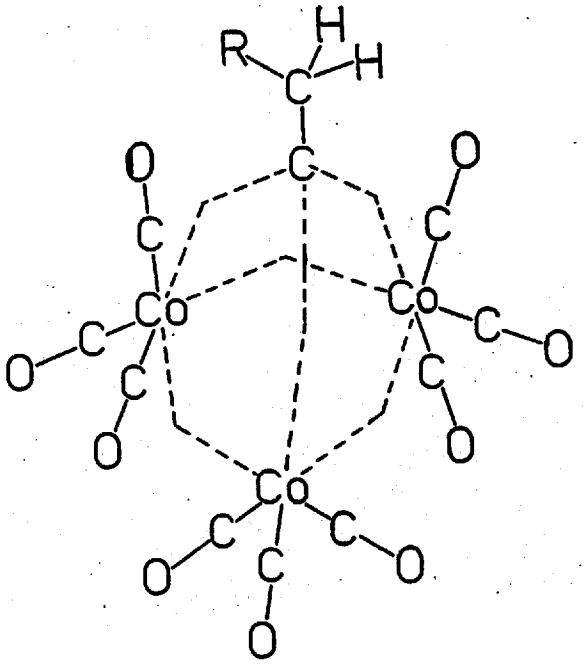

Fig. 10. $HCo_3(CO)_9RCCH$.

in these compounds.

Acetylenic compounds of type $HCo_3(CO)_9RCCH$ have been prepared and characterised by chemical and spectroscopic studies (52). A structure was proposed of a RHC_2 - C group equivalently bonded to three $Co(CO)_3$ groups situated at the corners of an equilateral triangle, with the four fragments bonded by bent σ-bonds (Fig. 10). Similar structures are proposed for the compounds $Co_3(CO)_9CY$ (Y=Me,Ph,F,Cl,CO_2H,CO_2Et, $CH(OAc)_2$ and CF_3) (53), $Co_3(CO)_9S$ (54), and the mixed metal compound $FeCo_2(CO)_9S$ (55).

The metal-metal distances, in the chalcogen and acetylene bridged compounds (14), are of the same order as those in compounds with bridging carbonyl groups.

Tabulation of the compounds in this section is not worthwhile because of the large number which are known.

(B) SURVEY OF METAL - METAL BONDED CARBONYL COMPLEXES

It is intended, in this section, to deal with physical and chemical data, which give indications of the stabilities of the metal-metal bonds in the complexes under consideration. However, there is a complete lack of data on metal-metal bond energies, except in $Mn_2(CO)_{10}$ (25), so that comparisons are impossible except in some instances within a metal group.

X-ray structural data, considered in the previous section

will only be reiterated when used to give credence to structures derived from spectroscopic investigations.

(1) VANADIUM GROUP

The diamagnetic compound, $V_2(CO)_{12}$, was reported contemporaneously with the paramagnetic $V(CO)_6$. However there is now little doubt that the dimer formulation was in error (56). The formation of seven coordinate vanadium, to satisfy the E.A.N. rule, is energetically unfavourable in this instance.

The compounds, $[AzV(CO)_4]_2$ (57) and $[V(CO)_4(P(C_6H_{11})_3)_2]_2$ (58), have been reported. Although no data is available for the former, the analagous manganese compound, $[AzMn(CO)_3]_2$ is known (59).

Some substituted phosphines react with $V(CO)_6$, in hexane, to yield the paramagnetic trans species, $V(CO)_4L_2$ ($L=PPh_3$, PPh_2H, $PPhH_2$, PEt_3, PPr_3). Conversely, tricyclohexylphosphine gives a diamagnetic product under the same conditions (58). The compound was formulated as $[V(CO)_4(P(C_6H_{11})_3)_2]_2$ from I.R. studies, which indicated the presence of bridging carbonyl groups and a dimer-monomer equilibrium in solution.

(2) CHROMIUM GROUP

The complex anions, $[M_2(CO)_{10}]^{2-}$ (M=Cr, Mo, W) and

$[M_3(CO)_{14}]^{2-}$ (M=Cr, Mo), are known (2).

The I.R. spectra of the binuclear anions are very similar to those of the isoelectronic $M_2(CO)_{10}$ carbonyls of the manganese group, and thus the two groups of complexes are considered to be isostructural of D_4d symmetry (3).

No structural data are available for the trinuclear anions.

The anions interconvert on reaction with carbon monoxide (2):

$$[M_3(CO)_{14}]^{2-} + 2CO \rightarrow [M_2(CO)_{10}]^{2-} + M(CO)_6$$

$$[M_2(CO)_{10}]^{2-} + CO \rightarrow [M(CO)_5]^{2-} + M(CO)_6$$

The protonated binuclear anions, $[HM_2(CO)_{10}]^-$, have structures of similar symmetry to the parent complexes (6). Proton resonance data indicates that the proton is equivalently associated with the two metal atoms (60), and an X-ray diffraction study of $[HCr_2(CO)_{10}]^-$ confirmed this inference (61). The molecular symmetry of the anion is D_4h with the proton assigned to a position on the Cr - Cr axis midway between the atoms. The Cr - Cr distance of 3.41A is significantly longer than the normal σ- bonded metal-metal distances.

The binuclear cyclopentadiene complexes, $[CpM(CO)_3]_2$ (M=Cr, Mo, W) and $Cp(CO)_3MoW(CO)_3Cp$ (7), are well characterised.

A crystal structure determination of the molybdenum compound showed that the $CpMo(CO)_3$ moeities are bonded directly between the metal atoms (62). The other compounds are assummed to be isostructural with it from I.R. data.

The mass spectra of the chromium and molybdenum compounds are strikingly different (57). The molybdenum compound degrades by stepwise loss of carbonyl groups to give the series of ions, $[Cp_2Mo_2(CO)x]^+$ (x=0,2,3,4,5,6), whereas the highest mass ion, formed from the chromium analogue, is $[CpCr(CO)_3]^+$. These data indicate that the Cr - Cr bond fissions on vapourisation to give $CpCr(CO)_3$ monomers. This is also in accord with the much lower sublimation temperature of the chromium compound ($\sim 100^{\circ}C$ at 0.1 mm), as compared to the molybdenum ($\sim 150^{\circ}C$ at 0.1 mm).

The molybdenum, tungsten and mixed metal compounds dissolve in concentrated sulphuric acid to give monoprotonated species, $[HCp_2M_2(CO)_6]^+$, which revert to the parent compounds on diluting the solution with water (63). Proton resonance data showed that the proton is equivalently associated with both metal atoms. However it was not possible to distinguish between a static, symmetrically bridged, model (I), and a model, (II), in which rapid intramolecular exchange is occurring:

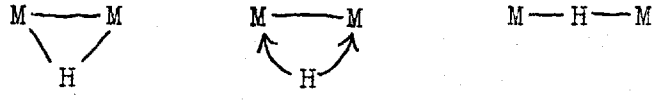

I II III

Model III, proposed for $[HCr_2(CO)_{10}]^-$, is also consistent with the n.m.r. data. A three-centre, one electron-pair, bond has been postulated for this type of structure (61).

Homolytic fission of the metal-metal bond occurs in the

following reactions of the compounds:

$$[CpM(CO)_3]_2 + 2Na \rightarrow 2Na\,[CpM(CO)_3] \quad (M=Mo, W) \quad (5)$$

$$[CpCr(CO)_3]_2 + 2NO \rightarrow 2CpCr(CO)_2NO + 2CO \quad (64)$$

$$[CpM(CO)_3]_2 + H_2 \rightleftharpoons 2CpM(CO)_3H \quad (M=Cr, Mo, W) \quad (65)$$

$$[CpM(CO)_3]_2 + I_2 \rightarrow 2CpM(CO)_3I \quad (M=Mo, W) \quad (62)$$

$$[CpM(CO)_3]_2 + E_2R_4 \rightarrow [CpM(CO)_2ER_2]_2 + 2CO \quad (M=Mo, W) \quad (6)$$

$$[CpMo(CO)_3]_2 + As_2(CF_3)_4 \rightarrow 2CpMo(CO)_3As(CF_3)_2 \quad (6)$$

The physical and chemical data are consistent with a lower metal-metal bond energy for the chromium, as compared to the molybdenum and tungsten compounds.

(3) MANGANESE GROUP

The binary compounds, $M_2(CO)_{10}$(M=Mn, Tc, Re) and $MnRe(CO)_{10}$ (2), are very well characterised. Their I.R. spectra have been extensively studied (66, 67), and show that the crystalline molecular symmetry of D_4d is probably retained in solution, although a structure of D_4h symmetry cannot be ruled out on spectroscopic grounds. The Raman spectrum of $Re_2(CO)_{10}$ has been reported, and a bond at about 120 cm^{-1} was assigned to the Re - Re stretching mode (67).

A mass spectrometric study of $Mn_2(CO)_{10}$ shows that fragmentation occurs through stepwise removal of carbonyl groups to form $[Mn_2(CO)_n]^+$ ions (68). The $Mn(CO)_5$ radical does not seem to occur in the fission scheme. However, the ion $[Mn(CO)_5]^-$ appears to be the predominant species in the

negative ion spectrum. It is likely that it is formed by a dissociative electron-capture process:

$$Mn_2(CO)_{10} + e \rightarrow [Mn(CO)_5]^- + Mn(CO)_5$$

A new polynuclear carbonyl of rhenium, $[Re(CO)_4]_n$, was reported recently and shown to have only terminal carbonyl groups (89).

Chemical reaction studies of this group of compounds have been mainly confined to $Mn_2(CO)_{10}$ due to its greater availability.

$Mn_2(CO)_{10}$ sparingly dissolves in concentrated sulphuric acid, and the U.V. spectrum suggests that a monoprotonated species, $[HMn_2(CO)_{10}]^+$, is formed (63).

The carbonyl hydrides, $M(CO)_5H$ (M=Mn, Tc, Re), are prepared by the reduction and subsequent acidification of the $M_2(CO)_{10}$ compounds (5):

$$M_2(CO)_{10} + 2Na/Hg \rightarrow 2Na[M(CO)_5] \xrightarrow{H+} 2M(CO)_5H$$

However only a trace of $Tc(CO)_5H$ is formed, the main product being $[HTc(CO)_4]_3$. The analagous rhenium compound has been isolated and structures have been proposed for these compounds which are essentially the same as that of $Os_3(CO)_{12}$ but with bridging protons (70).

The halogens react with $Mn_2(CO)_{10}$ (71), $Tc_2(CO)_{10}$ (69), and $Re_2(CO)_{10}$ (90) to effect homolytic fission of the metal-metal bond:

$$M_2(CO)_{10} + X_2 \rightarrow 2M(CO)_5X \ (X=Cl, Br, I)$$

The rates of reaction are in the order $Cl_2 > Br_2 > I_2$.

On the other hand, substitution with retention of the metal-metal bond occurs in the reactions of the halide ions with $Mn_2(CO)_{10}$ (72):

$$Mn_2(CO)_{10} + 2X^- \rightarrow [Mn_2(CO)_8X_2]^{2-} + 2CO \quad (X=Cl,Br,I)$$

The infrared spectra of the compounds suggests that their structures are derived from that of the parent compound by replacement of the axial carbonyl groups.

Similar structures were proposed for the compounds $Mn_2(CO)_8L_2$ which are products of the reactions between $Mn_2(CO)_{10}$ and substituted phosphines, arsines and stibenes (73). Preliminary X-ray data shows that the compounds $Mn_2(CO)_8(PR_3)_2$ (R=F, Et) are of D_4d symmetry (74). Early work (75) reported the existence of paramagnetic monomers $Mn(CO)_4L$ ($L=PPh_3$, PEt_3, $AsPh_3$, $SbPh_3$), as well as diamagnetic dimers, but the preparation of the monomeric radicals has since proved to be unrepeatable (73, 76). The monosubstituted compounds $Mn_2(CO)_9L$ ($L=RCN,py,PPh_3$) have also been prepared (77). $Re_2(CO)_{10}$ reacts with triphenylphosphine to yield a di-substituted product, $Re_2(CO)_8(PPh_3)_2$, but under more rigourous conditions the paramagnetic monomer, $Re(CO)_3(PPh_3)_2$, is formed (78, 79).

Similar monomeric species can be prepared from $Mn_2(CO)_{10}$ by reaction with bidentate ligands such as o- phenylenebis-dimethylarsine (D) (6). This ligand reacts to give both the

diamagnetic dimer, $[Mn(CO)_3D]_2$, and the paramagnetic monomer, $Mn(CO)_3D$, the latter being formed under more rigourous conditions (91).

The disubstituted dimers of manganese and rhenium undergo homolytic fission of the metal-metal bond when treated with bromine (73, 79):

$$M_2(CO)_8L_2 + Br_2 \rightarrow 2t - M(CO)_4LBr$$

(4) IRON GROUP

The following polynuclear binary complexes are known for the iron group:- $Fe_2(CO)_9$, $[Fe_2(CO)_8]^{2-}$, $M_3(CO)_{12}$ (M=Fe, Ru, Os), $[Fe_3(CO)_{11}]^{2-}$ and $[Fe_4(CO)_{13}]^{2-}$ (2).

$Fe_2(CO)_9$ was formulated as a binuclear compound from X-ray data (31), but its unusual properties of low solubility and lack of volatility suggested some type of polymeric structure (2). However support for the formulation has come from a recent mass spectral study, which found no ions of greater mass than $Fe_2(CO)_9^+$ or any with more than two metal atoms (80). The ruthenium and osmium analogues were reported but were subsequently shown to be of formule $M_3(CO)_{12}$ (27).

The structure of $Fe_3(CO)_{12}$ was the subject of dispute for many years but this was resolved by the recent publication of a three-dimensional X-ray analysis (30). (See section I (A) (2) (a)).

In contrast with $Ru_3(CO)_{12}$, $Os_3(CO)_{12}$ and $[HFe_3(CO)_{11}]^-$ (33, 88), $Re_3(CO)_{12}$ does not appear to retain its solid-state molecular structure in solution. A linear bridged structure, similar to that of $Fe_2(CO)_9$, has been proposed to occur in solution (81).

The stability of the metal-metal bonds in the $M_3(CO)_{12}$ compounds is attested by mass spectral studies. The ruthenium (57) and osmium (82) complexes only exhibit metal-metal bond fission in the M_3^+ ions, which are formed by stepwise loss of carbonyl groups. In contrast, this process occurs in the $Fe_3(CO)_3^+$ ion, formed from the ion complex (57). Thus it appears that the metal-metal bonds of $Fe_3(CO)_{12}$ are weaker with respect to the metal-carbon bonds, than in the ruthenium and osmium complexes.

Reported reactions of the iron group carbonyls are virtually confined to those of iron, and a large number are known and reviewed (1 - 13).

Chemical information on the relative stabilities of the metal-metal bonds in the iron carbonyls is much more difficult to assess than in the chromium and manganese group compounds and will not be discussed here. The only typical cleavage reaction is the reduction of $Fe_3(CO)_{12}$ (5):

$$Fe_3(CO)_{12} + 6Na/Hg \rightarrow 3Na_2[Fe(CO)_4]$$

The cyclopentadiene compounds, $[CpM(CO)_2]_2$ (M=Re, Ru, Os) are known (7).

The iron and ruthenium complexes dissolve in concentrated sulphuric acid to give monoprotonated species, $[Cp_2M_2H(CO)_4]^+$ (63). The I.R. spectrum of the iron species, which can be isolated, shows the absence of bridging carbonyl groups, but the neutral, bridged compound is recovered on dilution with water.

The compounds of iron and ruthenium cleave on reduction (5):

$$[CpM(CO)_2]_2 + 2Na/Hg \rightarrow 2Na[CpM(CO)_2]$$

(5) COBALT GROUP

The following polynuclear binary carbonyls are known for this group: $M_2(CO)_8$ and $M_4(CO)_{12}$ (M=Co, Rh, Ir) (2), and $Rh_6(CO)_{16}$ (16).

There is E.S.R. and mass spectral evidence for the formation of $Co(CO)_4$ radicals when $Co_2(CO)_8$ is vapourised. The hyperfine splitting of the E.S.R. signal was interpreted as due to spin-spin coupling of the unpaired electron of the radical, of D_{4h} symmetry, with the ^{59}Co nucleus (I=7/2) (83). The mass spectrum indicated that fragmentation occurs by successive loss of carbonyl groups either from $Co_2(CO)_8$ to form $[Co_2(CO)_n]^+$ ($n \leqslant 8$) ions, or from the $Co(CO)_4$ radical to form $[Co(CO)_n]^+$ ($n \leqslant 4$) ions (68).

In contrast, mass spectral studies of $Co_4(CO)_{12}$ (57, 82) and $Co_3(CO)_9(CY)$ (Y=Me, Cl) (57) show that metal-metal bond

fission occurs only after the complete removal of carbonyl groups.

The bridged form of $Co_2(CO)_8$ exists in equilibrium with an unbridged form in solution (36), and this latter form appears to be the reactive species found in previous kinetic studies of carbon monoxide exchange (84), and acetylene (85) reactions.

$Co_2(CO)_8$ reacts with triphenyl-phosphine to yield mono and disubstituted products, $Co_2(CO)_7PPh_3$ and $Co_2(CO)_6(PPh_3)_2$ (86). Comparing these reactions with the analagous $Mn_2(CO)_{10}$ reactions shows that $Co_2(CO)_8$ is very much more reactive.

Decomposition occurs when $Co_2(CO)_8$ is treated with the halogens (1), but the compound is cleaved on reduction (5):

$$Co_2(CO)_8 + 2Na/Hg \rightarrow 2Na\left[Co(CO)_4\right]$$

Very little is known of the reactions of the other compounds in this group.

(6) NICKEL GROUP

A series of salts and protonated species of the carbonylnickelates, $\left[Ni_2(CO)_6\right]^{2-}$, $\left[Ni_3(CO)_8\right]^{2-}$, $\left[Ni_4(CO)_9\right]^{2-}$ and $\left[Ni_5(CO)_5\right]^{2-}$, have been prepared by reduction of $Ni(CO)_4$ (86). These anions are illcharacterised but structures can be drawn for them which conform to the E.A.N. rule.

The cyclopentadiene compounds $[CpM(CO)]_2$ are known for nickel (87) and platinum (37), and they undergo the characteristic cleavage reaction with iodine:

$$Cp_2M_2(CO)_2 + I_2 \rightarrow 2CpM(CO)I$$

However, attempts to cleave the nickel compound, with sodium amalgam, failed to yield $Na[CpNi(CO)]$, but a paramagnetic complex, $Cp_3Ni_3(CO)_2$, was isolated (5).

II GENERAL EXPERIMENTAL

(A) PREPARATION AND PURIFICATION OF MATERIALS

The $Mn_2(CO)_{10}$ was a gift from Professor G. Wilkinson of this department and was purified by recrystallisation from 60/80 petroleum ether. With this compound as a starting material $Mn(CO)_5Br$(71), $Mn(CO)_5I$(92), $Mn_2(CO)_9PPh_3$(76), $Mn_2(CO)_8(PPh_3)_2$(73) and $Mn_2(CO)_8(P(OPh)_3)_2$(73) were prepared and purified as described in the literature and identified by their I.R. spectra.

The triphenylphosphine and triphenylphosphite were obtained from B.D.H. Ltd., and triphenylphosphine was purified for kinetic runs by recrystallisation from ethanol. Analar bromine and iodine were used as supplied by Hopkin and Williams Ltd. A sample of bromine, which had been fractionally distilled at room temperature under reduced pressure, showed no difference in kinetic behaviour.

Benzoyl peroxide was recrystallised from 60/80 petroleum ether prior to use.

Spectrosol grade cyclohexane and CCl_4, and micro-analytical reagent decalin, supplied by Hopkin and Williams Ltd., were dried over molecular sieves and used without further purification. $CF_2Cl.CFCl_2$ supplied by Koch-Light Ltd., was fractionally distilled and dried over molecular sieves. Other solvents were fractionally distilled if not of Analar grade and all were dried over molecular sieves.

(B) MEASUREMENT OF SPECTRA

(1) ULTRAVIOLET/VISIBLE SPECTRA

Spectra were measured in silica cells of path lengths of 1 cm. or 1 mm. against a solvent reference and using Perkin-Elmer recording spectrophotometers, Models 350 and 137 U.V. A Unicam S.P. 500 single beam instrument was used to measure the absorbances which were used to calculate the molar extinction coefficients of peaks.

The instruments were wavelength calibrated by using holmium oxide and didymium glass filters and their absorbance scales were checked for linearity by using solutions of potassium dichromate.

(2) INFRARED SPECTRA

Spectra were measure in solution using cells with NaCl windows and with suitable path length. A solvent reference was used. Accurate band positions in the carbonyl stretching region were obtained with a Grubb-Parsons Spectromaster spectrometer. Extinction coeffients were determined from the peak heights using the Perkin-Elmer diffraction-grating instruments, Models 237 and 257. A polystyrene standard was used for the calibration of wavelengths and $Mn_2(CO)_{10}$ solutions were used to check the linearity of the percent transmission scales by using the expression $C \propto \log_{10} 100/T$. The accuracy of the transmission scales of the Perkin-Elmer instruments was such that measurement of concentrations to better than 2% was possible in the region, 100 to 10% transmission.

(C) DETERMINATION OF RATES OF REACTION

The quantitative analyses of reactant and product concentrations, during the course of a reaction, were carried out by using U.V./Vis. or I.R. spectroscopic techniques.

(1) U.V./Vis TECHNIQUES

The majority of kinetic runs were carried out in 1cm. path length, stoppered silica cells in a thermostatted compartment in the spectrometer. The reactions were followed by observing changes in the absorbance due to the absorption maxima of the reactants against a solvent reference. The measurements were done at suitable time intervals either at predetermined wavelengths with the Unicam S.P. 500 spectrometer, or by scanning selected regions of the spectrum with the Perkin-Elmer 137 U.V. recording instrument. If necessary concentrations were calculated from absorbances by using the expression $C = A/\epsilon l$.

Some of the high temperature reactions,(60 to 125°C), were followed by measuring the absorbances, at room temperature of aliquots abstracted from reaction vessels in the thermostat baths.

(2) I.R. TECHNIQUES

The Perkin-Elmer recording instruments, Models 237 and 257 were used to follow the reations by scanning aliquots, from thermostatted reaction vessels, in the carbonyl stretching region at room temperature. A solvent reference was used. The peak heights of well resolved reactant and product bands

were measured in percent transmission units (T), and were converted into absorbances using the expression $A = \log_{10} 100/T$.

(D) CONTROL OF REACTION TEMPERATURES

Most of the reactions in the temperature range, 30 to 80°C, were carried out in 1 cm. path length cells in Adkins electrically heated thermostat blocks. These blocks were situated in the cell compartments of the Unicam SP..500 and Perkin-Elmer 137 U.V. instruments and gave temperature control to better than ± 0.05°C. Temperatures at ambient and below were achieved by using a flow of thermostatted liquid, from a bath, through a block containing the cells, in the SP. 500. Temperature variations in the cell were undetectable and so less than ± 0.02°C. Oil baths were used to thermostat reaction vessels in the temperature range 80 to 135°C and these gave temperature control which was usually about ± 0.05°C but never worse that ± 0.1°C.

Temperature measurement was by mercury in glass thermometers, graduated to 0.1°C, which were either calibrated at the National Physical Laboratory, Teddington or were calibrated against such thermometers.

III ULTRAVIOLET/VISIBLE AND INFRARED SPECTRA

The main features of the spectra are tabulated showing the positions of absorption maxima (λ_{max}(U.V.) and ν_{max}(I.R.)) with their molar extinction coefficients (ϵ) in various solvents. The U.V./Vis. spectra, in the region 200 to 750 mμ, are presented in Table 3 and the I.R. spectra, in the carbonyl stretching region between 1900 to 2200 cm^{-1}, are presented in Table 4.

Published values are given in parentheses for comparison when available and in some instances are recorded when used in this work but not remeasured.

TABLE 3

U.V./Vis. Spectra

Solvent	λ max (mμ)	ϵ ($l.moles^{-1}cm^{-1}$)	Ref.
	$Mn_2(CO)_{10}$		
$CHCl_3$	340 (344)	20,000 (20,000)	(93)
CCl_4	342	20,800	
$CF_2Cl.CFCl_2$	343	21,000	
Cyclohexane	343	20,200	
n-octane	343	20,500	
Decalin	342	19,800	
	$Mn(CO)_5Br$		
$CHCl_3$	(386)	(420)	(93)

TABLE 3 (cont.)

Solvent	λ_{max} (mμ)	ϵ (l.moles^{-1}cm^{-1})	Ref.
	$Mn(CO)_5I$		
$CHCl_3$	(404)	(390)	(93)
	Br_2		
CCl_4	417 (417)	(207)	(94)(a)
$CF_2Cl.CFCl_2$	417	200	
Cyclohexane	420 (420)	(210)	(94)(a)
	I_2		
CCl_4	512 (517)	900 (918)	(94)(b)
Cyclohexane	514 (490)	1000 (1010)	(94)(b)
n-octane	512	830	
Decalin	525	890	

TABLE 4

I.R. Spectra

Solvent	ν_{max} (cm^{-1})	ϵ^* (l.moles^{-1}cm^{-1})	Ref.
	$Mn_2(CO)_{10}$		
	1982 (1980)	5,000 (4,590)	
CCl_4	2013 (2014)	28,500 (25,500)	(67)
	2047 (2046)	12,500 (12,100)	
	1983 (1983)	7,800	
Cyclohexane	2013 (2014)	41,300	(74)
	2047 (2045)	13,100	

TABLE 4 (cont)

Solvent	ν_{max} (cm^{-1})	ϵ* ($l.moles^{-1}cm^{-1}$)	Ref.
	1986	6,700	
Decalin	2015	40,000	
	2047	11,000	
	$Mn(CO)_5Br$		
	2000 (2001)	2,900 (m)	
CCl_4	2020 (2019)	250 (w)	(69)
	2053 (2050)	10,200 (s)	
	2133 (2133)	450 (w)	
	2003	6,500	
Cyclohexane	2023	500	
	2053	16,700	
	2135	500	
	$Mn(CO)_5I$		
	2004 (2005)	5,300 (m)	
Decalin	2015 (2016)	4,000 (w)	(69)
	2045 (2044)	16,900 (s)	(Soln.in CCl_4)
	2127 (2125)	900 (w)	
	$Mn_2(CO)_9PPh_3$		
	1942 (1937)	5,100 (s)	
	1974 (1969)	3,800 (w)	
Decalin	1997 (1997)	25,000 (vs)	(76) (Soln.in xylene)
	2015 (2015)	5,200 (s)	
	2093 (2098)	2,700 (s)	

TABLE 4 (cont.)

Solvent	ν_{max} (cm^{-1})	ϵ ($l.moles^{-1}cm^{-1}$)	Ref.
	$Mn_2(CO)_8(PPh_3)_2$		
Cyclohexane	1963 (1956)	10,000 (vs)	(73)
	1987 (1980)	w (sh)	(soln.in $CHCl_3$)

* in some cases relative intensities are given: vs, very strong; s, strong; m, medium; w, weak; sh, shoulder.

IV KINETIC, MECHANISTIC AND THERMODYNAMIC STUDIES ON THE DECOMPOSITION OF DIMANGANESE DECACARBONYL AND ITS REACTIONS WITH TRIPHENYLPHOSPHINE AND IODINE IN SOLUTION

(A) INTRODUCTION

It may seem unusual to compare the homolytic fission reaction :

$$Mn_2(CO)_{10} + I_2 \rightarrow 2Mn(CO)_5I$$

with the substitution reaction :

$$Mn_2(CO)_{10} + 2PPh_3 \rightarrow Mn_2(CO)_8(PPh_3)_2 + 2CO$$

However we have found similarities in the kinetic behaviour of the two reactions which lead us to suggest a common primary step for the two reactions.

Evidence will be given which shows that these reactions and the decomposition of $Mn_2(CO)_{10}$ in solution occur by an identical initial stage.

As mentioned above, (Section I (B) (3)), the orange complex $Mn_2(CO)_8(PPh_3)_2$ was initially reported by Hieber and Freyer (75) as a red paramagnetic monomer, $Mn(CO)_4PPh_3$. It was prepared by the reaction of $Mn_2(CO)_{10}$(1mM) and PPh_3(6mM) in xylene solution by heating the reactants in a sealed evacuated tube for 16 hours at 120°C. They also stated that the compound $Mn_2(CO)_8(P(OPh)_3)_2$ became paramagnetic in xylene solution on heating to 120°C, the colour changing from yellow to red. They postulated that this behaviour was evidence for the thermal equilibrium :

$$Mn_2(CO)_8(P(OPh)_3)_2 \rightleftharpoons 2Mn(CO)_4P(OPh)_3$$

Osborne and Stiddard (73) prepared $Mn_2(CO)_8(PPh_3)_2$ by both photochemical and thermal reactions but accepted the existence of the monomer. They stated that it reacted with chlorinated solvents to give $Mn(CO)_4(PPh_3)Cl$.

On the other hand, Wawersik and Basolo (76) were unable to repeat the preparation of the monomer and asserted that there was no evidence for Mn-Mn bond cleavage in this reaction. They prepared the known monosubstituted compound from equimolar amounts of the reactants and showed that it reacted with an excess of PPh_3 to produce the disubstituted product:

$$Mn_2(CO)_{10} \xrightarrow{PPh_3} Mn_2(CO)_9PPh_3 \xrightarrow{PPh_3} Mn_2(CO)_8(PPh_3)_2$$

These authors considered that the paramagnetism observed by Hieber and Freyer was due to impurities.

Accordingly, in addition to carrying out kinetic studies of the PPh_3 reaction with $Mn_2(CO)_{10}$, we have also attempted to detect monomeric radicals formed from $Mn_2(CO)_{10}$ and some of its derivatives.

The only published preparation of $Mn(CO)_5I$ is by reaction of an intimate mixture of $Mn_2(CO)_{10}$ and I_2 in a sealed evacuated tube at 140°C (92). This is in contrast with the solution reaction with Br_2 and Cl_2 at 40 and 0°C respectively (71). We have produced $Mn(CO)_5I$ by reaction of I_2 with $Mn_2(CO)_{10}$ in cyclohexane solution by catalysing the reaction with benzoyl peroxide in the light at room temperature. The results of these catalytic reactions are presented in Section VI

(B) ATTEMPTS TO PRODUCE MONOMERIC RADICALS FROM $Mn_2(CO)_{10}$ AND ITS SUBSTITUTED PHOSPHINE DERIVATIVES

(1) EXPERIMENTAL

Samples of $Mn_2(CO)_8(PR_3)_2$ (R=Ph, OPh) were prepared by the photochemical method of Osborne and Stiddard (73), and the published method for the preparation of $Mn(CO)_4PPh_3$ was followed (75).

The U.V. spectra of samples were measuredin degassed solutions in evacuated, 1cm. path length, silica cells. The cells were thermostatted in a Unicam SP.500 spectrometer.

Solution I.R. spectra, recorded in the 2000 cm.$^{-1}$ region using a Perkin-Elmer 237 spectrometer, were measure in thermostatted, 0·1 mm path length cells with NaCl windows and pressure tight ports. The thermostat consisted of an electrically heated block controlled by a stepless electronic unit designed and built by Mr. D. Alger of this department. This device operated in the temperature range from ambient to 250°C and the cell temperature was measured by using a thermocouple.

E.S.R. studies were done on degassed solutions in evacuated silica tubes. A Varian V-4502-15 3 cm. spectrometer was used to scan the samples over 1000 to 2,500 gauss ranges centred on 3,350 gauss. The samples were thermostatted by a stream of nitrogen from a Varian V-4540 variable temperature controller.

(2)RESULTS

Two attempts to prepare $Mn(CO)_4PPh_3$ yielded only the dimer $Mn_2(CO)_8(PPh_3)_2$ which had identical U.V. and I.R. spectra with that prepared by the photochemical method. Wawersik and Basolo obtained the same result (76). However, it was observed that the reaction solutions at 120°C were red, the colour reported for the monomer, but rapidly changed to orange on cooling to room temperature. This behaviour is similar to that reported for a solution of $Mn_2(CO)_8(P(OPh)_3)_2$ (75). Isolation of the red "species" was attempted by rapidly freezing a reaction solution in liquid nitrogen, but again the only product was the orange dimer.

The phenomenon proved to be impossible to measure by U.V. spectroscopy because of the decomposition of $Mn_2(CO)_8(PPh_3)_2$ in the dilute solutions necessary. A 10^{-4}M solution in xylene decomposed by 50% in 5 hours at room temperature.

A 5×10^{-4}M solution of $Mn_2(CO)_8(P(OPh)_3)_2$ in decalin, heated to 100 and 150°C, showed a decrease in the intensity of the I.R. spectrum and the growth of some new bands, but on cooling to room temperature the spectrum did not change. The identity of the product was not established.

Preliminary E.S.R. scans of saturated xylene solutions of $Mn_2(CO)_{10}$, $Mn_2(CO)_9PPh_3$, $Mn_2(CO)_8(PPh_3)_2$ and $Mn_2(CO)_8(P(OPh)_3)_2$ revealed no absorption in the temperature range from 25 to 125°C. Even after prolonged heating at 125°C (about 1 hour)

no signals were observed although some decomposition of the compounds was apparent.

(C) KINETIC STUDIES ON THE DECOMPOSITION OF $Mn_2(CO)_{10}$ AND ITS REACTIONS WITH PPh_3 AND I_2 IN SOLUTION

(1) EXPERIMENTAL

The initial runs in n-octane (B.P. = 125°C) or xylene (B.P. = 140°C) solution at 80°C were carried out in foil-wrapped, stoppered volumetric flasks which were thermostatted in an oil-bath. Oxygen was not excluded from the solutions. Samples were withdrawn from the flasks at suitable time intervals by means of a teat-pipette and were cooled to room temperature. If necessary, clear solutions were obtained by filtration. The majority of the reactions were followed by observing the decrease in the absorbance due to the absorption maximum of $Mn_2(CO)_{10}$ at 340 mμ . However all of the I_2 runs in xylene were followed by I.R. spectroscopy because of the masking of the $Mn_2(CO)_{10}$ absorption by the charge transfer peak due to the complex formed between I_2 and xylene (94(b)).

It was not necessary to correct the absorbance readings from U.V. measurements for product absorption because I.R. scans showed that the products decomposed under the experimental conditions.

The majority of the reactions were carried out in decalin (B.P. = 190°C) under an atmosphere of nitrogen with rigorous exclusion of oxygen and light. The studies on $Mn_2(CO)_{10}$ decomposition were an exception in that most of them were

carried out in an atmosphere of air. The reaction solutions were contained in tubes fitted with rubber syringe caps and were thermostatted in an oil-bath. Samples were ejected, at suitable time intervals, through stainless steel or glass small bore tubing under pressure of nitrogen, or of air in the case of the decomposition reactions. The samples were cooled to room temperature and either scanned immediately or stored in sample tubes under nitrogen for periods of time always lessthan one hour before scanning. No changes were detected in samples which had been stored in this way for two hours. I.R. and U.V./Vis spectroscopy was used to follow the reactions. Some of the decomposition and iodine reaction runs were followed by the latter technique, but all of the PPh_3 runs were scanned in the I.R. region because of appreciable product absorption at 340 mμ .

The reaction of $Mn_2(CO)_9PPh_3$, using decalin as solvent, was studied by using identical techniques to those used for the $Mn_2(CO)_{10}$ reaction with PPh_3 in the same solvent.

Three runs of the $Mn_2(CO)_{10}$ reaction with PPh_3, using degassed xylene as solvent, were carried out at 125°C in sealed evacuated silica tubes in the cavity of an E.S.R. spectrometer. The E.S.R. techniques used were as given in Section IV (B)(1).

(2) RESULTS

Initial,studies in n-octane at 80°C showed that the rate of reaction of $Mn_2(CO)_{10}$ ($\sim 5\times10^{-5}$M) with PPh_3 ($1-5\times10^{-3}$M)

was approximately the same as the decomposition rate. On the other hand, the rate of reaction in iodine ($1\text{-}5\times10^{-3}$M) was faster by factors of two to seven.

The decomposition rate in xylene was similar but the reactions with iodine were, on average, about fifty times faster and very irreproducible.

The rate of decrease of the absorbance at 340 mμ or in the 2000 cm^{-1} region was logarithmic in all the reactions which shows that they obey rate equations which are first-order in $[Mn_2(CO)_{10}]$. The first-order rate constants were not sufficiently reproducible to determine the dependency of the rate on $[I_2]$.

No carbonyl products were detected in these reactions but insoluble decomposition products were formed. The brown precipitates, from the decomposition and PPh_3 reactions, were not identified, but the white precipitate, from the I_2 reaction, was shown to be MnI_2 by its U.V. spectrum in chloroform.

It was considered that $Mn(CO)_5I$ was initially formed but decomposed rapidly. Attempts were made to prove this by carrying out the reaction in the presence of ligands such as ER_3 (E = P, As, Sb; R = Ph, OPh, C_4H_9 etc.), $RC_6H_4NH_2$ (R = H, Me) and C_5H_5N which are known to react with $Mn(CO)_5I$(95) and detecting the products formed by their I.R. spectra. $Mn(CO)_5I + 2L \rightarrow Mn(CO)_4LI$ or $Mn(CO)_3L_2I$. Unfortunately these ligands reacted with I_2. When symtribromoaniline, a ligand unreactive towards I_2, was used it proved not to react with

$Mn(CO)_5I$. This approach was then abandoned, but $Mn(CO)_5I$ was subsequently detected in the reactions carried out in deoxygenated decalin.

The rates of the three reactions were too slow at 80°C for convenient measurement ($t_{\frac{1}{2}}$ = 190 hours for the decomposition in n-octane) so the study was extended to elevated temperatures using decalin (B.P. = 190°C) as solvent.

The results of the initial studies, together with those using decalin as solvent, are given in Tables 5,6, and 9 in the following sections. Further investigation of the reactions using n-octane as solvent was done by R.E. James as an undergraduate research exercise in this department, and these results are also tabulated.

A spectroscopic interaction between $Mn_2(CO)_{10}$ and I_2 was observed in n-octane solution such that on increasing $[I_2]$ the absorption maximum due to $Mn_2(CO)_{10}$ at 343 mμ decreased. This phenomenon was further investigated in n-octane and cyclohexane solvents and the results are given in Section IV (D).

(a) THE DECOMPOSITION OF $Mn_2(CO)_{10}$

Kinetic data for reactions in xylene, n-octane, and decalin over the temperature range 60 to 125°C are presented in Table 5. Most of the reactions were followed by observing the decrease in absorbance at 340 mμ, due to $Mn_2(CO)_{10}$, over a period of at least two half-lives and the first-order rate constants were evaluated from linear logarithmic rate plots.

Parallel runs, followed in the 2000 cm^{-1} region of the

TABLE 5.

Rates of Decomposition of $Mn_2(CO)_{10}$ in Solution.

Solvent	Atmosphere	Temp. (°C)	$[Mn_2(CO)_{10}]_0$ ($\times 10^{-5}$M)	Rate Constant (sec^{-1})
N-octane	Air	60.0	5.1	5×10^{-8}
N-octane	Air	80.0	6.7	1.0×10^{-6}
N-octane	Air	80.0	6.1	1.2×10^{-6} *
N-octane	Air	80.0	5.1	1.4×10^{-6} *
Xylene	Air	80.0	100	4×10^{-6}
N-octane	Air	95.0	6.1	9.0×10^{-6} *
N-octane	Air	95.0	6.1	1.4×10^{-5} *
Decalin	Air	105.0	41	2.8×10^{-5}
Decalin	N_2	105.0	45	7.1×10^{-6}
Decalin	Air	115.0	41	6.5×10^{-5}
Decalin	Air	125.0	41	1.3×10^{-4}
N-octane	N_2	125 **	50	2.1×10^{-4} *

* R.E. James, personal communication; ** solution refluxed.

infra-red, showed that no carbonyl products were formed.

The assumption is made here that the decomposition of $Mn_2(CO)_{10}$ is identical in n-octane and decalin. This is supported by the results of the reactions with PPh_3 where data obtained using the two solvents give a linear Arrhenius plot and thus reactions in the two solvents can be directly compared.

An Arrhenius plot (Fig. 11) illustrates the temperature dependence of the reaction. The activation energy between 60 and 95°C is about 37 Kcal/mole and the first order rate constants are given by the expression $k = 9 \times 10^{16} e^{-37,000/RT}$. But above 95°C the rate increases less rapidly with temperature.

The rate in deoxygenated decalin is a factor of four slower than the rate with oxygen present. The rate in refluxing n-octane under nitrogen is about twice as fast as the rate in decalin at 125°C.

(b) THE REACTION OF $Mn_2(CO)_{10}$ WITH PPh_3

The reaction in decalin was followed over the temperature range 105 to 125°C at values of $[Mn_2(CO)_{10}]$ of about 4×10^{-4}M and of $[PPh_3]$ of 0.01M. At 115 and 125°C the effect of varying $[PPh_3]$ was determined.

The I.R. spectra of the samples from reaction mixtures usually comprised eight well resolved bands in the region 1900 to 2100 $cm.^{-1}$. Fig. 12 illustrates a series of spectra, taken at different times during a run, in which can be observed

Fig. 11. Decomposition of $Mn_2(CO)_{10}$.

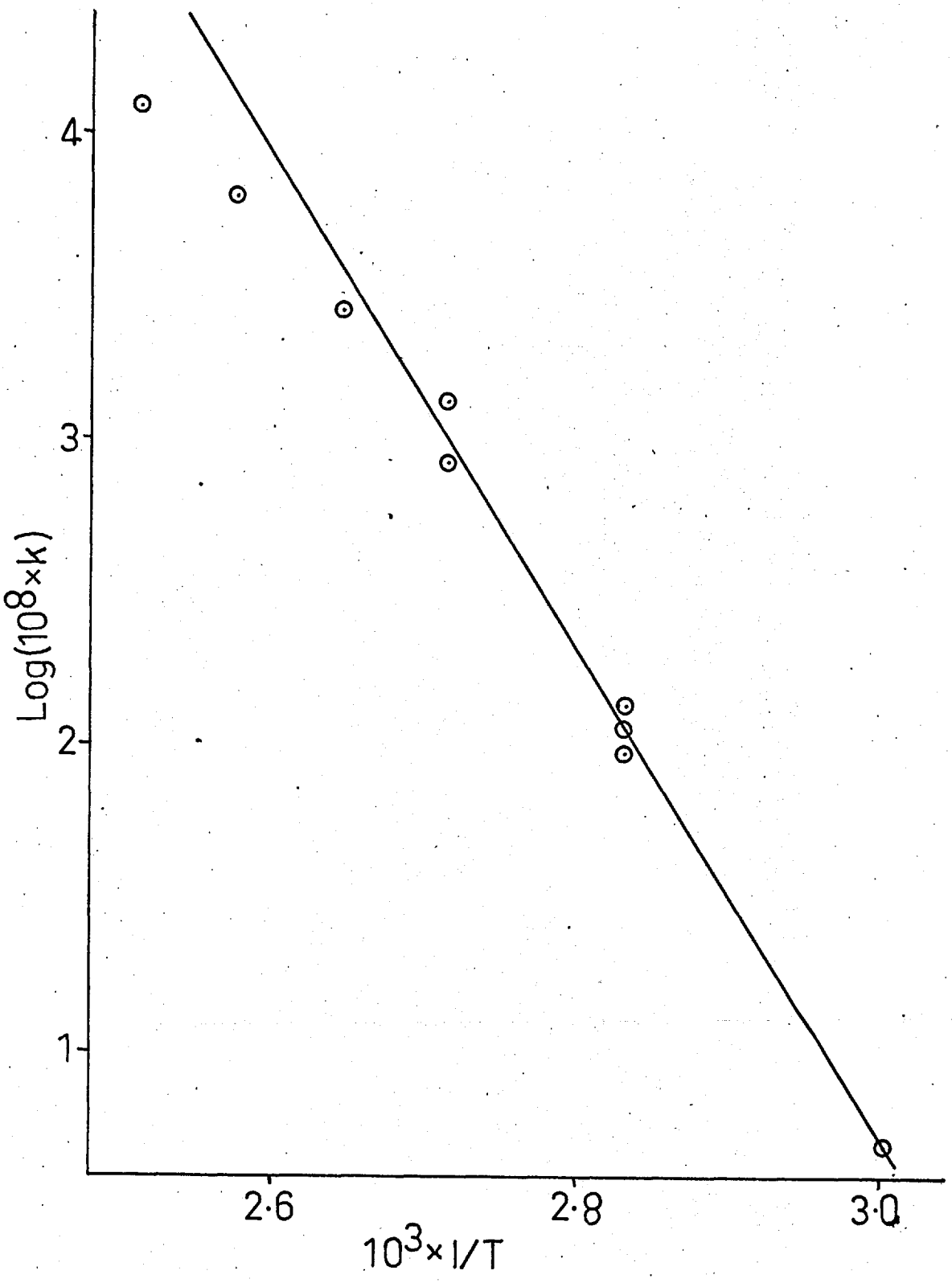

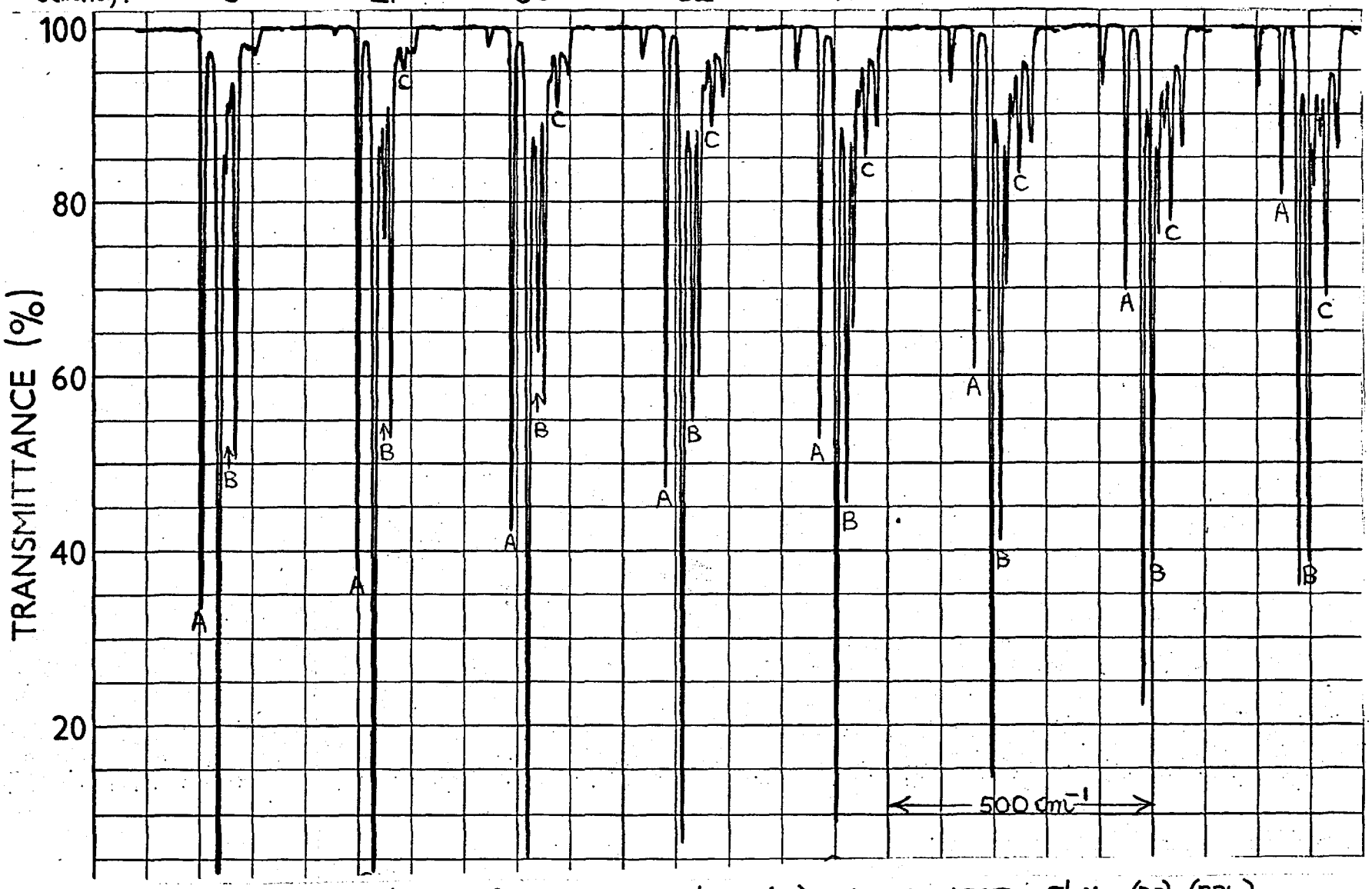

$Mn_2(CO)_{10}/PPh_3$ Reaction Spectra.

A = 2047 cm^{-1} $Mn_2(CO)_{10}$; B = 1997 cm^{-1} $Mn_2(CO)_9PPh_3$; C = 1963 cm^{-1} $Mn_2(CO)_8(PPh_3)_2$.

Fig. 12.

the decay of the spectrum due to $Mn_2(CO)_{10}$ (2047,2015,1986 cm.$^{-1}$) and the growth of spectra due to $Mn_2(CO)_9PPh_3$ (2093,2015,1997, 1974,1942 cm.$^{-1}$) and $Mn_2(CO)_8(PPh_3)_2$ (1963 cm.$^{-1}$).

It is convenient to report the rates of reaction of $Mn_2(CO)_{10}$ separately from the formation of the products of the reaction. Data from the reaction of $Mn_2(CO)_9PPh_3$ with PPh_3 is given in a third section.

(b)(i) RATES OF REACTION OF $Mn_2(CO)_{10}$

Linear logarithmic rate plots were obtained by following the decrease of $[Mn_2(CO)_{10}]$ and the first-order rate constants for the reactions in n-octane and decalin are presented in Table 6.

The rate dependence on $[PPh_3]$, determined at 115°C, showed that with increasing $[PPh_3]$ the rate rapidly became independent of $[PPh_3]$. The data are adequately represented by an empirical function :

$$k_{ob} = \frac{k'[PPh_3]}{1+k''[PPh_3]}$$

with values of the constants of $k' = 0.094$ l.moles^{-1}sec.$^{-1}$ and $k'' = 550$ l. moles^{-1}. The data are plotted as k_{obs} versus $[PPh_3]$ in Fig. 13 which also shows the curve calculated from the above expression.

The rate constants of the three runs in decalin at $[PPh_3]$ of 0.01M precisely obey the Arrhenius Law and give an activation energy of 36.6 Kcal/mole. This value is in

TABLE 6.

Rates of Reaction of $Mn_2(CO)_{10}$ with PPh_3

Solvent	Temp. (°C)	$[Mn_2(CO)_{10}]_0$ ($\times 10^{-4}$M)	$[PPh_3]_0$ (M)	Rate Constant. ($sec.^{-1}$).
N-octane	80.0	0.51	1.2×10^{-3}	1.4×10^{-6}*
N-octane	80.0	0.51	2.1×10^{-3}	1.4×10^{-6}*
N-octane	80.0	0.63	5.1×10^{-3}	1.3×10^{-6}
N-octane	95.0	0.61	2.0×10^{-3}	1.2×10^{-5}*
Decalin	105.0	4.5	1.0×10^{-2}	3.8×10^{-5}
Decalin	115.0	4.1	4.6×10^{-4}	5.8×10^{-5}
Decalin	115.0	3.7	4.0×10^{-3}	1.30×10^{-4}
Decalin	115.0	4.6	1.0×10^{-2}	1.36×10^{-4}
Decalin	115.0	4.0	4.0×10^{-2}	1.63×10^{-4}
Decalin	115.0	4.2	1.0×10^{-1}	1.70×10^{-4}
Decalin	125.0	4.0	4.6×10^{-3}	4.0×10^{-4}
Decalin	125.0	4.9	1.0×10^{-2}	4.5×10^{-4}
N-octane	125**	5.0	2.0×10^{-3}	1.16×10^{-3}*
N-octane	125**	5.0	2.0×10^{-2}	1.11×10^{-3}*
N-octane	125**	5.0	2.0×10^{-2}	1.37×10^{-3}*

* R.E. James, personal communication; ** solutions refluxed.

Fig. 13. $Mn_2(CO)_{10}/PPh_3$ Reaction.

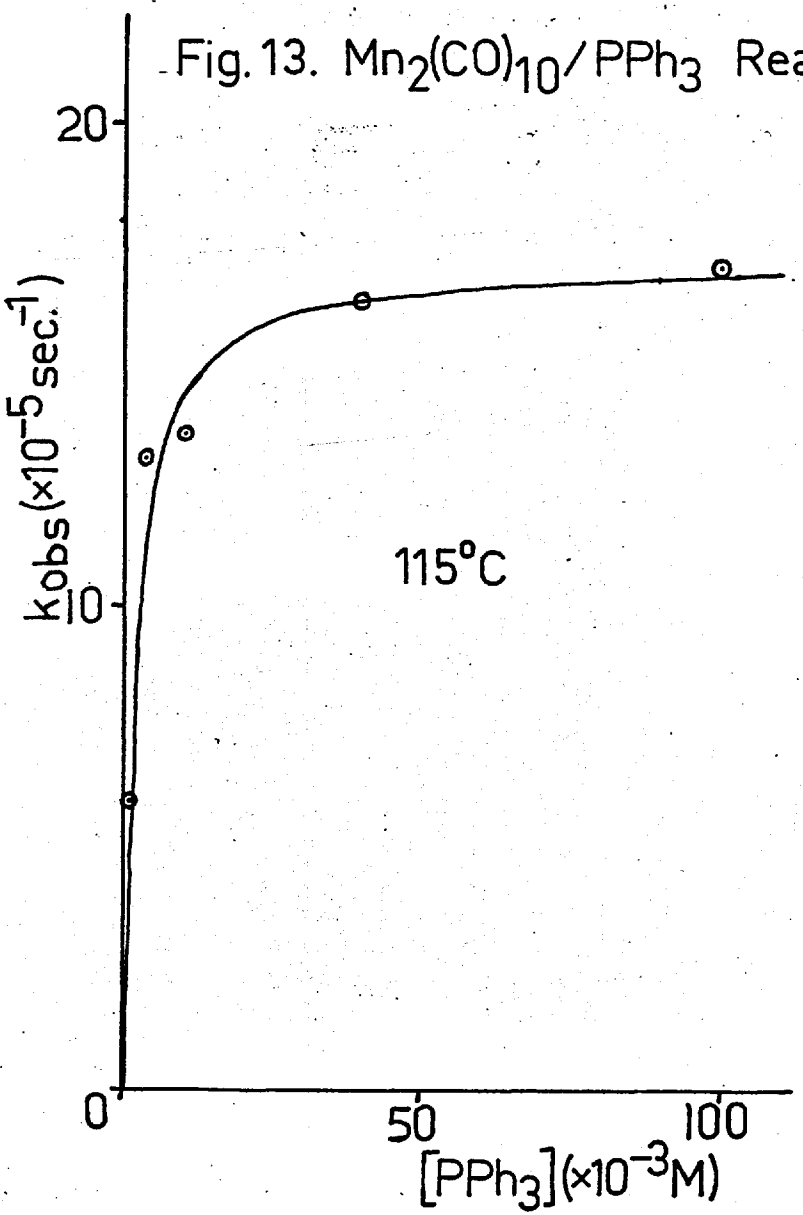

Fig. 14. $Mn_2(CO)_{10}/PPh_3$ Reaction.

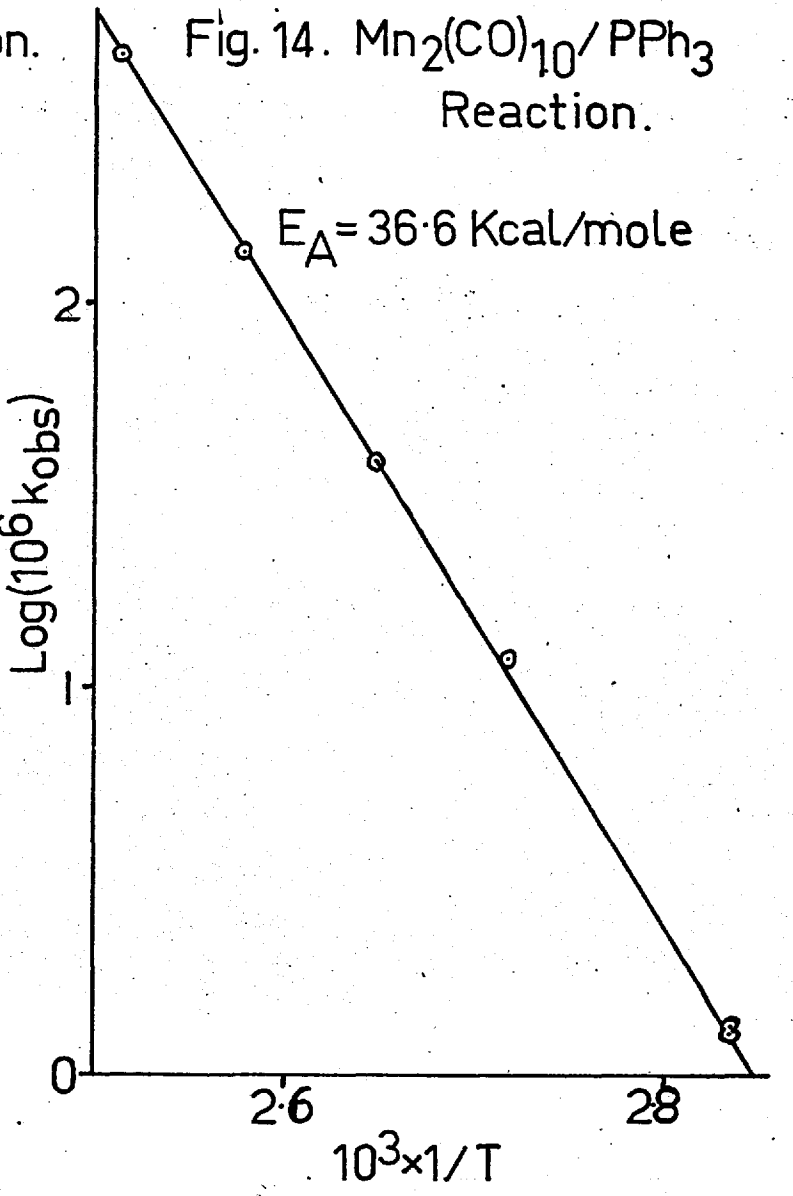

excellent agreement with that obtained from the rate constants of the reactions in n-octane at 80 and 95°C (Fig.14) and the data are well represented by the expression $k = 5.2 \times 10^{16} e^{-36,600/RT}$. These data are regarded as good evidence for the identity of the reactions in the two solvents.

However three runs in refluxing n-octane gave internally consistent results which were more than twiceas fast as the runs in decalin at 125°C. But because the lower temperature runs in n-octane are more consistent with the higher temperature runs in decalin than with the reflux runs, it is considered that the reflux runs are anomalous.

(b) (ii) THE FORMATION OF THE PRODUCTS OF THE REACTION IN DECALIN SOLUTION

The concentrations of the three carbonyl species in any reaction sample are calculated using the expression : $C = A_t/\epsilon l$ where $A_t = \log_{10}(100/T_t)$. $[Mn_2(CO)_{10}]$ and $[Mn_2(CO)_9PPh_3]$ are calculated from the peak heights of their bands at 2047 and 1997 $cm.^{-1}$ respectively using the extinction coefficients measured in decalin (Table 4). Unfortunately, it was impossible to quantitatively dissolve $Mn_2(CO)_8(PPh_3)_2$ in decalin without some decomposition occurring. Therefore the extinction coefficient of the 1963 cm^{-1} band in cyclohexane is used to calculate $[Mn_2(CO)_8(PPh_3)_2]$.

The data are presented in Table 7 as percentages of each carbonyl species with respect to the initial concentration

TABLE 7

FORMATION OF THE PRODUCTS OF THE REACTION OF $Mn_2(CO)_{10}$ WITH PPh_3

Key : t = time (min); A = 100 $[Mn_2(CO)_{10}]_t / [Mn_2(CO)_{10}]_0$;
B = 100 $[Mn_2(CO)_9PPh_3]_t / [Mn_2(CO)_{10}]_0$;
C = 100 $[Mn_2(CO)_8(PPh_3)_2]_t / [Mn_2(CO)_{10}]_0$; Tot. = A+B+C

Temp. = 105.0°C

$[Mn_2(CO)_{10}]_0 = 4.5 \times 10^{-4}$M; $[PPh_3] = 0.01$M

t:	10	41	72	122	191	250	310	350
A:	98	91	84	80	67	58	51	47
B:	2	4	7	11	16	18	19	20
C:	2	4	7	11	18	24	29	36
Tot:	102	99	98	102	101	100	99	103

Temp. = 115.0°C

(a) $[Mn_2(CO)_{10}]_0 = 4.1 \times 10^{-4}$M; $[PPh_3] = 4.6 \times 10^{-4}$M

t:	10	25	40	55	70	90	110	130	150
A:	95	88	81	76	76	71	66	61	56
B:	5	12	18	24	27	32	34	34	37
C:			←		~ 2			→	
Tot:	100	100	99	100	103	103	100	95	93

TABLE 7 (cont.)

(b) $[Mn_2(CO)_{10}]_0 = 3.8 \times 10^{-4}M$; $[PPh_3] = 4.0 \times 10^{-3}M$.

t:	4	19	34	49	64	87	150
A:	97	84	76	71	63	53	32
B:	3	13	18	25	29	32	38
C:		3	3	3	5	8	13
Tot:	100	100	97	99	97	93	83

(c) $[Mn_2(CO)_{10}]_0 = 4.6 \times 10^{-4}M$; $[PPh_3] = 0.01M$.

t:	6	21	36	52	76	106	146	206	254
A:	94	85	74	63	54	41	30	18	12
B:	4	11	17	22	30	33	35	37	33
C:	2	4	9	11	15	17	24	35	32
Tot:	100	100	100	96	99	91	89	90	77

(d) $[Mn_2(CO)_{10}]_0 = 4.0 \times 10^{-4}M$: $[PPh_3] = 0.04M$.

t:	8	23	38	53	68	88	118	158
A:	93	85	78	68	50	45	33	23
B:	3	5	5	10	10	10	10	5
C:		3	5	8	8	10	13	10
Tot:	96	93	88	86	68	65	56	38

(e) $[Mn_2(CO)_{10}]_0 = 4.2 \times 10^{-4}M$: $[PPh_3] = 0.1M$.

t:	7	23	62	87	106	137	172
A:	93	81	60	45	36	25	17
B:	5	5	10	10	10	10	7
C:		5	11	23	22	27	31
Tot:	98	91	81	78	68	62	55

TABLE 7 (cont.)

Temp. = 125.0°C

(a) $[Mn_2(CO)_{10}]_0 = 4.0 \times 10^{-4}M$; $[PPh_3] = 4.6 \times 10^{-3}M$.

t:	4	9	14	19	24	31	39	49	94	124
A:	90	85	73	65	58	50	40	33	13	5
B:	8	15	23	30	35	43	48	53	53	45
C:		3	5	8	8	10	13	15	23	23
Tot:	100	103	101	103	101	103	101	101	89	73

(b) $[Mn_2(CO)_{10}]_0 = 4.9 \times 10^{-4}M$; $[PPh_3] = 0.01M$.

t:	10	20	30	40	51	60	70	81	96
A:	74	57	45	35	25	20	14	10	6
B:	14	25	33	39	39	41	39	35	27
C:	12	18	23	27	31	35	33	29	29
Tot:	100	100	101	101	95	96	86	74	62

of $Mn_2(CO)_{10}$ at given times during a run. As an example, the concentration-time curves of the three carbonyl species are depicted in Fig. 15 for the reactions with $[PPh_3]$ of 0.01M at the three temperatures.

In any run, except those with $[PPh_3]$ of value greater than 0.01M, the concentration of carbonyl species, in samples taken during the first half-life of reaction, have a standard deviation of less than $\pm$ 2%. Thus this data is sufficiently accurate for detailed kinetic analysis.

Precipitation of an orange solid, shown to be $Mn_2(CO)_8(PPh_3)_2$, occurred when $[Mn_2(CO)_8(PPh_3)_2]$ reached

Fig. 15.
Concentration–Time Curves – The $Mn_2(CO)_{10}$/PPh_3 (0·01 M) Reaction.

Key : A = $Mn_2(CO)_{10}$, B = $Mn_2(CO)_9PPh_3$, C = $Mn_2(CO)_8(PPh_3)_2$

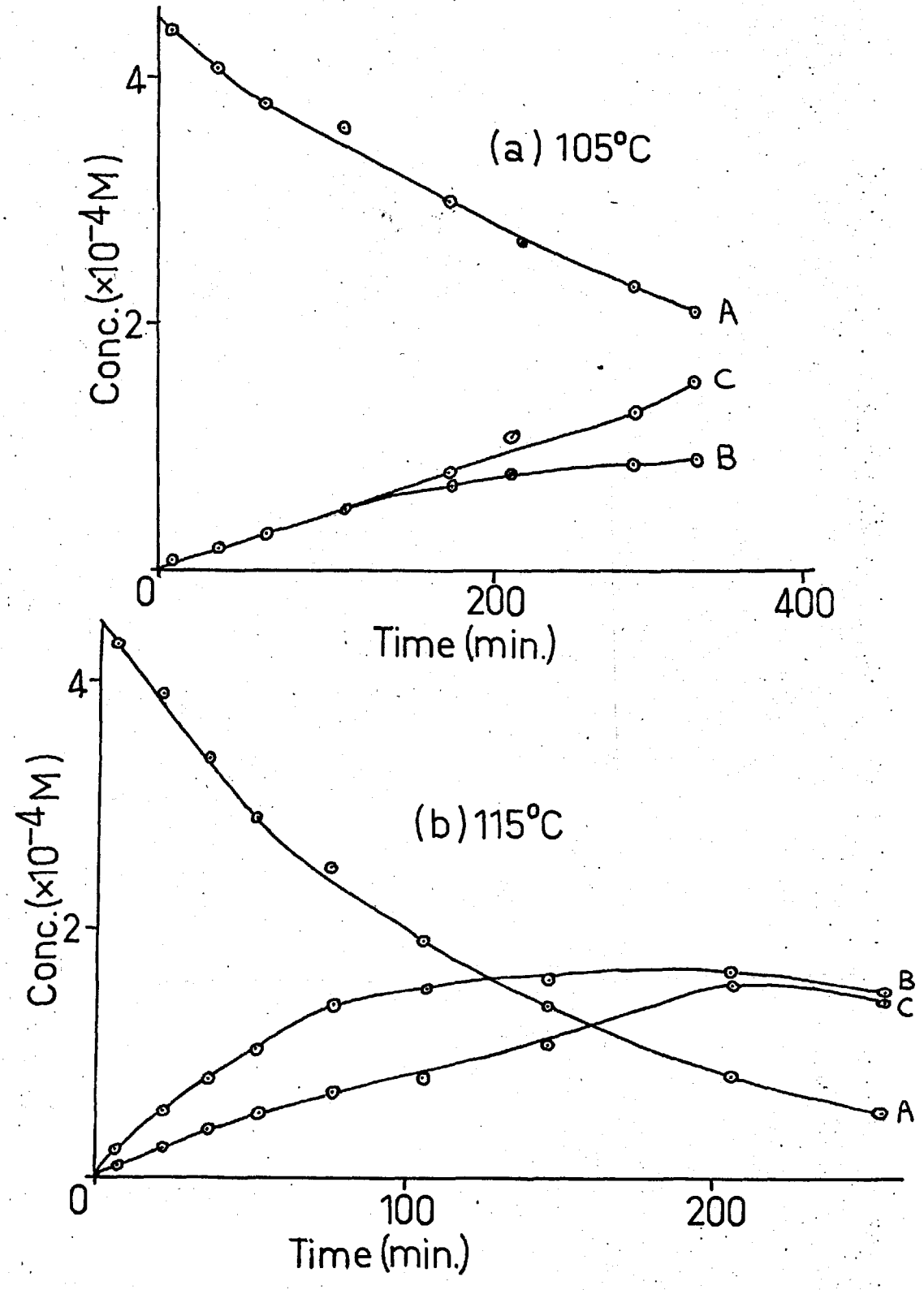

Fig. 15. (cont.)

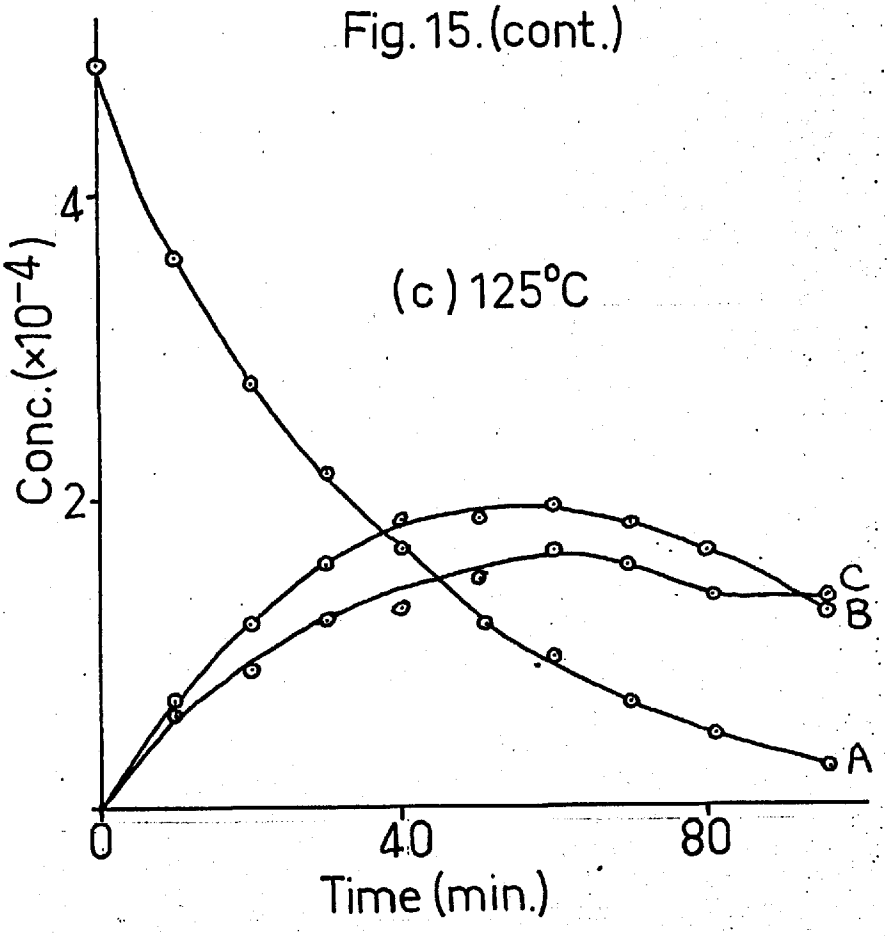

Fig. 16.

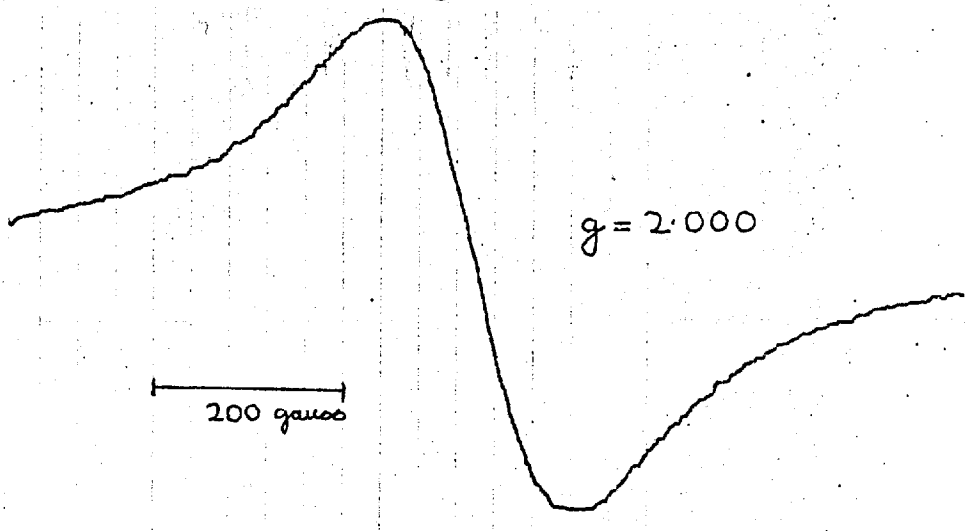

E.S.R. Signal. ($Mn_2(CO)_{10}$/PPh_3 Reaction)

about 1·5 x10^{-4}M. This behaviour is shown in the concentration-time curve of $Mn_2(CO)_8(PPh_3)_2$ in Fig. 15 (b) and (c).

Brown precipitates, which contained only traces of carbonyl species, came down in the runs with $[PPh_3]$ greater than 0.01M.

(b) (iii) THE REACTION OF $Mn_2(CO)_9PPh_3$ WITH PPh_3

This reaction was studied in the temperature range of 115 to 135°C at values of $[Mn_2(CO)_9PPh_3]$ of about 4 x 10^{-4}M and of $[PPh_3]$ of 0.01M in decalin. The effects of varying $[Mn_2(CO)_9PPh_3]$ and $[PPh_3]$ were determined at 125°C.

The reaction was zero-order in $[Mn_2(CO)_9PPh_3]$ in all the runs except one at 115°C which gave a sigmoid relationship of $[Mn_2(CO)_9PPh_3]$ versus time. The zero-order rate constants, evaluated from linear absorbance-time plots, are given in Table 8.

The runs at 125°C show that the rates are independent of $[Mn_2(CO)_9PPh_3]$ at $[PPh_3]$ of 0.01M and that doubling of $[PPh_3]$ leads to a reduction in the rate by about 30%. The rate of reaction at $[PPh_3]$ of 0.001M is about half of that at 0.01M.

The effect of varying temperature at constant initial concentrations of $Mn_2(CO)_9PPh_3$ revealed no systematic changes in rates and tend to show that the reaction is independent of temperature, albeit with a deviation of about ± 50%.

The product of the runs with $[PPh_3]$ of 0.01M or greater was $Mn_2(CO)_8(PPh_3)_2$ but the formation of traces of $Mn_2(CO)_{10}$ ($< 10^{-5}$M) was also observed. Conversely in the reaction with

TABLE 8

Rates of Reaction of $Mn_2(CO)_9PPh_3$ with PPh_3

Temp. (°C)	$[Mn_2(CO)_9PPh_3]_0$ ($\times 10^{-4}$M)	$[PPh_3]$ (M)	Rate constant ($\times 10^{-8}$ moles l^{-1} $sec.^{-1}$)
115.0	4.0	0.010	3.8
115.0	4.0	0.010	sigmoid
120.0	3.8	0.010	7.6
125.0	2.1	0.0010	0.93
125.0	2.2	0.010	1.8
125.0	4.0	0.010	1.9
125.0	2.4	0.019	1.2
130.0	3.9	0.010	6.4
135.0	3.5	0.010	5.9

$[PPh_3]$ of 0,001M, the product was $Mn_2(CO)_{10}$ with only barely detectable traces of $Mn_2(CO)_8(PPh_3)_2$ ($<10^{-5}$M).

In all the reactions, the rates of formation of products were much less than the rate of reaction of $Mn_2(CO)_9PPh_3$. Both precipitation of $Mn_2(CO)_8(PPh_3)_2$ and decomposition occurred. However 100% concentrations of carbonyl species were observed in the initial samples of 60% of the runs.

The problems encountered here, which appear to be mainly due to the lack of solubility of $Mn_2(CO)_8(PPh_3)_2$ in the solvent, make it doubtful if these results are of quantitative value.

(b) (iv) THE $Mn_2(CO)_{10}$ REACTION WITH PPh_3 FOLLOWED BY E.S.R. SPECTROSCOPY

In contrast with the preliminary E.S.R. scans of saturated solutions of $Mn_2(CO)_{10}$ and some of its substituted phosphine derivatives in xylene (Section IV (B) (2)), signals were detected from $Mn_2(CO)_{10}/PPh_3$ reaction solutions in xylene. The signals were broad of line-width of 206 gauss and g factor of 2.000 ± 0.001 (Fig.16).

A preliminary run was carried out with $[Mn_2(CO)_{10}]$ of 0.01M and $[PPh_3]$ of 0.02M, but the signal to noise ratios were low over the initial stages of the reaction. Therefore the growth of the absorption was followed in two runs at 125°C with $[Mn_2(CO)_{10}]$ of 0.1M and $[PPh_3]$ of 0.2M. At any time the amplitude of the signal was comparatively unaffected by lowering the temperature to -150°C but no fine structure was observed in the signals at any temperature. The growth of the absorption was accompanied by the precipitation of an orange reaction product which was identified by its I.R. spectrum as a mixture of $Mn_2(CO)_9PPh_3$ and $Mn_2(CO)_8(PPh_3)_2$.

The amplitudes of the derivative spectra were used as a measure of the relative concentrations of the absorbing species. Atherton, Melville, and Wiffen (96) show that this method yields values which are accurate to 5%. These values were calibrated by an absolute concentration calculated from one spectrum by numerical double integration of the derivive curve by using the method of Wyard (97), and by comparing this area with the

area calculated from a standard Cu E.D.T.A. solution curve (98). Values of the absorbing species concentration versus time are given in Fig. 17 for the two runs together with values of $([Mn_2(CO)_{10}]_0 - [Mn_2(CO)_{10}]_t)$ calculated from the known rate of reaction ($k = 4.0 \times 10^{-4} sec.^{-1}$). At any time the species concentrations were about 5% of the amount of $Mn_2(CO)_{10}$ reacted and in one run the concentration was $1.0 \times 10^{-2}M$ after keeping the solution at 125°C for 12 hours.

(c) THE REACTION OF $Mn_2(CO)_{10}$ WITH I_2

The reactions in decalin were studied over the temperature range 105 to 125°C with initial values of $[Mn_2(CO)_{10}]$ of about $4 \times 10^{-4}M$ and with $[I_2]$ varied from about 10^{-3} to $2 \times 10^{-2}M$. The runs at 105 and 125°C were kindly carried out by L.I.B. Haines in this laboratory.

Linear logarithmic rate plots were obtained by following the decrease of $[Mn_2(CO)_{10}]$ and the first-order rate constants for the reactions in xylene, n-octane, and decalin are presented in Table 9.

The reaction rates in decalin, at a given temperature, are dependent on the initial $[I_2]$, such that the observed rate constants obey the relationship :

$$k_{obs} = k_a + k_b [I_2]$$

Values of k_a and k_b, obtained graphically (Fig.18) are given in Table 10.

Fig. 17.

Radical Formation in the $Mn_2(CO)_{10}/PPh_3$ Reaction.

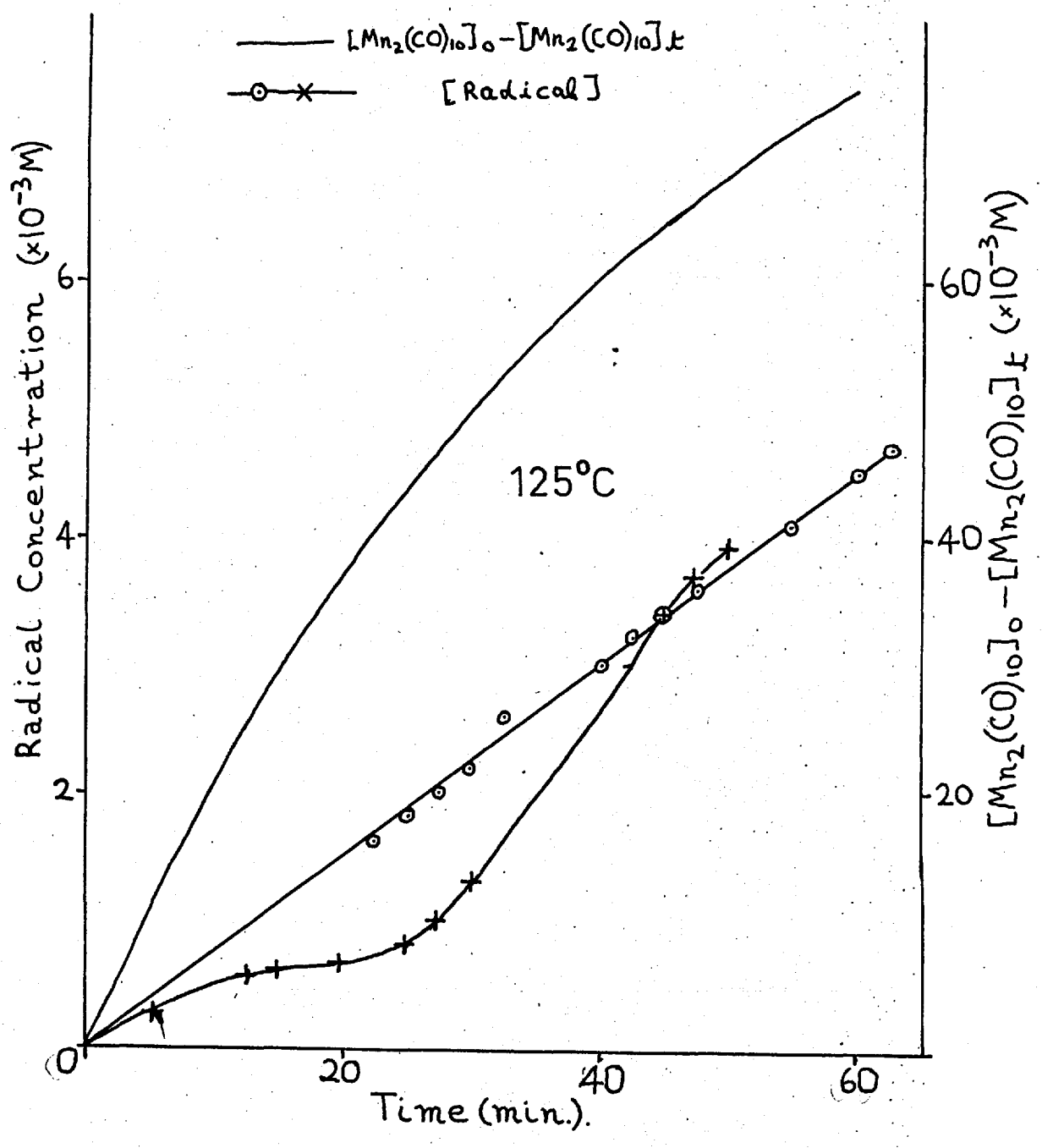

TABLE 9

Rates of Reaction of $Mn_2(CO)_{10}$ with I_2.

Solvent	Temp. (°C)	$[Mn_2(CO)_{10}]_0$ ($\times 10^{-4}$M)	$[I_2]_0$ ($\times 10^{-3}$M)	Rate Constant. ($\times 10^{-5}$ sec.$^{-1}$)
N-octane	80.0	0.72	1.0	0.21 *
N-octane	80.0	0.50	1.0	0.70
N-octane	80.0	0.50	5.0	0.45
Xylene	80.0	2.8	1.6	13
Xylene	80.0	5.0	1.8	7.7
Xylene	80.0	5.2	2.0	2.9
Xylene	80.0	50	200	1.8
Decalin	104.9	4.1	5.6	4.8 **
Decalin	104.9	4.0	9.1	6.0 **
Decalin	104.9	3.8	15.2	8.0 **
Decalin	115.0	4.6	1.3	12.0
Decalin	115.0	4.2	3.6	14.0
Decalin	115.0	3.8	12.5	21.5
Decalin	115.0	4.4	21.0	28.0
Decalin	124.6	3.9	6.0	54.0 **
Decalin	124.6	4.1	10.4	65.0 **
Decalin	124.6	4.0	15.5	78.5 **

* R.E. James, personal communication; ** L.I.B. Haines, personal communication.

Fig. 18. $Mn_2(CO)_{10}/I_2$ Reaction.

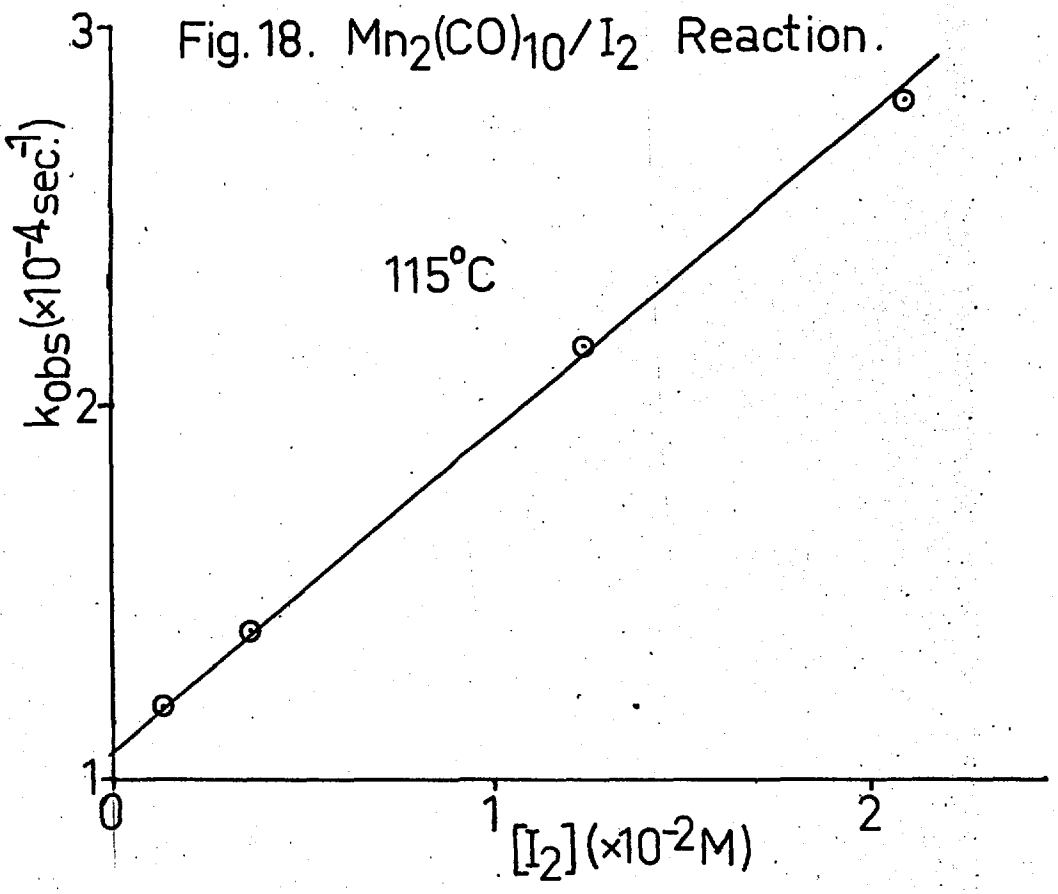

Fig. 19. $Mn_2(CO)_{10}/I_2$ Reaction.

$k_{obs} = k_a + k_b[I_2]$.

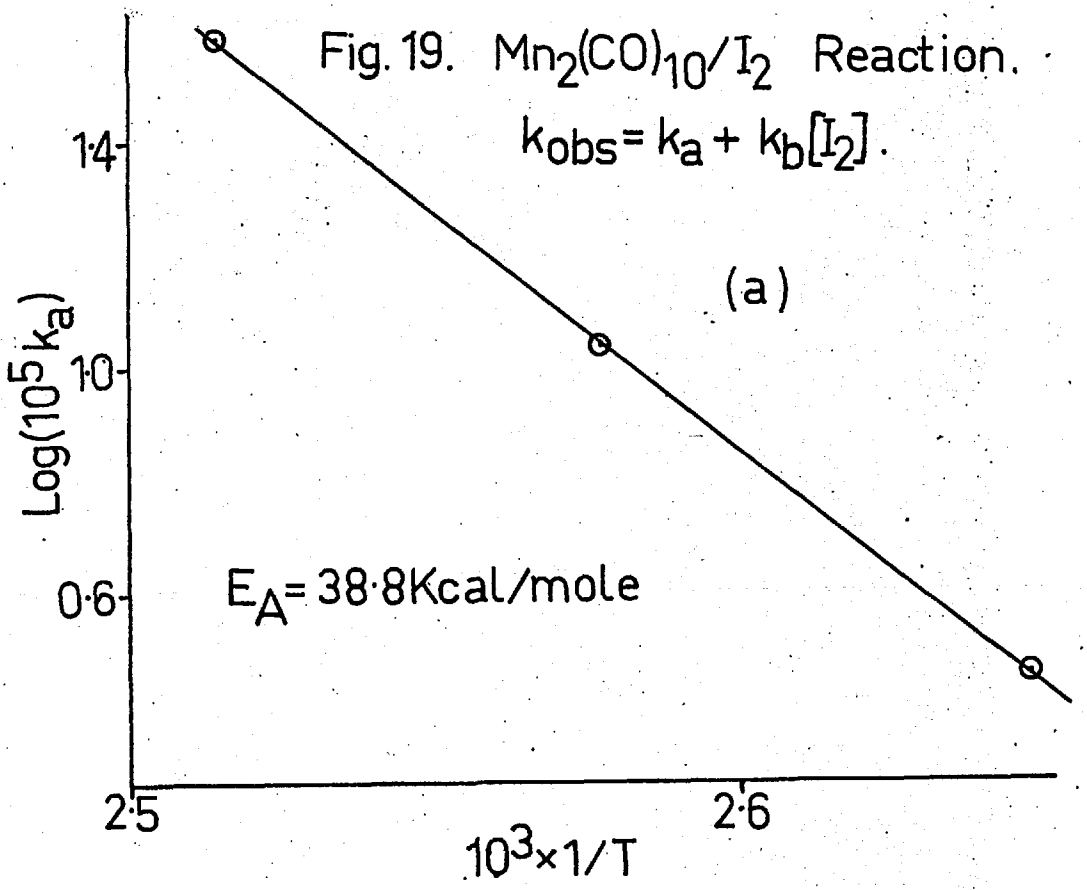

Fig. 19(b)

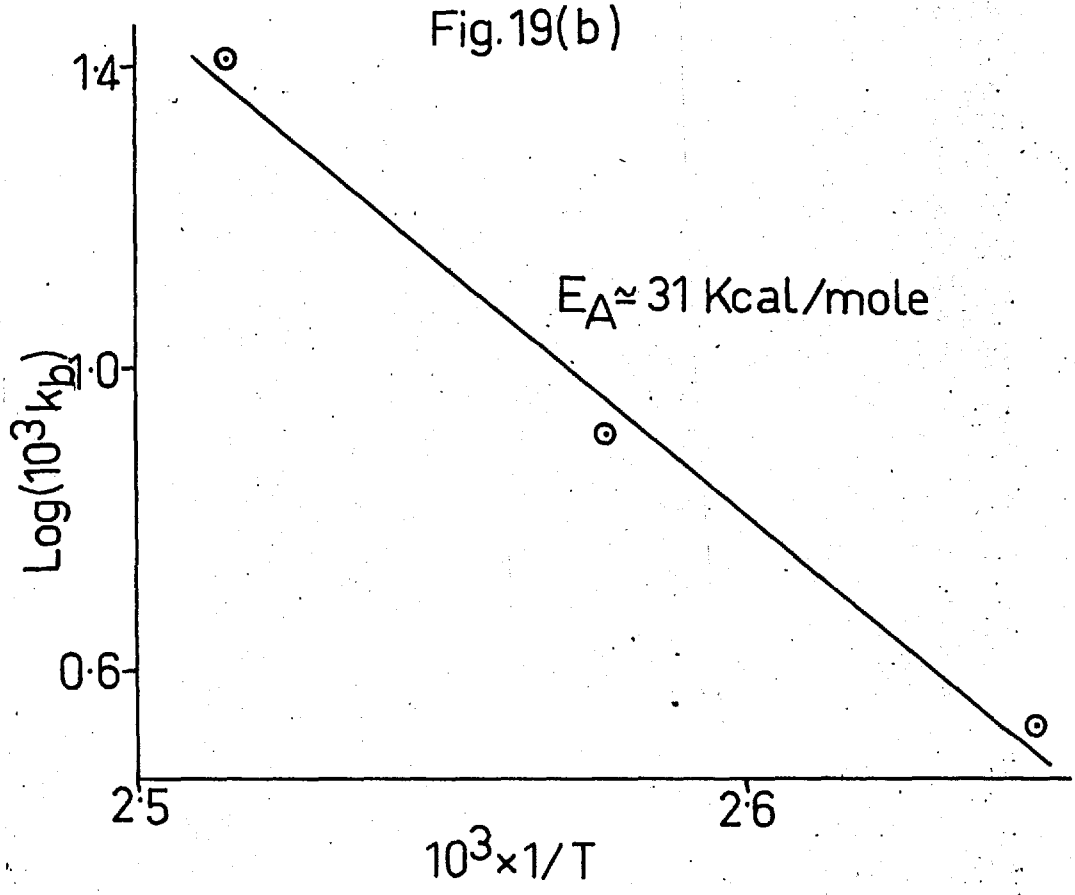

Fig. 20. Concentration–Time Curves $Mn_2(CO)_{10}/I_2$ Reaction.

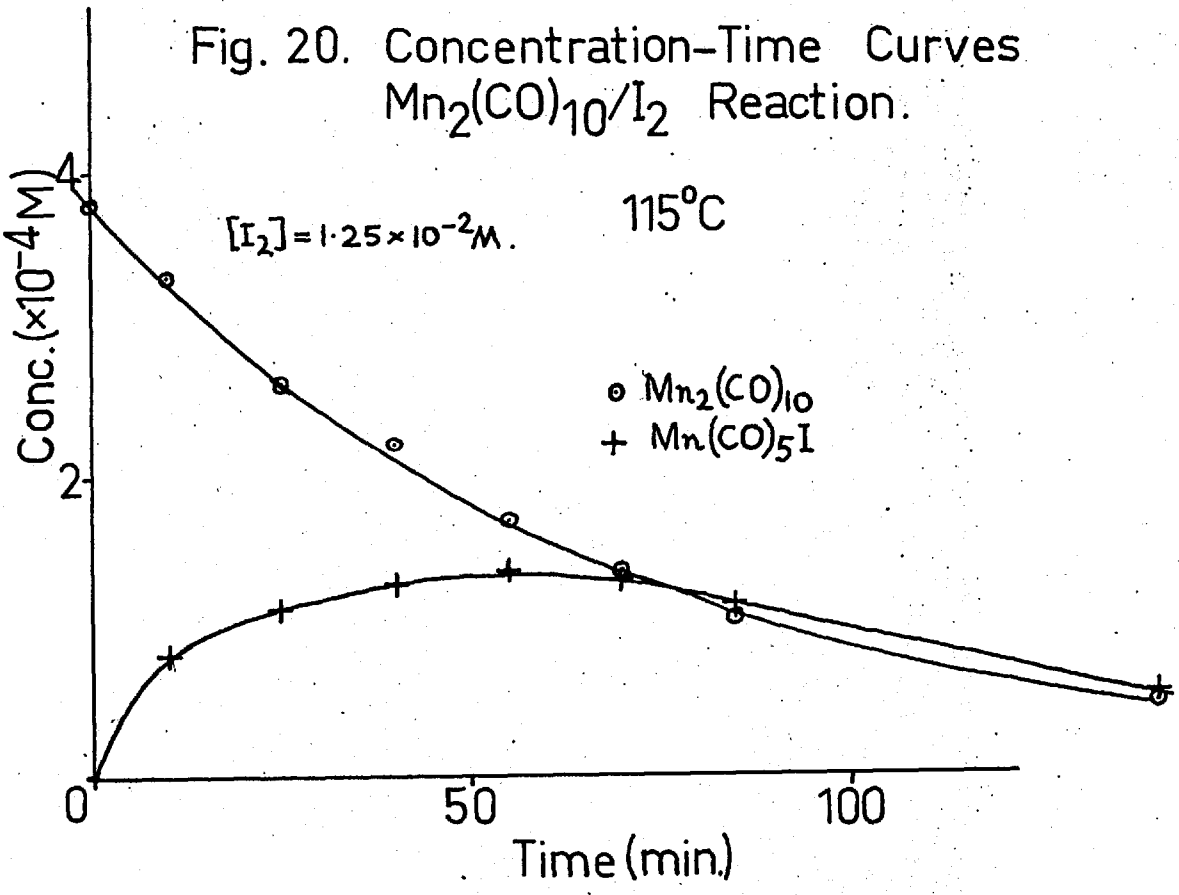

TABLE 10

Rate Parameters for the $Mn_2(CO)_{10}$ Reaction with I_2 in Decalin

$$k_{obs} = k_a + k_b[I_2]$$

Temp.(°C)	k_a($\times 10^{-5}$ sec^{-1})	k_b($\times 10^{-3}$ l. $moles^{-1} sec.^{-1}$)
104.9	2.90	3.3
115.0	11.0	8.2
124.6	38.0	26.0

Both k_a and k_b give linear Arrhenius plots (Fig.19) with activation energies of 38.8 and 31 Kcal/mole respectively. The rate constants are given by the expressions $k_a = 7.2 \times 10^{17} e^{-38,800/RT}$ and $k_b = 3 \times 10^{15} e^{-31,000/RT}$.

$Mn(CO)_5I$ was detected as the initial product of the reaction but it subsequently decomposed to MnI_2. The known decomposition product $[Mn(CO)_4I]_2$ (71) was not detected.

Concentration-time curves are given (Fig.20) for one run at 115°C in which a 100% yield of $Mn(CO)_5I$ was observed over the first 10% of reaction. The other runs, analysed by I.R. spectroscopy also gave similar growth and decay curves for $[Mn(CO)_5I]$ but with less than quantitative amount observed over the initial reaction.

(D) THE INTERACTION BETWEEN $Mn_2(CO)_{10}$ AND I_2 IN SOLUTION

(1) EXPERIMENTAL

To a solution of $Mn_2(CO)_{10}$ were added aliquots of a concentrated solution of I_2 from a microsyringe such that

the total volume of added solution was less than 1% of the initial $Mn_2(CO)_{10}$ solution. Thus corrections for volume changes were not made. The absorbances of the resulting solutions were measured at room temperature ($23 \pm 1^{\circ}C$) in calibrated silica cells, at the absorption maxima of $Mn_2(CO)_{10}$ and I_2, using a Unicam SP.500 spectrometer. This instrument was also used to plot the spectra of solutions of $Mn_2(CO)_{10}$, I_2, and $Mn_2(CO)_{10}$ plus I_2 in the region 650 to 220 mμ. These spectra were also recorded on a Perkin-Elmer 350 spectrometer. The I.R. spectra of some solutions of higher relative concentrations were recorded in the 2000 cm^{-1} region using a Grubb-Parsons Spectromaster spectrometer.

(2) RESULTS

Solutions of $Mn_2(CO)_{10}$ and of I_2 obeyed Beer's Law precisely over the range of concentrations used and in a solution of the two reactants the I_2 peak at about 510 similarly obeyed the law but the absorbance of the peak at about 340 mμ, due to $Mn_2(CO)_{10}$, was dependent on $[I_2]$. The rate of change of the absorbance at 340 mμ, on adding I_2, was too fast to be measured and the value of absorbance attained did not change over a period of two hours. No changes in the I.R. spectrum of $Mn_2(CO)_{10}$ were detected.

$[I_2]$, in any solution, was calculated from the absorbance of the peak at 510 mμ using a measured extinction

coefficient (Table 3) and this value was used to correct the absorbance of 340 mμ for absorption by I_2 ($\epsilon_{340}I_2$= 18 and 170 in cyclohexane and n-octane respectively). The resulting absorbance was assumed to be due only to $Mn_2(CO)_{10}$ and the difference between this and the initial absorbance was assumed to be proportional to the concentration of a complex formed between $Mn_2(CO)_{10}$ and I_2.

Measurements on the spectra of $Mn_2(CO)_{10}$ and I_2 apart and together did not reveal any absorbance changes in the region 650 to 220 mμ other than the symmetrical decrease centred on 340 mμ . Absorption by a complex is possibly obscured by the high intensity absorption of $Mn_2(CO)_{10}$ and I_2 in the far U.V. region. The simplest possibility is the formation of a 1 : 1 complex and equilibrium constants were calculated from the data on this basis :

$$Mn_2(CO)_{10} + I_2 \rightleftharpoons Mn_2(CO)_{10}\cdot I_2$$

$$K = \frac{[Mn_2(CO)_{10}\cdot I_2]}{[Mn_2(CO)_{10}][I_2]}$$

$\therefore$ as $[Mn_2(CO)_{10}]$ init = $[Mn_2(CO)_{10}] + [Mn_2(CO)_{10}\cdot I_2]$

then $$\frac{[Mn_2(CO)_{10}\cdot I_2]}{[Mn_2(CO)_{10}]} = \frac{A \text{ init} - A + AI_2}{A - AI_2}$$

(where A is the absorbance due to $Mn_2(CO)_{10}$ at 340 mμ and $AI_2 = A_{510} \times \epsilon_{340I_2}/\epsilon_{510I_2}$)

$$K = \frac{(A \text{ init} - A + AI_2)}{(A - AI_2)} \times \frac{\epsilon_{510I_2} \times \ell}{A_{510}}$$

Values of K calculated using this expression are given in Table 11. Statistically random values of K, for increasing $[I_2]$, are obtained in 6 out of the 8 series of determinations, with standard deviations of 10% or less for 5 of them. However there is no constancy observed between the average values of K for either of the solvents. A systematic decrease of K is obtained for increase of $[I_2]$ in two of the series.

In view of these results, the data from two of the series of determinations in cyclohexane are given in Table 12 to show the magnitude of the effect. The data are given for one series which gave random values of K (a) and for one which showed systematic decrease of K with increase of $[I_2]$ (b).

Thus although there is no doubt as to the positivity of the effect, it has proved impossible to analyse the data to give reliable parameters.

TABLE 11

Constants evaluated for the Equilibrium:

$$Mn_2(CO)_{10} + I_2 \rightleftharpoons Mn_2(CO)_{10} \cdot I_2$$

$[Mn_2(CO)_{10}]_0$ ($\times 10^{-5}$M)	Range of $[I_2]$ ($\times 10^{-4}$M)	K (M^{-1})	σ (%)	Number of determinations
	Cyclohexane			
0.19	0.41 – 1.6	550	20	4
1.1	4.6 – 39	42	10	6
2.8	0.76 – 64	380 74		21
4.2	3.7 – 37	90	7	10
4.3	3.1 – 27	36	3	9
8.5	4.3 – 80	84 17		7
	N-octane			
2.8	6.3 – 41	245	5	9
3.9	3.2 – 35	127	5	6

TABLE 12

Data from Two Series of Determinations of the $Mn_2(CO)_{10}$ Interaction with I_2

(a) $[Mn_2(CO)_{10}] = 4.2 \times 10^{-5}M$; $[I_2] = (3.7 - 37) \times 10^{-4}M$

$K = 90M^{-1} \pm 7\%$

A_{340}	A_{514}	A_{340I_2}	$(A-AI_2)^*_{340}$	$K(M^{-1})$
0.845	0.004		0.840	
0.827	0.370	0.007	0.815	83
0.810	0.553	0.010	0.795	102
0.805	0.730	0.013	0.787	92
0.790	1.08	0.019	0.766	90
0.780	1.42	0.026	0.749	85
0.760	1.71	0.031	0.724	94
0.745	2.3	0.041	0.699	88
0.725	2.8	0.050	0.670	91
0.700	3.3	0.059	0.636	97
0.690	3.7	0.067	0.618	97

(b) $[Mn_2(CO)_{10}] = 2.8 \times 10^{-5}M$; $[I_2] = (7.6 - 640) \times 10^{-5}M$

$K = 380 - 74M^{-1}$

A_{340}	A_{514}	A_{340I_2}	$(A-AI_2)^*_{340}$	$K(M^{-1})$
0.562	0.003		0.557	
0.547	0.076	0.001	0.541	380
0.540	0.149	0.003	0.532	315
0.535	0.220	0.004	0.526	267
0.533	0.295	0.005	0.523	221

Table 12 (cont.)

A_{340}	A_{514}	A_{340I_2}	$(A-AI_2)^*_{340}$	$K(M^{-1})$
0.530	0.368	0.007	0.518	205
0.524	0.440	0.008	0.511	204
0.520	0.588	0.011	0.504	179
0.517	0.760	0.014	0.499	154
0.512	0.870	0.016	0.491	155
0.507	1.015	0.018	0.484	149
0.502	1.155	0.021	0.476	148
0.500	1.30	0.023	0.472	139
0.497	1.45	0.026	0.466	135
0.495	1.59	0.029	0.461	131
0.488	1.75	0.031	0.452	133
0.483	1.90	0.034	0.444	134
0.482	2.40	0.043	0.434	118
0.478	2.9	0.052	0.421	108
0.480	3.8	0.068	0.407	97
0.483	4.9	0.088	0.390	87
0.494	6.4	0.115	0.374	74

* values corrected for mismatch of cells.

(E) DISCUSSION

It is convenient to discuss first the rates of decrease of $[Mn_2(CO)_{10}]$ in the reactions and it will be shown that marked similarities exist between all three reactions.

(1) RATES OF DECREASE OF $Mn_2(CO)_{10}$

First-order rate laws are obeyed by $Mn_2(CO)_{10}$ in its decomposition reactions, both in the presence and absence of O_2 and in its reactions with PPh_3 and I_2:

$$-d\left[Mn_2(CO)_{10}\right]/dt = k_{obs}\left[Mn_2(CO)_{10}\right]$$

The temperature dependences of k_{obs} were determined as follows:

(a) Decomposition in the presence of O_2 in the temperature range 60 to 95° C:

$$k_{obs} = 9 \times 10^{16}\ e^{-37,000/RT}$$

(b) Reaction with PPh_3 at $[PPh_3]$ of 0.01M:

$$k_{obs} = 5.2 \times 10^{16}\ e^{-36,600/RT}$$

(c) Reaction with I_2 where $k_{obs} = k_a + k_b[I_2]$

then $k_a = 7.2 \times 10^{17}\ e^{-38,800/RT}$

and $k_b = 3 \times 10^{15}\ e^{-31,000/RT}$

Thus the relationships of k_{obs} are identical within experimental error for the decomposition and limiting PPh_3 reactions, and these are similar to the relationship of k_a from the I_2 reaction. Thus it is probable that the same rate determining step occurs in all three reactions.

(2) THE REACTION WITH PPh_3

The dependence of this reaction on $[PPh_3]$ is of the form:

$$k_{obs} = \frac{k[PPh_3]}{1 + k'[PPh_3]} \quad \text{.....} \quad \text{(Fig 13)}$$

This type of rate law suggests that $Mn_2(CO)_{10}$ reversibly dissociates into a reactive fragment or gragments:

$$Mn_2(CO)_{10} \underset{k_{-1}}{\overset{k_1}{\rightleftharpoons}} (X.Y) \xrightarrow[k_3]{PPh_3} Mn_2(CO)_9PPh_3$$

By using a steady-state treatment, this mechanism gives an expression in k_{obs} of:

$$k_{obs} = \frac{k_1 (k_3 / k_{-1}) [PPh_3]}{1 + (k_3/ k_{-1}) [PPh_3]}$$

Thus when $(k_3/k_{-1}) [PPh_3] \gg 1$ then $k_{obs} = k_1$. The values of k and k' (Fig 13) determined at 115° C gives values of $k_1 = 1.70 \times 10^{-4}$ sec $^{-1}$ and $(k_3/k_{-1}) = 550M^{-1}$.

Therefore the limiting rate of the reaction is the rate of formation the reactive fragment or fragments (X.Y) which has an activation energy of 37 Kcal/mole.

The symbol (X.Y) refers to the two fragments trapped in a cageof solvent molecules. This cage effect, which is well discussed by North (99), causes the fragments to remain near neighbours for periods of time which are about 10^2 to 10^3 times longer than molecular vibration frequencies. This behaviour has to be postulated here in view of the first-order dependence on $[Mn_2(CO)_{10}]$ of the reaction. The reaction would be more complex if the reverse reaction involved a second-order recombination of non-geminate X and Y fragments.

The simplest mechanism which leads to the production of $Mn_2(CO)_9PPh_3$ is one in which the primary step is of CO dissociation, ie (X.Y) is $(Mn_2(CO)_9 \cdot CO)$. This mechanism

has been proposed by Basolo and Wawersik (100) who studied the $Mn_2(CO)_{10}$ reaction with PPh_3 using xylene as solvent. Their data were obtained at high $[PPh_3]$ and agree with ours. In addition they have shown that the reaction is partially inhibited by CO in agreement with the mechanism. Also they have found that the reaction of $Mn_2(CO)_9PPh_3$ with PPh_3 was first-order in $[Mn_2(CO)_9PPh_3]$ again using xylene solutions. We prefer their data on this reaction in view of the difficulties we encountered with this reaction using decalin as solvent. From the point of view of solubility decalin is a much less suitable solvent than xylene. These results lead them to propose that the reaction of $Mn_2(CO)_{10}$ to give $Mn_2(CO)_8(PPh_3)_2$ in the presence of excess $[PPh_3]$ is by two consecutive first-order CO dissociative steps:

$$Mn_2(CO)_{10} \xrightarrow{k_A} Mn_2(CO)_9PPh_3 \xrightarrow{k_B} Mn_2(CO)_8(PPh_3)_2$$

However this postulate is easily tested by kinetic analysis of the rates of formation of the two products.

The treatment of series first-order reactions is as given by Frost and Pearson (101). Values of K ($K = k_B/k_A$), given in Table 13, were calculated from the data given in Table 7 for the runs at $[PPh_3]$ of 0.01M or less by using the Time-Ratio Method at 15 and 35% reaction. These data are reliable as evidenced by the constancy of the concentrations of the three carbonyl species over the first half-life of the reactions. Initial rates of formation of the products, which were measured graphically, are also given in Table 13.

TABLE 13

ANALYSIS OF PRODUCT FORMATION IN THE $Mn_2(CO)_{10}$ REACTION WITH PPh_3

Temp (°C)	$[PPh_3]$ ($\times 10^{-3}$M)	K (k_B/k_A)	dB/dt* ($\times 10^{-8}$ moles $l.^{-1}$ sec^{-1})	dC/dt** ($\times 10^{-8}$ moles $l.^{-1}$ sec^{-1})
105.0	10.0	0.2	0.8	0.8
115.0	0.46	0.1	2.8	0
115.0	4.0	0.3	4.4	0.5
115.0	10.0	0.4	4.4	1.8
125.0	4.6	0.1	13	3
125.0	10.0	0.2	12	10

*dB/dt = d $[Mn_2(CO)_9PPh_3]$ /dt; **dC/dt = [d $[Mn_2(CO)_8(PPh_3)_2]$ /dt

---

Although these values of K are very approximately independent of $[PPh_3]$ they are not large enough to account for the observed concentration of $Mn_2(CO)_8(PPh_3)_2$ over the first part of the reaction. Fig. 21 depicts theoretical concentration-time curves for the series first order reactions $A \xrightarrow{k_A} B \xrightarrow{k_B} C$ for K ($K = k_A/k_B$) values of 0.4 and 2. Comparison of these with the experimental curves shown in Fig. 15 shows that the forms of the experimental and theoretical curves are quite different at $K = 0.4$, which

Fig. 21.
Series First-Order Reaction.

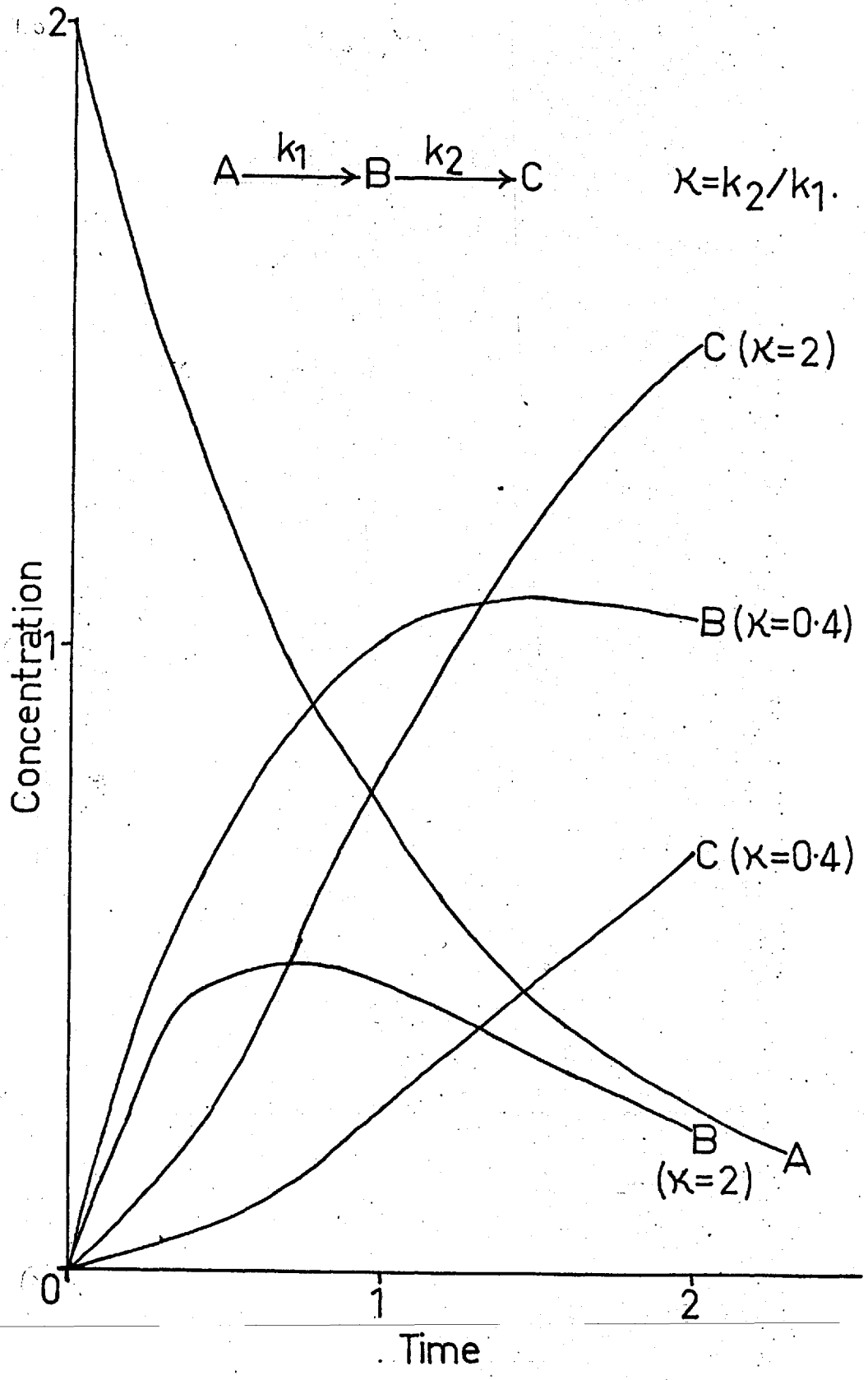

is the highest value given in Table 13 and that even at a higher value of K, such as 2, the forms of the curves are still quite different. These data show that $Mn_2(CO)_8(PPh_3)_2$ is formed directly from $Mn_2(CO)_{10}$ as well as from $Mn_2(CO)_9PPh_3$. At $[PPh_3]$ of 0.01M the initial rates of formation of the mono- and bi -phosphine products are quite comparable (Table 13; Fig 15).

Therefore a CO dissociative mechanism can be ruled out.

The most probable alternative primary step is homolytic fission of the Mn - Mn bond to give a pair of $Mn(CO)_5$ radicals, of which either one or both can react with PPh_3 before recombination occurs. Thus the following mechanism can be written:

$$Mn_2(CO)_{10} \underset{k_{-1}}{\overset{k_1}{\rightleftharpoons}} (2Mn(CO)_5)$$

$$(2Mn(CO)_5) + PPh_3 \xrightarrow{k_3} (Mn(CO)_5 \cdot Mn(CO)_4PPh_3) + CO$$

$$(Mn(CO)_5 \cdot Mn(CO)_4PPh_3) \xrightarrow{k_4} Mn_2(CO)_9PPh_3$$

$$(Mn(CO)_5 \cdot Mn(CO)_4PPh_3) + PPh_3 \xrightarrow{k_5} (2Mn(CO)_4PPh_3)_2 + CO$$

$$(2Mn(CO)_4PPh_3)_2 \longrightarrow Mn_2(CO)_8(PPh_3)_2$$

The reaction of $Mn_2(CO)_9PPh_3$ with PPh_3 to give $Mn_2(CO)_8(PPh_3)_2$ will be ignored here as only the initial rates of formation of the products will be considered. The above mechanism gives the same rate expression, $k_{obs} = \dfrac{k_1(k_3/k_{-1})\,[PPh_3]}{1+(k_3/k_{-1})\,[PPh_3]}$, as before

and the following expressions for the rate of production of products:

$$\frac{d\left[Mn_2(CO)_9\,PPh_3\right]}{dt} = \frac{dB}{dt} = \frac{k_1 k_3 k_4 \left[Mn_2(CO)_{10}\right]\left[PPh_3\right]}{(k_{-1} + k_3\left[PPh_3\right])(k_4 + k_5\left[PPh_3\right])} \quad \cdots\cdots$$

$$\frac{d\left[Mn_2(CO)_8(PPh_3)_2\right]}{dt} = \frac{dC}{dt} = \frac{k_1 k_3 k_5 \left[Mn_2(CO)_{10}\right]\left[PPh_3\right]^2}{(k_{-1} + k_3\left[PPh_3\right])(k_4 + k_5\left[PPh_3\right])} \quad \cdots\cdots$$

These equations simplify to:

$$\frac{dB}{dt} = \frac{k_{obs} k_4 \left[Mn_2(CO)_{10}\right]}{(k_4 + k_5\left[PPh_3\right])}$$

$$\frac{dC}{dt} = \frac{k_{obs} k_5 \left[Mn_2(CO)_{10}\right]\left[PPh_3\right]}{(k_4 + k_5\left[PPh_3\right])}$$

$$\therefore \quad \frac{dC/dt}{dB/dt} = \frac{k_5\left[PPh_3\right]}{k_4} = \frac{Ct}{Bt}$$

Values of k_5/k_4, calculated from the initial rates given in Table 13, are as follows:

k_5/k_4 = 100; 35 ± 6; and 67 ± 16 M^{-1} at 105, 115 and 125°C respectively. Remembering that the initial rates were obtained graphically these values are reasonably consistent. Therefore the proposed mechanism is consistent with the data available at present and it appears that k_5/k_4 is not greatly dependent on temperature within experimental error.

The retarding effect of CO can be explained on this mechanism by the reversible steps:

$$(2Mn(CO)_5) + PPh_3 \underset{k_{-3}}{\overset{k_3}{\rightleftharpoons}} (Mn(CO)_5 \cdot Mn(CO)_4PPh_3) + CO$$

and similarly for k_5. Thus the reaction would not go to completion but would attain an equilibrium mixture of $Mn_2(CO)_{10}$ and products. The reaction of $Mn_2(CO)_9PPh_3$ with PPh_3 of concentration of 0.001M, in which $Mn_2(CO)_{10}$ was formed in the presence of CO from decomposed compound, possibly demonstrates this effect. The reactions of $Mn_2(CO)_{10}$ with PPh_3 conducted by Basolo and Wawersik (100), which were retarded in the presence of CO, were not apparently followed over a sufficiently large extent of reaction to show that either the reactions went to completion or that an equilibrium mixture was attained. Unfortunately we have not as yet followed reactions in the presence of CO to clarify this point.

In contrast with the data reported by Hieber and Freyer (75) we have found no evidence that $Mn(CO)_4PR_3$ (R = Ph, OPh) radicals are sufficiently stable to exist in detectable concentrations in xylene solution in the temperature range of 25 to 125°C. The sensitivity of the E.S.R. spectrometer used was such that radical concantrations of $1.5 \times 10^{-9} \times \Delta H$ M (ΔH is the signal line-width in gauss) are detectable. Assuming $\Delta H \simeq 200$ gauss, as was found for the signals from the $Mn_2(CO)_{10}$ reaction with PPh_3 then concentrations of radicals of about 10^{-7}M are detectable. The concentrations of $Mn_2(CO)_8(PR_3)_2$ in saturated solutions are about 10^{-2}M so than K is less than about 10^{-13}M for the equilibrium:

$$Mn_2(CO)_8(PR_3)_2 \rightleftharpoons 2Mn(CO)_4PR_3$$

However we detected the growth of a signal on following the $Mn_2(CO)_{10}$ reaction with PPh_3 at concentrations such that the products precipitated from solution. The g value of 2.000 strongly indicates that the absorbing species was a free radical. The small temperature dependence of the signal suggests that the radicals were trapped in crystal matrices in the precipitate. Thus the absorption is probably due to either one of or both $Mn(CO)_5$ and $Mn(CO)_4PPh_3$. However in the absence of hyperfine splittings due to spin-spin coupling of the unpaired electron with the Mn^{55} nucleus (I = 5/2; 100% abundance), the presence of a Mn containing radical cannot be proved.

In summary, the data from the $Mn_2(CO)_{10}$ reaction with PPh_3 strongly suggests that the primary step of the reaction is homolytic fission of the Mn-Mn bond with an activation energy of 37 Kcal/mole.

(3) THE DECOMPOSITION OF $Mn_2(CO)_{10}$ IN SOLUTION

In n-octane solution and in the low temperature range, 60 to 95°C, the rate of decomposition of $Mn_2(CO)_{10}$ is identical with the limiting rate of the PPh_3 reaction, but at higher temperatures in decalin solution the rate of decomposition progressively decreases with respect to the values of the PPh_3 reaction (Fig 11)

At 105°C the decomposition is slower by a factor of 4 in the absence of O_2 than the reaction carried out in an atmosphere of air. Thus we propose the following mechanism:

$$Mn_2(CO)_{10} \underset{k_{-1}}{\overset{k_1}{\rightleftharpoons}} (2Mn(CO)_5) \xrightarrow{k_2} 2Mn(CO)_5 \downarrow \text{Decomp.}$$

$$(2Mn(CO)_5) + O_2 \xrightarrow{k_3} \text{Decomp.}$$

The decomposition product was not charactised apart from showing that it did not contain CO groups.

Step 2 is a diffusion controlled escape of the radicals from the solvent cage which accounts for the decomposition in the absence of O_2. The above mechanism gives a rate law whereby:

$$k_{obs} = \frac{k_1(k_2/k_{-1} + (k_3/k_{-1})\,[O_2])}{1 + k_2/k_{-1} + (k_3/k_{-1})\,[O_2]}$$

When $(k_3/k_{-1})\,[O_2] \gg (1 + k_2/k_{-1})$ then $k_{obs} = k_1$ and this behaviour was observed in the temperature range of 60 to 95°C.

In the absence of O_2, $k_{obs} = \frac{k_1(k_2/k_{-1})}{1 + k_2/k_{-1}}$ and knowing k_1 from the PPh_3 reaction, we can calculate the value of k_2/k_{-1} of 0.17 at 105°C ($k_1 = 4.8 \times 10^{-5}$ sec.$^{-1}$).

If we make some assumptions about the variation of k_2/k_{-1} with temperature we can calculate values of $(k_3/k_{-1})\,[O_2]$. The rate of diffusion from the solvent cage is proportional to the diffusion coefficient of the $Mn(CO)_5$ radicals which is given by the Stokes-Einstein equation (99):

$$k_2 \propto D = \frac{kT}{4\pi\eta r_s} \qquad \text{(k=Boltzmann constant)}$$

Thus the variation of k_2 with temperature is dependent only

on the variation of the viscosity of the solvent. This variation can represented by an apparent activation energy (E_2) of 3 Keal/mole which was calculated from viscosity data of decalin (102(a)).

Assuming that E_{-1}, the activation energy for the step k_{-1}, is zero, we then calculate k_2/k_{-1} at 115 and 125°C to be 0.19 and 0.21 respectively. From these values we find $(k_3/k_{-1})[O_2]$ at 105, 115 and 125°C to be 1.25, 0.45 and 0.09 respectively. In order to calculate the temperature dependence of (k_3/k_{-1}) it is necessary to know only the temperature dependence of $[O_2]$ and not absolute values. $[O_2]$ will decrease over the temperature range 105 to 125°C due to (a) decreasing solubility and (b) the increasing vapour pressure of the solvent which decreases the partial pressure of O_2 in the atmosphere above the reaction solution. There is no published data on the solubility of O_2 in decalin but as solubilities of gases are usually governed by the Clausius-Clapeyron equation then:

$$\ln \frac{[O_2]_2}{[O_2]_1} = \frac{L}{R}\left\{\frac{1}{T_1} - \frac{1}{T_2}\right\}$$

where L is the heat of vapourisation of the gas from the solution. For O_2 dissolved in nonpolar organic solvents L is usually in the range 200 to 300 cal/mole (103) so that the decrease in $[O_2]$ in decalin cannot be more than 1% over the 20°C temperature range. Vapour pressure data for decalin (102(b)) show that the decrease of $[O_2]$, over the 20°C temperature range, due to this effect is 9%. Accordingly we standardise the data to $[O_2]_{105}$

using the expression:

$$[O_2]_{105} = 1.05\,[O_2]_{115} = 1.10\,[O_2]_{125}$$

Therefore the values of $[O_2]_{105}$ are 1.25, 0.47 and 0.10 at 105, 115 and 125°C respectively. A plot of log $(k_3/k_{-1})\,[O_2]_{105}$ against I/T gives a straight line whose gradient shows that:

$$E_3 - E_{-1} = -38 \text{ Kcal/mole}$$

As k_3 is probably diffusion controlled, E_3 = 3 Kcal/mole and this gives a value of E_{-1} of 41 Kcal/mole. Using this value to recalculate (k_2/k_{-1}) at 115 and 125°C and repeating the procedure until the value of E_{-1} used to calculate (k_2/k_{-1}) agrees with the value of E_{-1} given by the temperature dependence of $(k_3/k_{-1})\,[O_2]_{105}$, we obtain the parameters given in Table 14. The value of E_{-1} calculated by this procedure is 24 Kcal/mole and the Arrhenius plot of $(k_3/k_{-1})\,[O_2]_{105}$ is shown in Fig 22.

TABLE 14

Parameters Calculated for the Decomposition of $Mn_2(CO)_{10}$

Temp (°C)	k_{obs} ($X10^{-5}sec^{-1}$)	k_1 ($X10^{-5}sec^{-1}$)	(k_2/k_{-1})	$(k_3/k_{-1})\,[O_2]$	$(k_3/k_{-1})\,[O_2]_{105}$
105	2.8	4.8	0.17	1.25	1.25
115	6.5	17	0.08	0.54	0.57
125	13	56	0.04	0.27	0.30

Fig. 22.
Decomposition of
$Mn_2(CO)_{10}$.

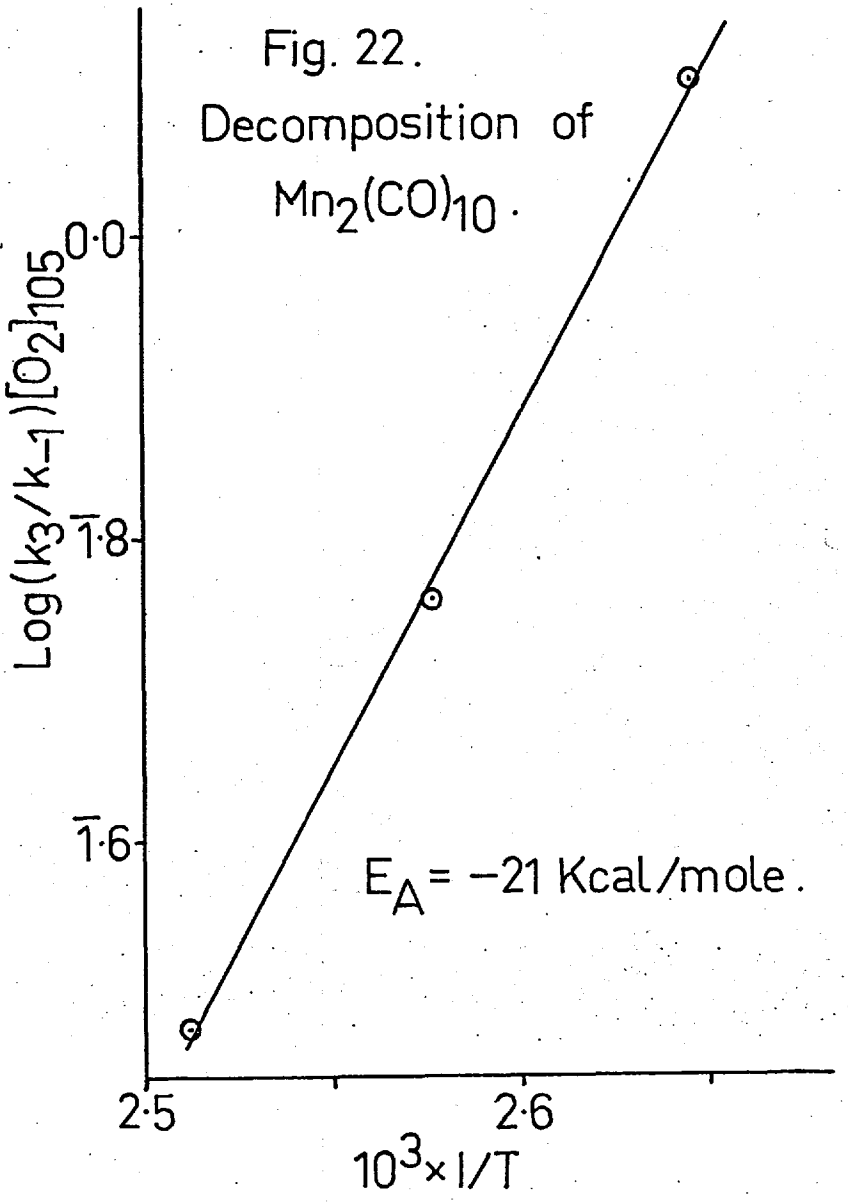

Fig. 23. Enthalpy Curve.

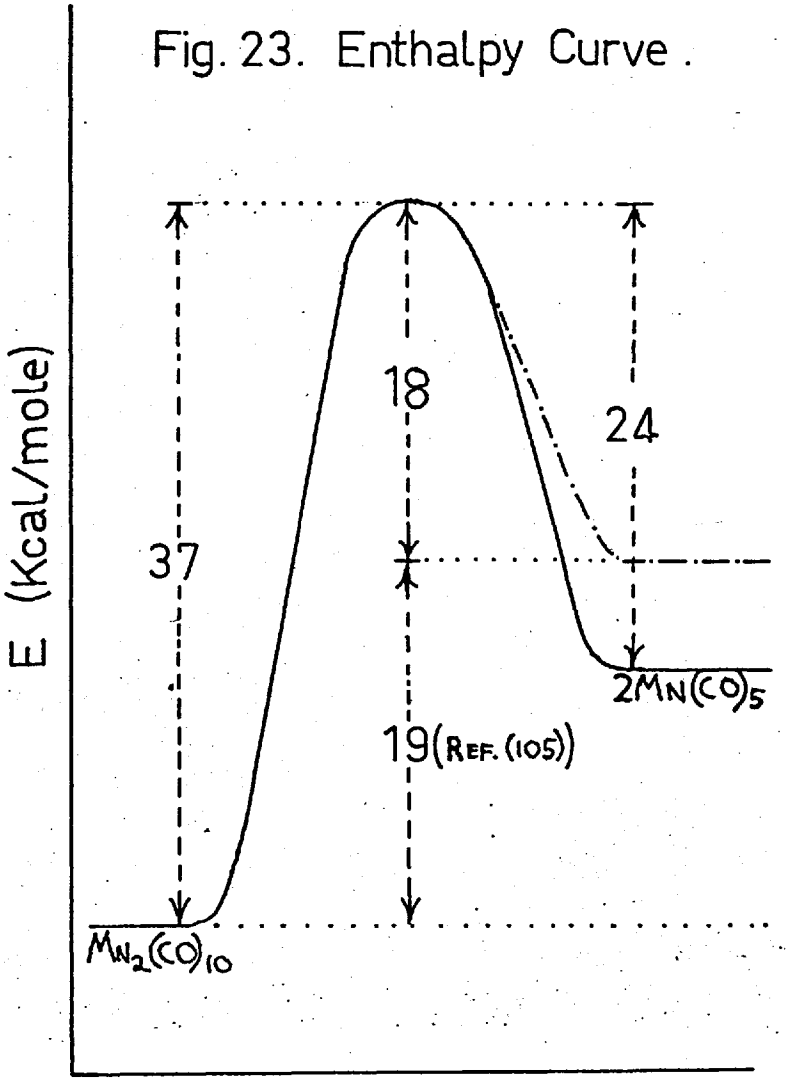

The data from the $Mn_2(CO)_{10}$ reaction with PPh_3 at 115°C was shown to be consistent with a rate law $k_{obs} = \frac{k_1(k_3/k_{-1})[PPh_3]}{1+(k_3/k_{-1})[PPh_3]}$ (Fig 13). However the data are better represented at low $[PPh_3]$ (4.6×10^{-4}M) by a rate law similar to that proposed for the decomposition reaction:

$$k_{obs} = \frac{k_1(k_2/k_{-1} + (k_3/k_{-1})[PPh_3])}{1 + k_2/k_{-1} + (k_3/k_{-1})[PPh_3]}$$

Using $k_1 = 1.70 \times 10^{-4}$ sec.$^{-1}$ and $k_2/k_{-1} = 0.08$ gives $(k_3/k_{-1}) = 570M^{-1}$ (determined previously as $550M^{-1}$).

Bamford and Denyer (104) have reported some data on the decomposition of $Mn_2(CO)_{10}$ in the absence of O_2 at 80°C. They report the initial rates of CO evolution, from $[Mn_2(CO)_{10}]$ of 1.50×10^{-3}M. to be 6.8×10^{-9} mole l^{-1} sec.$^{-1}$ independently of whether the solvent was methyl methacrylate, benzene, or ethyl acetate and 1.26×10^{-8} mole l^{-1} sec.$^{-1}$ in the same solvents in the presence of $[CCl_4]$ of 0.142M. They postulate that one mole of CO is evolved per mole of $Mn_2(CO)_{10}$ decomposing in the absence of CCl_4:

$$Mn_2(CO)_{10} \longrightarrow Mn_2(CO)_9 + CO$$

and that in the presence of CCl_4 two moles of CO are evolved due to a second step:

$$Mn_2(CO)_9 + CCl_4 \longrightarrow CCl_3 + CO + ?$$

No mention is made of the fate of $Mn_2(CO)_9$ in the absence of CCl_4 and their postulate is obviously incorrect as we have shown that the decomposition reaction yields no carbonyl products.

Using the equation:

$$d\,[CO]/10\,dt = -d\,[Mn_2(CO)_{10}]/dt = k_{obs}\,[Mn_2(CO)_{10}]$$

gives a value of k_{obs} of 4.5×10^{-7} sec.$^{-1}$ which together with our value of $k_1 = 1.55 \times 10^{-6}$ sec.$^{-1}$ and the equation $k_{obs} = \frac{k_1(k_2/k_{-1})}{1 + (k_2/k_{-1})}$ enables (k_2/k_{-1}) to be directly calculated at 80°C as we have done at 105°C. These data give $(k_2/k_{-1}) = 0.41$ which is in comparison with a value of 1.0, calculated using the data given in Table 14.

If in the presence of CCl_4, 10 moles of CO are evolved per mole of decomposing $Mn_2(CO)_{10}$ then $k_{obs} = 8.4 \times 10^{-7}$ sec.$^{-1}$ and so some recombination of caged $Mn(CO)_5$ radicals would be occurring. Alternatively this lower value of k_{obs} as compared with k, might be caused by the formation of some $Mn(CO)_5Cl$ and $[Mn(CO)_4Cl]_2$ which would involve less CO release. The latter explanation is probably correct as $Mn_2(CO)_{10}$ reacts readily with CCl_4 in the light to give the above products (69).

The values of E_1 and E_{-1} obtained in this work are in quite good agreement with the mass spectral work of Bidinosti and McIntyre (105) who estimated a bond dissociation energy of 19 Kcal/mole for the Mn-Mn bond in $Mn_2(CO)_{10}$. The appearance potentials for $Mn(CO)_5^+$ from $Mn_2(CO)_{10}$ and from $Mn(CO)_5$, produced by pyrolysis in a graphite effusion cell at 210 to 300°C, were combined to give this value which if it is that for the formation of $Mn(CO)_5$ in its most stable configuration, in that temperature range, then we obtain the enthalpy curve shown in Fig 23.

Further work is obviously necessary firstly to measure rates of decomposition in the absence of O_2 at several temperatures in order to directly estimate E_{-1} and secondly to measure rates under atmospheres of O_2 and N_2 mixtures of various composition. The above mechanism, although regarded as tentative, is certainly consistent with all the data available at present.

(4) THE REACTION WITH I_2

The preliminary studies showed that the reaction in xylene solution was significantly faster but of lesser reproducibility than n-octane. I_2 is known to associate with aromatic compounds to give a 1 : 1 complex (94(b)) which, in this case, is presumably more reactive than free molecular I_2. Thus we chose to study the reaction in aliphatic solvents to eliminate this complicating factor.

The reaction with I_2 in decalin, gives direct evidence for Mn-Mn bond fission as the primary step in the reactions we are discussing. It is difficult to imagine an alternative mechanism which satisfactorily accounts for the quantitative production of $Mn(CO)_5I$ at least over the initial stages of the reaction. The rate law, whereby $k_{obs} = k_a + k_b[I_2]$, suggests that two reactions proceed in parallel, one by a pseudo first-order process similar to the PPh_3 and decomposition reactions (a) and one by a second-order process(b).

The values of k_a obtained differ from the values of k_1 obtained from the PPh_3 reaction such that the ratio k_a/k_1 is 0.60, 0.65 and 0.68 at 105, 115, and 125°C respectively.

This apparent inconsistency is resolved by the following mechanism:

(a) $Mn_2(CO)_{10} \underset{k_{-1}}{\overset{k_1}{\rightleftharpoons}} (2Mn(CO)_5) \xrightarrow{k_2} 2Mn(CO)_5$

$(2Mn(CO)_5) + I_2 \xrightarrow{k_3} (Mn(CO)_5I + Mn(CO)_5 + I)$

$\downarrow$ fast

$2Mn(CO)_5I$

$Mn(CO)_5 + I_2 \xrightarrow{\text{fast}} (Mn(CO)_5I + I$

(Iodine atom attack on $Mn_2(CO)_{10}$ is an unfavourable process as shown by the reaction catalysed by benzoyl peroxide (Section VI(C)) and so the fate of the iodine atoms, produced according to the above mechanism, can be disregarded).

(b) $Mn_2(CO)_{10} + I_2 \xrightarrow{k_2} 2Mn(CO)_5I$

This mechanism gives the rate law:

$$k_{obs} = \frac{k_1(k_2/k_{-1} + (k_3/k_{-1})[I_2])}{1 + k_2/k_{-1} + (k_3/k_{-1})[I_2]} + k_2'[I_2]$$

Since k_1 and k_2/k_{-1} are known values, k_3/k_{-1} and k_2' are calculable from the data given in Table 9. Simultaneous equations were solved to obtain an approximate value of k_2' at each temperature. The values of k_2' and (k_3/k_{-1}) given in Table 15, were determined by varying the approximate k_2' values by increments and decrements of less than 5% to obtain calculated values of (k_3/k_{-1}) of least spread. The values of k_{obs} calculated using the parameters given in Table 15 are in good agreement with the experimental values except in the run at

TABLE 15

Rate Parameters for the $Mn_2(CO)_{10}$ Reaction with I_2

Temp (°C)	k_1 ($X10^{-5}$ $sec.^{-1}$)	$\left(\frac{k_2}{k_{-1}}\right)\left(\frac{k_3}{k_{-1}}\right)$ (M^{-1})	k_2' ($X10^{-3}$ $l.mole^{-1}$ $sec.^{-1}$)	$[I_2]$ ($X10^{-3}M$)	k_{obs} ($X10^{-5}$ sec^{-1}) exp.	calc.
104.9	4.8	0.17	320	2.6	5.6	4.8	4.7
					9.1	6.0	6.0
					15.2	8.0	7.9
115.0	17	0.08	480	6.5	1.3	12.0	8.0
					3.6	14.0	13.5
					12.5	21.5	22.5
					21.0	28.0	29.0
124.6	56	0.04	600	17	6.0	54.0	54.0
					10.4	65.0	66.0
					15.5	78.5	77.0

low $[I_2]$ at 115°C, where the error is 33%.

Arrhenius plots of the parameters (k_3/k_{-1}) and k_2' are depicted in Figs 24 and 25 respectively and give the following expressions:

$$(k_3/k_{-1}) \simeq 5 \times 10^7 \; e^{-9,000/RT}$$

$$k_2' = 5.9 \times 10^{13} \; e^{-28,400/RT}$$

The second order reaction can either be of two body collision type or occur by decomposition of a complex of the type $Mn_2(CO)_{10}{\cdot}I_2$ for which we have some spectroscopic evidence at room temperature. However, if the second explanation is true, a curvature of the k_{obs} versus $[I_2]$ plots (Fig. 18) is

Fig. 24.

$Mn_2(CO)_{10}/I_2$ Reaction.

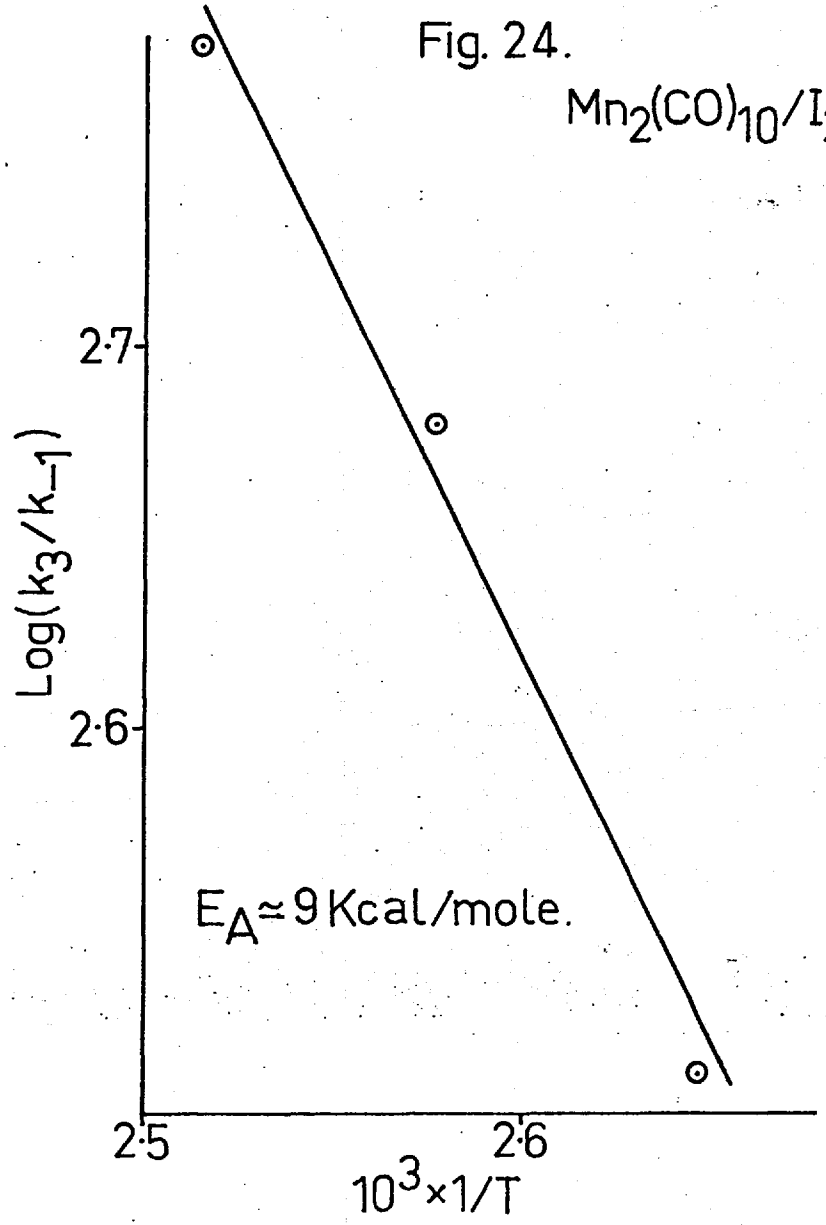

Fig. 25.

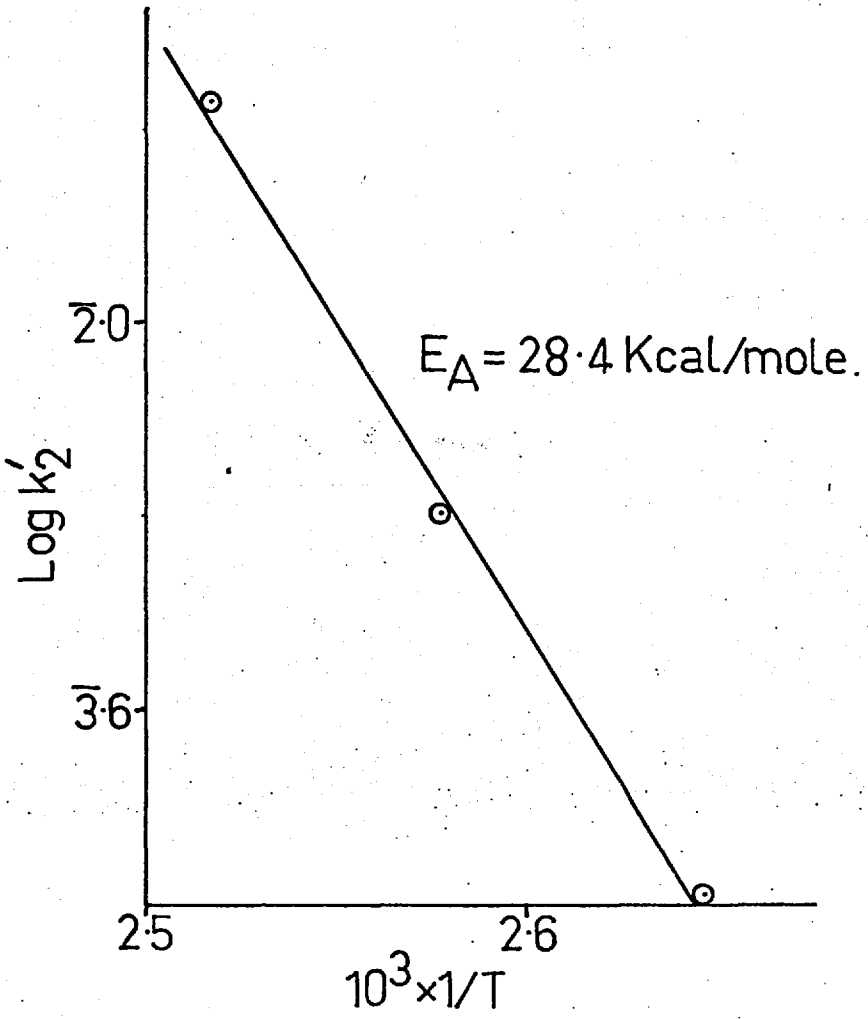

expected which was not observed. As we have not measured the temperature dependence of the association then either the association constant is small at high temperatures or association does not produce kinetically useful pairs. In any case the value of 28 Kcal/mole represents the energy difference between separated $Mn_2(CO)_{10}$ and I_2 and $Mn_2(CO)_{10}$ combined in the transition state.

The first-order reaction we have explained by an Mn-Mn bond fission primary step. A CO dissociative mechanism would involve the inelegant mechanism:

$$Mn_2(CO)_{10} \underset{k_{-1}}{\overset{k_1}{\rightleftharpoons}} (Mn_2(CO)_9 \cdot CO)$$

$$(Mn_2(CO)_9 \cdot CO) + I_2 \xrightarrow{k_3} (Mn_2(CO)_9 I_2 \cdot CO)$$

$$2Mn(CO)_5I \longleftarrow (Mn(CO)_5 \cdot Mn(CO)_4 I \cdot I \cdot CO)$$

Some formation of $[Mn(CO)_4I]_2$ would be expected on this mechanism but none was observed. However there is a definitive test between the two mechanisms in that the Mn-Mn bond fission one would not be inhibited by CO whilst the other mechanism would. Such experiments are to be carried out.

(5) SUMMARY

We propose a Mn-Mn bond fission primary step in the decomposition of $Mn_2(CO)_{10}$ and its reactions with PPh_3 and I_2 on the following evidence:

(a) The direct formation of $Mn_2(CO)_8(PPh_3)_2$ from $Mn_2(CO)_{10}$ in the presence of excess $[PPh_3]$;

(b) The quantitative formation of $Mn(CO)_5I$ and the absence of $[Mn(CO)_4I]_2$ over the initial stages of the reaction of $Mn_2(CO)_{10}$ with I_2 ;

(c) The formation of $Mn(CO)_5$ radicals by pyrolysis of $Mn_2(CO)_{10}$ as shown by mass spectral studies (105); and

(d) The very satisfactory quantitative agreement between the experimental results and the proposed mechanisms.

Some tentative conclusions can be drawn from the parameters obtained in this work.

The activation energy for recombination of a pair of caged $Mn(CO)_5$ radicals (E_{-1}) appears to be about 20 Kcal/mole (Fig 23). This presumably represents a rearrangement energy of about 10 Kcal/mole between each stable form of $Mn(CO)_5$, of possible trigonal-bipyramidal structure, analagous to $Fe(CO)_5$(2), and the form produced in the activated $Mn_2(CO)_{10}$ molecule.

The ratio k_5/k_4 of $35 \pm 6\ M^{-1}$, obtained from the reaction with PPh_3 at 115°C, for the competition:

$$(Mn(CO)_5 \cdot Mn(CO)_4PPh_3) \xrightarrow{k_4} Mn_2(CO)_9PPh_3$$

$$(Mn(CO)_5 \cdot Mn(CO)_4PPh_3) \xrightarrow[PPh_3]{k_5} (Mn(CO)_4PPh_3)$$

is significantly lower than the ratio k_3/k_{-1} of $570M^{-1}$ for the competition

$$(2Mn(CO)_5) \xrightarrow{k_{-1}} Mn_2(CO)_{10}$$

$$(2Mn(CO)_5) \xrightarrow[PPh_3]{k_3} (Mn(CO)_5 \cdot Mn(CO)_4PPh_3)$$

Now k_3 and k_5 both represent attacks on $Mn(CO)_5$ radicals by PPh_3 and so it is reasonable to assume that $k_3 = 2k_5$. Therefore k_4/k_{-1} is approximately equal to 8 indicating the greater facility of recombination of a $Mn(CO)_4PPh_3$ radical as compared with a $Mn(CO)_5$ radical.

Two further points of interest are the activation energy of about 30 Kcal/mole ($E_3 - E_{-1} \simeq 9$) for I_2 attack on $Mn(CO)_5$ as compared with an activation energy of 28 Kcal/mole for I_2 attack on $Mn_2(CO)_{10}$, and the approximate identities of k_3 for $I_2(k_3/k_{-1} = 480M^{-1})$ and $PPh_3(k_3/k_{-1} = 570M^{-1})$ attack on $Mn(CO)_5$ at 115°C.

(6) ERRORS

The treatments accorded to the data given in this section have been mainly by trial and error cyclisation to obtain best fits of experimental data to rate laws derived from possible mechanisms by steady-state treatment. We have not carried out statistical treatments to obtain standard deviations of the derived parameters because there are insufficient data to make this meaningful. The various figures depicting Arrhenius plots give a reasonable indication of the reliability of the data.

(V) THE THERMAL REACTIONS OF DIMANGANESE DECACARBONYL WITH BROMINE

(A) INTRODUCTION

Initial studies showed that in cyclohexane and CCl_4 solutions the reaction of Br_2($\sim 10^{-3}$ to 10^{-2}M) with $Mn_2(CO)_{10}$($\sim 5 \times 10^{-5}$ to 5×10^{-4}M) was suitable for a kinetic study. In both solvents the reaction was complete in 5 to 10 min. at room temperature and in the light, and the I.R. spectra showed smooth changes from that characteristic of $Mn_2(CO)_{10}$ to that of $Mn(CO)_5Br$ (Table 4). Measurement of the peak absorbances showed that 100% yields of $Mn(CO)_5Br$ were obtained:

$$Mn_2(CO)_{10} + Br_2 \longrightarrow 2\ Mn(CO)_5Br.$$

The reaction was also followed by observing the decrease in absorbance at 340 mμ due to $Mn_2(CO)_{10}$ in 1cm silica cells. Considerable reaction occurred before the first reading was taken (i.e. $\sim$ 2 to 4 min. after mixing) but subsequent reaction in the dark was much slower. In cyclohexane it was found that reaction of Br_2 with the solvent occurred ($\sim$ 20% in 21 hr.) in addition to formation of $Mn(CO)_5Br$.

Quantitative study of the reaction was carried out in the temperature range 40 to 60°C using the solvents cyclohexane, CCl_4, and $CF_2Cl{\cdot}CFCl_2$. Some observations on the photochemical reactions in cyclohexane and $CF_2Cl{\cdot}CFCl_2$ are given in Section VII.

(B) EXPERIMENTAL

Reaction solutions were contained in 1cm, stoppered, silica cells which were thermostatted in the cell compartment of a

Unicam S.P.500 spectrometer. The general techniques are described in Section II.

Br_2 was added, from a glass micropipette, to the $Mn_2(CO)_{10}$ solution, which in some cases contained additives, after the solution had reached thermal equilibrium by being in the thermostat block for 10 minutes. The addition of Br_2 and all subsequent operations were carried out in inactive light (red lamp) and between readings the reaction cell was removed from the spectrometer beam. In some runs the reactions were carried out using solvents deoxygenated by passing nitrogen for 30 minutes.

The reactions were followed by observing the decrease of the 340 mμ absorption maximum due to $Mn_2(CO)_{10}$ in the presence of excess $[Br_2]$. $[Br_2]$ was calculated from the absorbance of the peak at about 400 mμ using known extinction coefficients (Table 3). The absorbance due to formation of $Mn(CO)_5Br$ is negligible and no corrections were made but the 340 mμ absorbances were corrected for absorption due to $[Br_2]$.

(c) RESULTS

Sigmoid rate plots were obtained in the majority of the runs (~80%), with the rate of decrease of $[Mn_2(CO)_{10}]$ being essentially constant from 10-20 to 70-80 % reaction (See Fig 29) In cyclohexane the rate of decrease of absorbance at 420 mμ, due to Br_2 reaction with the solvent subsequent to the completion of the $Mn_2(CO)_{10}$ reaction, was also sigmoid. Linear and logarithmic type decreases of $[Mn_2(CO)_{10}]$ were also observed but

the sigmoid behaviour can be regarded as typical. As a preliminary step, the rate of reaction at 50% reaction ($R_{\frac{1}{2}}$) was taken as an empirical parameter whereby the effect of varying the conditions could be evaluated.

(1) THE REACTION IN CYCLOHEXANE

Some results are given in Table 16 with $[Mn_2(CO)_{10}] \simeq 5 \times 10^{-5}$M under various conditions. It is notable that greater reproducibility was obtained within a series of runs (as referenced by letters in Table 16) than was achieved overall under apparently identical conditions.

Runs E1-7 show that $R_{\frac{1}{2}}$ is a function of $[Br_2]$. The dependence on $[Br_2]$ can be expressed as $R_{\frac{1}{2}} \simeq k[Br_2]^{\frac{1}{2}}$ or as $R_{\frac{1}{2}} \simeq k_a [Br_2] / (1 + k_b [Br_2])$ as shown in Fig 24 and 25 respectively.

The importance of purity of the solvent is shown by Run A1 in which the reaction was completely inhibited in fractionally distilled GPR cyclohexane. The only detectable impurity, as shown by the U.V. spectrum, was benzene but Run F2 shows this was not the inhibitor. Runs F3 and 4 show that ethanol is an effective inhibitor of the reaction. A 4 day old $Mn_2(CO)_{10}$ solution which had been stored at 0°C exhibited inhibition of about a factor of 3. The U.V. spectrum of the solution showed that no detectable decomposition had occurred. Accordingly the Run Series B and C were carried out to estimate the effect of ageing of a fresh $Mn_2(CO)_{10}$ solution in the thermostat block prior to the start of the reaction. No effect was detectable although the lack of precision of the

TABLE 16

Rates of Reaction of $Mn_2(CO)_{10}$ with Br_2 under various conditions, using Cyclohexane as solvent

$$[Mn_2(CO)_{10}]_0 \simeq 5.0 \times 10^{-5} M$$

Ref. No.	$[Br_2]_0$ ($\times 10^{-3}$ M)	$R_{\frac{1}{2}}$* ($\times 10^{-9}$ moles $l.^{-1}$ $sec.^{-1}$)	Conditions
		Temp. = 39.9 - 40.2°C	
A 1	5.0	-	G.P.R. solvent
B 1	4.8	4.0	15 min. at 40°C before start of reaction
2	4.5	9.6	100 min.
C 1	4.5	1.4	15 min.
2	3.5	1.4	70 min.
3	5.4	5.9	200 min.
		Temp. = 50.9 - 51.2°C	
D 1	5.0	51	4 day old soln.
E 1	0.8	32	
2	3.0	110	
3	3.5	130	
4	4.8	150	
5	5.0	130	
6	5.5	130	
7	15	210	

T A B L E 16(Contd.)

Rates of Reaction of $Mn_2(CO)_{10}$ with Br_2 under various conditions, using Cyclohexane as solvent.

Ref. No.	$[Br_2]_0$	$R_{\frac{1}{2}}$*	Conditions
		Temp. = 50.9 - 51.2°C	
F 1	7.0	160	
2	8.0	180	$[Benzene] = 2.3 \times 10^{-3}M$
3	7.5	28	$[EtOH] = 3.5 \times 10^{-3}M$
4	6.0	6.3	$[EtOH] = 1.4 \times 10^{-2}M$

* $R_{\frac{1}{2}} = -d[Mn_2(CO)_{10}]/dt$ at 50% reaction.

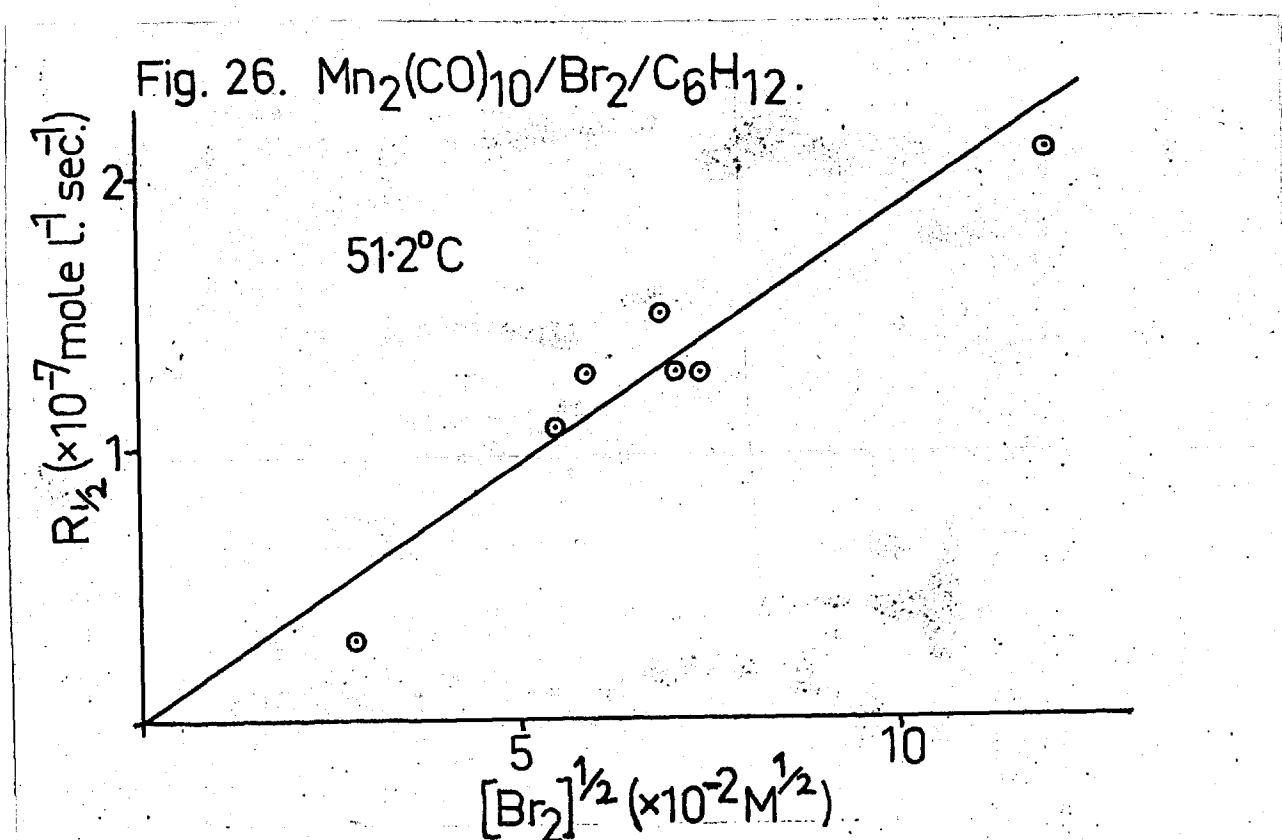

Fig. 27. $Mn_2(CO)_{10}/Br_2/C_6H_{12}$.

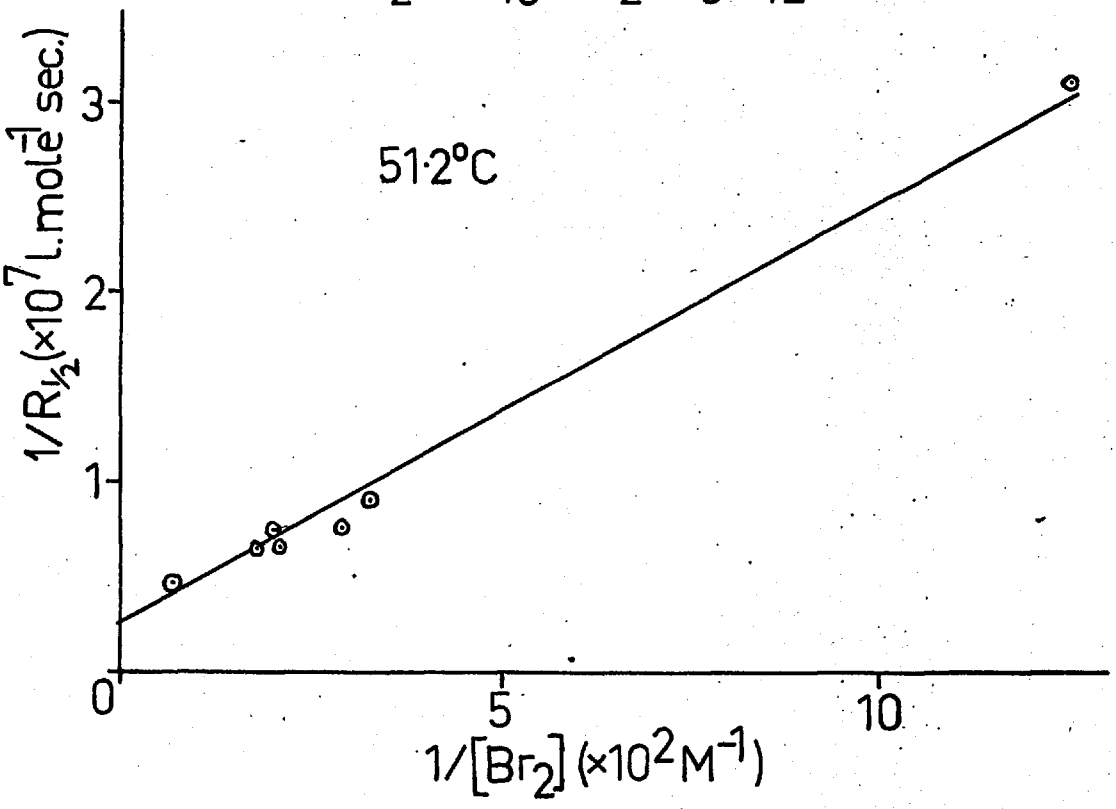

Fig. 28. Br_2/C_6H_{12}.

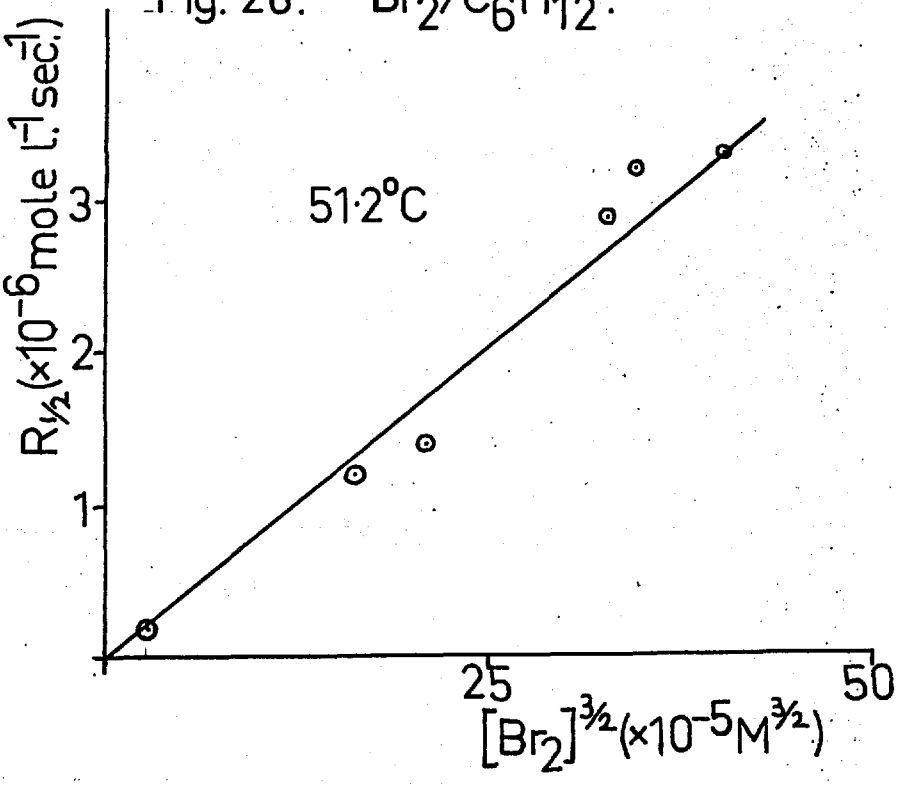

data quite likely precludes this.

At the completion of the $Mn_2(CO)_{10}$ reaction with Br_2 there was no detectable reaction of Br_2 with the solvent as measured by the absorbance of the 420 mμ peak. However a reaction rate of Br_2 with cyclohexane comparable of that with $Mn_2(CO)_{10}$ would have been undetectable. Sigmoid rate plots of the decrease in $[Br_2]$ were obtained subsequent to the completion of the $Mn_2(CO)_{10}$ reaction and the rates at 50% reaction ($R_{\frac{1}{2}}$) are given in Table 17 from the Run Series E.

TABLE 17

Rates of Reaction of Br_2 with Cyclohexane Subsequent to Completion of the Reaction with $Mn_2(CO)_{10}$ (Run Series E, Table 16)

$[Mn(CO)_5Br] \simeq 10^{-4}M$; Temp = 51.2°C

Ref. No.	1	2	3	4	5	6
$[Br_2]$ ($X10^{-3}M$)	0.8	3.0	3.5	4.8	5.0	5.5
$R_{\frac{1}{2}}^{*}$ ($X10^{-6}$ mole $l.^{-1}$ $sec.^{-1}$)	0.2	1.2	1.4	2.9	3.2	3.3

$^{*}R_{\frac{1}{2}} = -d[Br_2]/dt$ at 50% reaction

HBr was evolved during the reaction. The dependence of $R_{\frac{1}{2}}$ on $[Br_2]_o$ can be expressed as $R_{\frac{1}{2}} \simeq k[Br_2]_o^{3/2}$ as shown in Fig 28, with $k = 8.0 \times 10^{-3}$ $mole^{-\frac{1}{2}}$ $l.^{\frac{1}{2}}$ sec^{-1}.

The sigmoid nature of most of the $[Mn_2(CO)_{10}]$ rate plots suggested the possibility of autocatalytic phenomena

and so the effect of addition of various products was examined as well as of other changes in the conditions. These results are listed in Table 18.

Runs 1 to 4 show again the rather low level of reproducibility obtained in the absence of additives. Correcting for differences in $[Br_2]$ according to the square root dependence we have $R_{\frac{1}{2}}$ values from these runs (at $[Br_2]$ = 5.0×10^{-3}M) of 2.7, 1.8, 1.1 and 1.6×10^{-8} mole $l.^{-1}sec.^{-1}$ with a mean value of $(1.8 \pm 0.4) \times 10^{-8}$ mole $l.^{-1}sec.^{-1}$. An identical value is obtained by correcting the $R_{\frac{1}{2}}$ values according to a first-order dependence on $[Br_2]$. The induction period, if it may be called without begging the question of the mechanism, is 43, 37, 55, and 25 min., respectively, when measured by the time taken to reach 50% reaction. In spite of this imprecision, the effect, or lack of it, of changing the conditions are quite detectable. Thus $Mn(CO)_5Br$ (Run 10), $C_6H_{11}Br$ (Run 11; purity of sample not known), and a solution of $Mn_2(CO)_{10}$ made up 15 days previously (Run 12), all extend the induction period by factors of 2 to 5 and the reactions were not followed further. On the other hand, Run 6 which contained some of the completely reacted, reaction mixture from Run 1 (so that $[Mn(CO)_5Br] \simeq 10^{-6}$M and $[C_6H_{11}Br] \simeq 10^{-4}$M) reduced the induction period to about 5 min. and roughly doubled the value of $R_{\frac{1}{2}}$. Addition of the product of the Br_2/cyclohexane reaction (so that $[C_6H_{11}Br] \simeq 10^{-4}$M) cut the induction period even more (to 2 min.) but the subsequent rate was unaffected (Run 7). Neither HBr or Et_4NBr had any noticable effect (Runs 8 and 9).

TABLE 18

Further Rates of Reaction of $Mn_2(CO)_{10}$ with Br_2 under various conditions, using Cyclohexane as solvent

$$[Mn_2(CO)_{10}]_0 \simeq 5.0 \times 10^{-5}M$$

Temp. = 40.0°C

Ref. No.	$[Br_2]_0$ ($\times 10^{-3}$M)	$R_{\frac{1}{2}}^{1}$* ($\times 10^{-8}$ moles $l.^{-1}$ $sec.^{-1}$)	Induction Period** (min.)	Conditions
1	4.0	2.4	43	
2	5.0	1.8	37	
3	5.5	1.2	55	
4	5.5	1.7	25	
5	5.0	-	> 40	20 min exposure to room light before start of reaction
6	5.0	3.9	5	1% of completely reacted soln. 1. present.
7	5.0	2.2	2	1% of completely reacted Br_2 (10^{-2}M)/c-hexane soln. present.
8	5.5	1.6	23	1% of satd. HBr soln present.
9	5.5	1.8	42	1% of satd. Et_4NBr soln. present.
10	5.0	-	> 104	$[Mn(CO)_5Br] \simeq 10^{-5}$M.
11	5.0	-	> 90	$[C_6H_{11}Br] \simeq 10^{-4}$M.
12	5.0	-	> 216	15 days old soln.

* $R_{\frac{1}{2}}^{1} = -d[Mn_2(CO)_{10}]/dt$ at 50% reaction; ** Induction period defined as time taken for 10% reaction.

Irradiation of the $Mn_2(CO)_{10}$ solution with room light, prior to the start of the reaction, did not remove the induction period (Run 5). To illustrate some of the above points, the rate plots of some of the runs are shown in Fig 29.

It was proposed to study the thermal reaction of Br_2 with cyclohexane but at 50°C no reaction was observed over a period of 3 hours. The reaction was, however, fast, of the order of a few minutes, on exposure to room light.

(a) Inhibition by Ethanol

Some initial runs at 60°C with $[Mn_2(CO)_{10}] = 5.0 \times 10^{-5}$M, $[Br_2] \simeq 6.5 \times 10^{-3}$M and $[EtOH] = 6.0 \times 10^{-2}$M showed that the reaction consisted of two distinct parts such that an initial fast reaction over about 30% reaction was followed by a reaction, of logarithmic decrease of $[Mn_2(CO)_{10}]$, which was about a factor of 5 slower. A comparable run, conducted with complete exclusion of active light, showed no initial fast reaction but only a logarithmic decrease of $[Mn_2(CO)_{10}]$ from zero time. Thus it is considered that the initial fast reaction was due to irradiation of the $Mn_2(CO)_{10}$/EtOH solution by room light (<10 sec.) prior to the addition of Br_2 in the dark. The results of the above runs and some runs, carried out to attempt to determine a quantitative relationship between the extents of preirradiation and of initial fast reaction, are given in Table 19. No effects due to preirradiation of $Mn_2(CO)_{10}$/EtOH solutions were detected at 50°C.

Fig. 29. $Mn_2(CO)_{10}/Br_2/C_6H_{12}$.

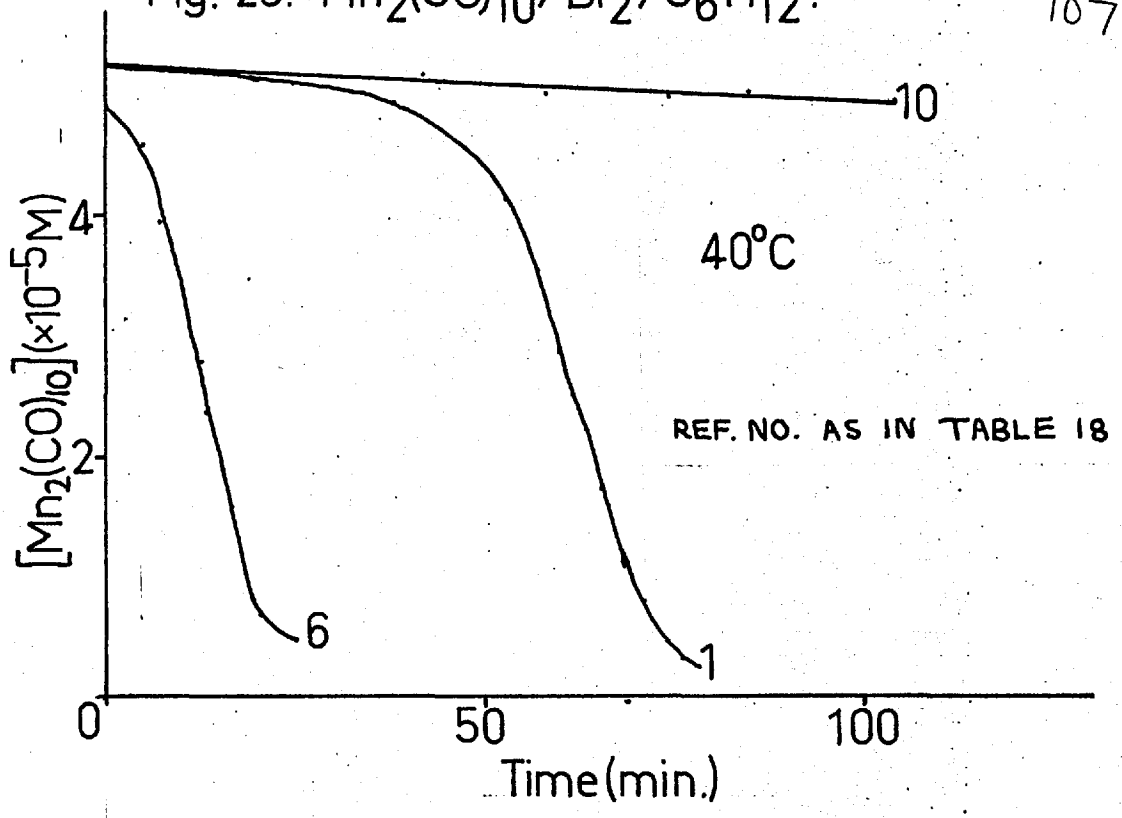

Fig. 30. $Mn_2(CO)_{10}/Br_2/CCl_4$.

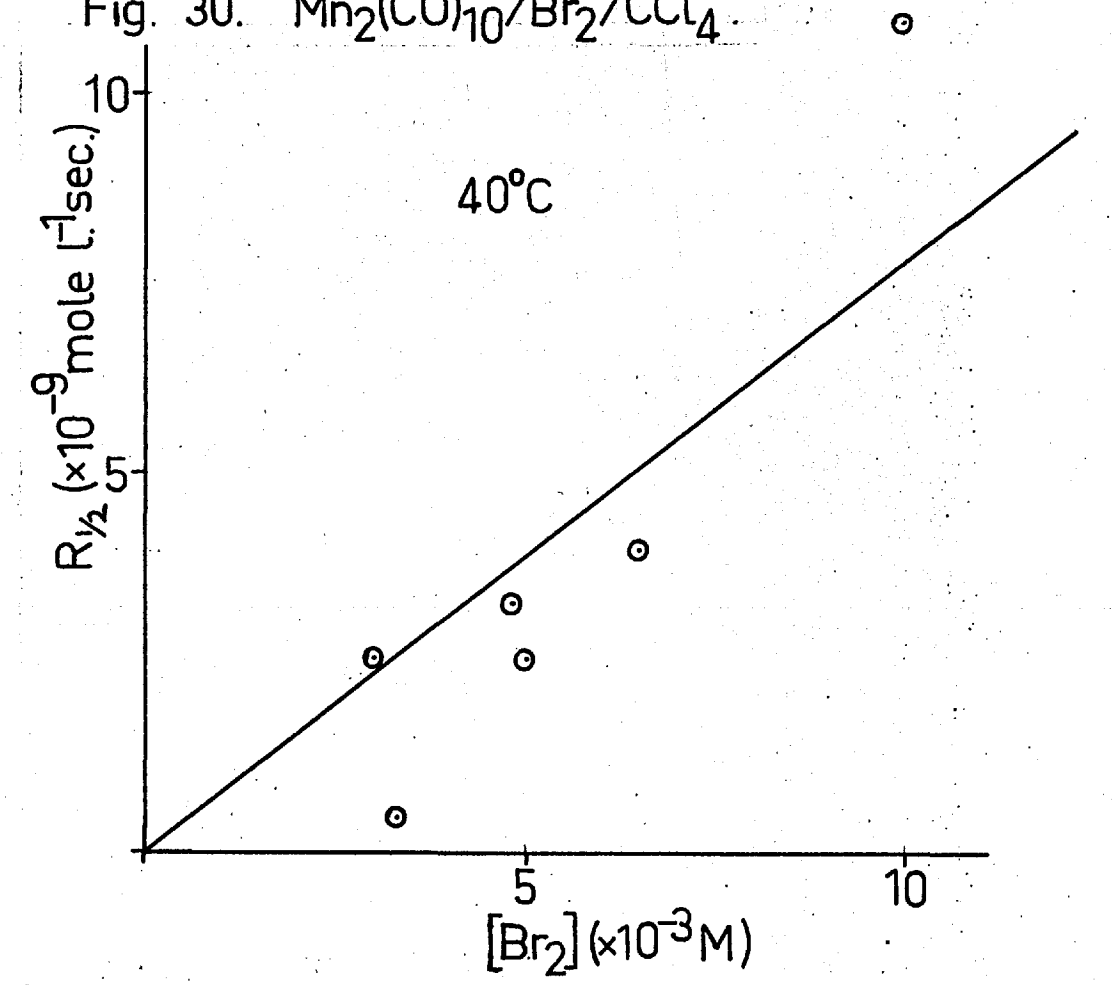

TABLE 19

Effect of Preirradiation by Room Light on the $Mn_2(CO)_{10}/Br_2$ Reaction in the Presence of EtOH

Irradiation Time (min.)	Extent of Fast Reaction (%)
0	0
? (10 sec)	12, 26, 31, 32, 36
1	12, 20
2	0
5	8

A series of runs were then carried out at 50 and 60°C, with complete exclusion of active light, at approximately constant $[Mn_2(CO)_{10}]$ ($\simeq 5.0 \times 10^{-5}$M) and $[Br_2]$ ($\simeq 7 \times 10^{-3}$M) to determine the dependency of the reaction on [EtOH]. The results are given in Table 20. All the runs, at sufficiently high [EtOH] (6.0×10^{-4}M) to exhibit inhibition, gave logarithmic rate plots of $[Mn_2(CO)_{10}]$. Thus first-order rate constants, k_{obs}, are given in addition to $R_{\frac{1}{2}}$ in Table 20. The runs at 60°C were quite reproducible, for example correcting for differences in $[Br_2]$, assumming a first-order dependence, gives the following mean values for k_{obs} at $[Br_2]$ of 7.0×10^{-3}M:-

At [EtOH] = 6.0×10^{-3}M, $k_{obs} = 7.0 \pm 0.1 \times 10^{-4}$ sec.$^{-1}$

At [EtOH] = 6.0×10^{-2}M, $k_{obs} = 6.9 \pm 0.3 \times 10^{-5}$ sec.$^{-1}$

Thus k_{obs} is inversely proportional to [EtOH] with a value of k of $4.2 \pm 0.2 \times 10^{-6}$ mole l.$^{-1}$ sec.$^{-1}$ from the

TABLE 20

Rates of Reaction of $Mn_2(CO)_{10}$ with Br_2 in the Presence of Ethanol, using Cyclohexane as solvent.

$[Mn_2(CO)_{10}]_0$ ($\times 10^{-5}$M)	$[Br_2]_0$ ($\times 10^{-3}$M)	[EtOH] (M)	k_{obs} ($sec.^{-1}$)	R_2^1* (moles $l.^{-1}$ $sec.^{-1}$)
		Temp. = 50.0°C.		
4.2	6.5	-	-	1.2×10^{-7}
4.7	6.5	-	-	1.1×10^{-7}
4.2	6.5	1.4×10^{-6}	-	7.9×10^{-8}
4.2	6.5	7.0×10^{-6}	-	1.2×10^{-7}
4.7	6.5	6.0×10^{-4}	6.0×10^{-4}	2.2×10^{-8}
4.7	6.5	1.5×10^{-3}	7.5×10^{-5}	1.4×10^{-9}
4.7	6.5	6.0×10^{-3}	8.9×10^{-5}	1.6×10^{-9}
5.1	6.5	6.0×10^{-3}	2.0×10^{-4}	4.4×10^{-9}
4.7	6.5	6.0×10^{-2}	7×10^{-6}	-
		Temp. = 60.0°C		
5.2	7.0	-	-	5×10^{-7}
5.2	6.5	-	-	4×10^{-7}
5.0	5.7	6.0×10^{-3}	5.6×10^{-4}	-
5.2	7.0	6.0×10^{-3}	7.1×10^{-4}	1.3×10^{-8}
5.2	7.4	6.0×10^{-2}	7.6×10^{-5}	1.8×10^{-9}
5.0	7.0	6.0×10^{-2}	7.2×10^{-5}	1.2×10^{-9}
4.9	7.0	6.0×10^{-2}	6.4×10^{-5}	-

equation $k_{obs} = k/[EtOH]$. Unfortunately the data at 50°C is very scattered although the general trend of decreasing rates with increasing $[EtOH]$ is shown.

(b) Catalysis by Benzoyl Peroxide

The results are reported in Section VI but it is convenient to mention here that on increasing benzoyl peroxide concentration the induction period was systematically reduced whilst $R_{\frac{1}{2}}$ was largely unchanged.

(2) THE REACTION IN CCl_4

The results are given in Table 21 with $[Mn_2(CO)_{10}] \simeq 5 \times 10^{-5}$M under various conditions with $R_{\frac{1}{2}}$ as a comperative parameter. The results are rather less reproducable than in cyclohexane. $R_{\frac{1}{2}}$ is very approximately first-order dependent on $[Br_2]$ as shown in Fig 30 for the runs at 40°C.

O_2 appears to have no effect on the reaction as shown by Runs F1-3; the values of $R_{\frac{1}{2}}$ obtained for the reactions under atmospheres of O_2, air, and N_2 lie within the deviation of the overall data.

Benzoyl peroxide (Run C2) has a very pronounced catalytic effect and the results of a systematic study of this reaction are given in Section VI.

Other effects to be noted are the catalysis by I_2, the inhibition by hydroquinone and the negligible effects of metadinitrobenzene and tetraphenyl tin.

Most of these runs gave sigmoid rate plots of $[Mn_2(CO)_{10}]$ and all the $Mn_2(CO)_{10}$ solutions were irradiated by room light for about 10 sec. prior to the addition of Br_2 in the dark.

TABLE 21

Rates of Reaction of $Mn_2(CO)_{10}$ with Br_2 under various conditions, using Carbon Tetrachloride as solvent.

$$\left[Mn_2(CO)_{10}\right]_0 \simeq 5.0 \times 10^{-5}M$$

Ref. No.	$[Br_2]_0$ ($\times 10^{-3}M$)	$R_{\frac{1}{2}}^{1}$* ($\times 10^{-9}$ moles $l^{-1}sec^{-1}$)	Conditions
		Temp. = 39.8 - 40.2°C.	
A 1	3.3	0.5	
2	6.5	4.0	
B 1	3.0	2.6	
2	4.8	3.3	N_2
3	10	11	N_2
C 1	5.0	2.6	N_2
2	5.5	220	N_2 $[(PhCOO)_2] = 10^{-2}M$
D 1	3.0	39	N_2 $[I_2] = 10^{-3}M$
2	10	4.4	N_2 $[Ph_4Sn] = 10^{-3}M$
		Temp. = 51.0°C	
E 1	4.0	46	N_2
2	4.3	38	N_2
3	7.1	120	N_2
4	5.3	2.6	N_2 [Hydroquinone] $=10^{-3}M$
5	4.7	260	N_2 $[I_2] = 10^{-3}M$

TABLE 21 (Contd.)

Rates of Reaction of $Mn_2(CO)_{10}$ with Br_2 under various conditions, using Carbon Tetrachloride as solvent.

Ref. No.	$[Br_2]_0$ ($\times 10^{-3}$M)	$R_{\frac{1}{2}}$* ($\times 10^{-9}$ moles l^{-1} sec^{-1})	Conditions
		Temp. = 51.0°C. (Contd.)	
F 1	3.1	18	
2	4.7	17	O_2
3	4.5	22	N_2
4	5.3	22	N_2
G 1	4.0	17	N_2
2	4.9	42	N_2 [m-dinitrobenzene]=10^{-3}M
3	4.0	88	N_2

* $R_{\frac{1}{2}} = -d[Mn_2(CO)_{10}]/dt$ at 50% reaction.

A later preliminary study of the effect of this preirradiation showed that no induction periods were observed when all operations were carried out in inactive light. The rate plots were of logarithmic or square-root type except that deviations from either analysis of the data were observed which were consistent with progressive inhibition of the reaction. As it appeared likely that this effect was due to autoinhibition by the product, two preliminary runs ($[Mn_2(CO)_{10}] = 5.0 \times 10^{-5}M$, $[Br_2] \simeq 7.0 \times 10^{-3}M$) were done at 40 and 50°C in the presence of $[Mn(CO)_5Br]$ of $10^{-3}M$. The runs were first-order in $[Mn_2(CO)_{10}]$ i.e. a logarithmic decrease of $[Mn_2(CO)_{10}]$ was observed, with rate constants of:

At 40.0°C $k_{obs} = 5 \times 10^{-5}$ sec.$^{-1}$ ($R_{\frac{1}{2}} = 1 \times 10^{-9}$ mole l^{-1} sec^{-1})

At 50.0°C $k_{obs} = 1.3 \times 10^{-4}$ sec^{-1} ($R_{\frac{1}{2}} = 3.2 \times 10^{-9}$ mole l^{-1} sec^{-1})

Further work is necessary to establish the rate dependence on $[Mn(CO)_5Br]$ and to firmly establish the autoinhibitory effect of $Mn(CO)_5Br$ produced during a reaction.

(3) THE REACTION IN $CF_2Cl.CFCl_2$

Some runs were carried out in the solvent (B.P. = 48°C) with $[Mn_2(CO)_{10}] = 5.0 \times 10^{-5}M$ at 40°C under various conditions. Linear rate plots of the decrease of $[Mn_2(CO)_{10}]$ were obtained and the zero-order rate constants (k_o) are given in Table 22.

TABLE 22

Rates of Reaction of $Mn_2(CO)_{10}$ with Br_2 under various conditions, using $CF_2Cl.CFCl_2$ as Solvent

$[Mn_2(CO)_{10}]$ = 5.0 X 10^{-5}M: Temp = 40.0°C

$[Br_2]$ (X10^{-3}M)	Conditions	k_o(X10^{-10}mole $l.^{-1}$ $sec.^{-1}$
7.1	-	4.3
7.1	[c-hexane] = 10^{-3}M	8.1
5.7	$[CCl_4]$ = 10^{-3}M	10.5
7.1	$[(PhCOO)_2]$ = 10^{-3}M	55
6.4	$[Mn(CO)_5Br]$ = 10^{-3}M	v.slow

The rate in the absence of additives is about 10 times slower than $R_{\frac{1}{2}}$ of the reactions in cyclohexane and CCl_4 at comparable $[Br_2]$. Benzoyl peroxide, cyclohexane, and CCl_4 catalysed the reaction with benzoyl peroxide being about 5 times as effective as the others. $[Mn(CO)_5Br]$ of 10^{-3}M not only effectively inhibited the thermal reaction but also inhibited the photochemical reaction. Irradiation by room light for 2 min. produced no detectable reaction whereas a 10 sec. period of irradiation caused about 20% reaction in the absence of $Mn(CO)_5Br$.

(D) DISCUSSION

The $Mn_2(CO)_{10}$ reaction with Br_2 is evidently a free-

radical chain reaction involving bromine atoms as evidenced by its catalysis by light and benzoyl peroxide and its inhibition by ethanol and hydroquinone (106(a)). Acceleration by light strongly indicates that a radical process is occurring and in addition benzoyl peroxide is a well known source of PhCOO radicals formed by homolytic thermal cleavage (106(b)).

However these catalytic processes cannot prove that a radical reaction is occurring in their absence, but inhibition by ethanol and hydroquinone is convincing evidence that the thermal reaction is of radical chain type. Such compounds inhibit this type of reaction by readily reacting with one or more of the radicals which propagate the chain to yield other unreactive radicals.

Accepting this, it is obvious that the chain propagating steps must be:

$$A_2 + B \xrightarrow{k_4} AB + A$$

and $$A + B_2 \xrightarrow{k_5} AB + B$$

(where A $\equiv$ $Mn(CO)_5$, B $\equiv$ Br)

The possible chain terminating steps are:

$$2A \xrightarrow{k_6} A_2$$

$$A + B \xrightarrow{k_7} AB$$

$$2B + M \xrightarrow{k_8} B_2 + M$$

A third-body, M, is necessary in atom recombinations to effect energy transfer otherwise the first molecular vibration will lead to dissociation. However account of third-body concentrations is not necessary in solution as the solvent molecules are always available for energy transfer. The cage effect, discussed previously in Section IV, facilitates radical recombination in solution by lengthening encounter times as compared with the gas phase(99)

Radical-radical reactions are generally so fast as to be diffusion-controlled in liquids i.e. reaction occurs at every encounter. The rate constants for such reactions are given by the Debye equation (99):

$$k = \frac{4RT}{10^3\eta}$$ (where η is the viscosity of the solvent)

For example, this equation applied to the recombination of iodine atoms in CCl_4 at 25°C predicts a value of k of 1.1×10^{10} l. mole^{-1} sec.$^{-1}$ which is in good agreement with the experimental value of 7×10^9 l. mole^{-1} sec.$^{-1}$ (99). The theory is also in accord with data from the quenching of fluorescence and the mutual termination reactions of a variety of polymeric radicals in several solvents (99). However, apart from the iodine case, there is a paucity of data on simple radical recombinations in solution. The only other reported instance is the recombination of trichloromethyl radicals in cyclohexane in which the observed rate constant at 30°C, 5×10^7 l. mole^{-1} sec.$^{-1}$, is a factor of 240 slower than the predicted value (99).

In the present instance we can reasonable assume that bromine atom recombination (k_8) is diffusion controlled with the other possible termination steps being slower. In Section IV we postulated that recombination of $Mn(CO)_5$ radicals involves an activation energy of about 20 Kcal/mole due to a re-arrangement energy of about 10 Kcal/mole per $Mn(CO)_5$ radical. Thus the relationship between the termination step rate constants is:

$$k_8 > k_7 > k_6$$

It will later be shown that the chain lengths in the reaction are long so that the rate of formation of $Mn(CO)_5Br$ is given by:

$$d[AB]/dt = R = k_4[A_2][B] + k_5[A][B_2]$$

and thus $k_4[A_2][B] = k_5[A][B_2]$

$$\frac{[B]}{[A]} = \frac{k_5[B_2]}{k_4[A_2]} \simeq 100k_5/k_4$$

(in most of the reactions $[A_2] \simeq 5 \times 10^{-5}M$, $[B_2] \simeq 5\text{-}7 \times 10^{-3}M$)

We will now determine the criteria for the termination processes which will predominate under various ratios of k_4 and k_5

(1) CRITERIA FOR PREDOMINANT TERMINATING STEP

(a) $k_4 = k_5$

$$[B] = 100[A]$$

$$\therefore R_6 = k_6[A]^2$$

$$R_7 = k_7[A][B] = k_7 100\,[A]^2$$

and $$R_8 = k_8[B]^2 = k_8 10^4[A]^2$$

(where $R_6 = d[A_2]/dt$, etc.)

Thus as $k_8 > k_7 > k_6$

then $R_8 \gg R_7 \gg R_6$

Therefore bromine atoms recombination is the terminating step in this case and also when $k_5 > k_4$.

(b) $k_4 = 100\,k_5$

$[B] = [A]$

and so $R_8 > R_7 > R_6$ $(R_8/k_8 = R_7/k_7 = R_6/k_6)$

(c) $k_4 = 10^4 k_5$

$[A] = 100\,[B]$

$R_6 = k_6 10^4 [B]^2$; $R_7 = k_7 100\,[B]^2$; $R_8 = k_8[B]^2$

$\therefore R_8 < R_7 < R_6$ unless $k_8 \geq 10^4 k_6$ and $k_7 \geq 100 k_6$

Thus $Mn(CO)_5$ recombination is the terminating step when $k_4 \gg k_5$ but the crossover point from bromine atom recombination is dependent on k_8/k_6. It is also possible for the $Mn(CO)_5$ reaction with Br to be the exclusive termination step when $k_4 \gg k_5$ if $k_8 > k_7 \gg k_6$.

In summary, Steps 6 and 7 can only terminate when $k_4 \gg k_5$, under other conditions Step 8 will terminate.

(2) INITIATION STEP AND RATE EQUATIONS

There are two possible initiation steps for the reaction:

$$A_2 \underset{k_{-1}}{\overset{k_1}{\rightleftharpoons}} (A \,.\, A) \xrightarrow{k_{diff}} 2\,A$$

$$B_2 \underset{k'_{-1}}{\overset{k'_1}{\rightleftharpoons}} (B \,.\, B) \xrightarrow{k'_{diff}} 2\,B$$

where the first stage is the formation of a caged radical pair and the second is the separation of the pair by diffusion. Either the radical pair or the separated species can initiate the reaction. The data discussed in Section IV show that $k_1 = 6.5 \times 10^{16}\ e^{-36,600/RT}$ and that $E_{-1} \simeq 20$ Kcal/mole. The gas-phase reaction of H_2 and Br_2 gives a value of $k'_1 \simeq 10^{13}\ e^{-45,200/RT}$ (94(c)) and E_{-1} is about zero. The value of k'_1 is probably valid in solution because the spectra of Br_2 in the gas phase and in solution in cyclohexane, CCl_4 and $CF_2Cl.CFCl_2$ are very similar (94(a)) and thus solvation effects are negligible. Thus $k_1 \gg k'_1$ and $k_{-1} < k'_{-1}$ and so $Mn_2(CO)_{10}$ dissociation is the initiation step of the reaction. We can write the following mechanism by analogy with the high temperature reactions (Section IV) which showed that attack occured on the radical pairs:

$$(A \,.\, A) + B_2 \xrightarrow{k_2} AB + A + B$$

$$(A \,.\, A) + B_2 \xrightarrow{k_3} 2AB$$

We will assume here that $k_2 \gg k_3$ and that $k_2 [B_2] \gg k_{-1}$ so that each dissociation of a $Mn_2(CO)_{10}$ molecule leads to the initiation of two chains. The chain propagation steps are, as was previously given:

$$B + A_2 \xrightarrow{k_4} AB + A$$

$$A + B_2 \xrightarrow{k_5} AB + B$$

These elementary reactions are treated by using the Steady-State Hypothesis with each of the possible termination steps to yield the rate equations given below (the calculations are given in the appendix):

(a) If $2A \xrightarrow{k_6} A_2$ is the termination step then:

$$-d[A_2]/dt = k_5(k_1/k_6)^{\frac{1}{2}} [A_2]^{\frac{1}{2}} [B_2]$$

(b) If $A + B \xrightarrow{k_7} AB$ is the termination step then:

$$-d[A_2]/dt = (k_1 k_4 k_5/k_7)^{\frac{1}{2}} [A_2] [B_2]^{\frac{1}{2}}$$

(c) If $2B \xrightarrow{k_8} B_2$ is the termination step then:

$$-d[A_2]/dt = k_4(k_1/k_8)^{\frac{1}{2}} [A_2]^{3/2}$$

The reactions in CCl_4 and cyclohexane are characterised by an induction period which is readily accounted for in terms of a build up in radical concentrations to the steady state although it could be due to inhibition by trace impurities which are consumed. In any case only the reaction succeeding the induction period can be expected to obey rate laws derived by using a steady-state treatment. Thus $R_{\frac{1}{2}}$ is a suitable parameter measured under steady-state conditions.

Scheme (c) can be immediately ruled out as the reactions are certainly dependent on $[Br_2]$ in the concentration range used here, and so $k_4 \gg k_5$ i.e. the reaction:

$$A + B_2 \xrightarrow{k5} AB + B$$

is the rate determining step of the propagation. However at higher $[Br_2]$ ($\geq 10^{-2}$M) it is possible that bromine atom recombination can become the termination process and the data from the reaction in cyclohexane suggests that this may be so i.e. if $R_{\frac{1}{2}} = k_1 [Br_2] / (1 + k_2 [Br_2])$ (Fig 27) proves to be the rate law rather than $R_{\frac{1}{2}} = k [Br_2]^{\frac{1}{2}}$ (Fig 26).

If we assume that there is a unique termination step rather than a combination of steps then we can decide between schemes (a) and (b) according to whether the dependences on either $[Mn_2(CO)_{10}]$ or $[Br_2]$ are square-root or first-order. The data on the $[Br_2]$ dependence of the reaction is ambiguous at present (Figs 26 - 28) and can be interpreted as either half- or first-order. Accordingly the rates of decrease of $[Mn_2(CO)_{10}]$ after the induction period in the runs given in Tables 16 and 21 were analysed according to both half- and first-order dependences. Most of the runs (24 out of 31), which did not contain either catalysts or inhibitors, gave linear plots of $[Mn_2(CO)_{10}]^{\frac{1}{2}}$ versus time from which rate constants (k) were calculated ($k = \left\{ - [Mn_2(CO)_{10}]^{\frac{1}{2}} \right\}_{t_1}^{t_2}$). Using the equation $k = k' [Br_2]$

gives the following averages values of k with standard deviations:

$$k_{\text{C-hex.}}\ (40^\circ) = (1.2 \pm 0.2) \times 10^{-4}\ \text{l.}^{\frac{1}{2}}\text{mole}^{-\frac{1}{2}}\ \text{sec}^{-1}$$

$$k_{\text{C-hex.}}\ (50^\circ) = (3.8 \pm 0.4) \times 10^{-3}\ \text{l.}^{\frac{1}{2}}\text{mole}^{-\frac{1}{2}}\ \text{sec}^{-1}$$

$$k_{CCl_4}\ (40^\circ) = (0.95 \pm 0.14) \times 10^{-4}\ \text{l.}^{\frac{1}{2}}\ \text{mole}^{-\frac{1}{2}}\ \text{sec}^{-1}$$

$$k_{CCl_4}\ (50^\circ) = (1.1 \pm 0.3) \times 10^{-3}\ \text{l.}^{\frac{1}{2}}\ \text{mole}^{-\frac{1}{2}}\ \text{sec}^{-1}$$

Plots of log $[Mn_2(CO)_{10}]$ versus time gave curves so it appears that scheme (a) is the mechanism of the reaction. These conclusions are regarded as very tentative due to the irreproducibility of the systems. Although internal consistency was obtained in a run series as evidenced by the k values given, the values of $R_{\frac{1}{2}}$ in Table 16 at 40°C are about a factor of 4 lower than the average $R_{\frac{1}{2}}$ values given in Table 18 obtained under apparently the same conditions in cyclohexane.

(3) CHAIN LENGTHS AND THE ROLE OF THE SOLVENT

The rate of formation of the radical pair from $Mn_2(CO)_{10}$ is given by the relationship (Section IV):

$$R_1 = 6.5 \times 10^{16}\ e^{-36,600/RT}\ [Mn_2(CO)_{10}]$$

Therefore the rates of formation of the pair at 50% reaction

($[Mn_2(CO)_{10}]_o \simeq 5 \times 10^{-5}$M) are:

At 40°C $R_1 = 2.3 \times 10^{-14}$ mole $l.^{-1}$ $sec.^{-1}$

At 50°C $R_1 = 1.9 \times 10^{-13}$ mole $l.^{-1}$ $sec.^{-1}$

Thus using the average experimental values of $R_{\frac{1}{2}}$ (Tables 16, 18, 21 and 22) in the three solvents at $[Br_2]$ of about 7×10^{-3}M, we obtain the approximate chain lengths (L) recorded in Table 23. ($L = R_{\frac{1}{2}}/2R_1$).

TABLE 23

Chain Lengths of the $Mn_2(CO)_{10}$ Reaction with Br_2

$[Mn_2(CO)_{10}]_o \simeq 5 \times 10^{-5}$M, $[Br_2] \simeq 7 \times 10^{-3}$M

Solvent	$R_{\frac{1}{2}}$ ($\times 10^{-9}$ mole $l.^{-1}$ $sec.^{-1}$)	L
	Temp. = 40°C	
$CF_2Cl \cdot CFCl_2$	0.4	1×10^4
CCl_4	4	1×10^5
Cyclohexane	20	4×10^5
	Temp. = 50°C	
CCl_4	120	3×10^5
Cyclohexane	150	4×10^5

The chain lengths in CCl_4 and cyclohexane are very approximately constant and longer by a factor of about 20 than that in $CF_2Cl \cdot CFCl_2$. Evidently the nature of the solvent is an important factor in these reactions which has not been accounted for in the previous steady-state treatments. In cyclohexane, the following reaction occurs subsequent to the completion of the $Mn_2(CO)_{10}$ reaction:

$$Br + C_6H_{12} \longrightarrow C_6H_{11} + HBr$$

$$C_6H_{11} + Br_2 \longrightarrow C_6H_{11}Br + Br$$

This propagation mechanism was postulated for the gas phase photochemical reaction (107(a)) and in this present work the HBr evolved was detected but it was not thought necessary to identify $C_6H_{11}Br$ in the reaction mixture. Similarly in CCl_4 the following reactions can occur:

$$Br + CCl_4 \longrightarrow BrCl + CCl_3$$

$$CCl_3 + Br_2 \longrightarrow CCl_3Br + Br$$

Although these chain reactions as such cannot increase the concentration of bromine atoms at the steady-state, they can catalyse the rate of approach to it and so reduce the induction period. These considerations possible explain the lower rate in $CF_2Cl \cdot CFCl_2$, which is relatively stable to bromine atom attack (108), such that a steady-state is not attained during the course of the reaction. The fact that CCl_4 and cyclohexane catalyse the reaction is consistent with this interpretation.

(4) CATALYSIS OF THE REACTIONS

Catalysis by benzoyl peroxide and light is discussed in Sections VI and VII respectively.

(a) Cyclohexane

Runs 6 and 7 in Table 18 show that the products of the Br_2/cyclohexane reaction reduce the induction period by a factor of about 10. Run 8 showed that HBr has no effect on the reaction so the catalyst must be $C_6 H_{11} Br$. Run 11 in which the reaction was inhibited by reagent grade $C_6 H_{11} Br$ can be ignored as the purity of the sample was not ascertained. $C_6 H_{11} Br$ seems to catalyse the rate of approach to the steady state and the only mechanism which is consistent with this is initiation by the step:

$$C_6 H_{11} Br \longrightarrow C_6 H_{11} + Br$$

The bond dissociation energy of this step is not known but by analogy with other aliphatic bromides should be about 60 Kcal/mole (107(b)). This value appears to be too high to give validity to the above postulate. It would be of interest to determine if $C_6 H_{11} Br$ catalyses the thermal reaction of Br_2 with cyclohexane.

(b) $C Cl_4$

The reaction was effectively catalysed by iodine (Table 21). This must be due to the formation of IBr:

$$Br + I_2 \longrightarrow IBr + I$$

$$I + Br_2 \longrightarrow IBr + Br$$

which has a greater rate of reaction with $Mn(CO)_5$ than Br_2 (the bond dissociation energies of Br_2 and IBr are 45 and 42 respectively (107))). Thus an alternative faster path is available for the rate determining propagation step. The above chain mechanism for the formation of IBr is possibly initiated by thermal dissociation of I_2 (D = 35 Kcal/mole):

$$I_2 \longrightarrow 2I$$

The other conceivable path which is iodine atom reaction with $Mn_2(CO)_{10}$ is not likely to occur (Section IV and VI).

(5) INHIBITION OF THE REACTIONS

(a) EtOH in Cyclohexane

Although the results at 50°C were irreproducable, those at 60°C showed that the rate of reaction was inversely proportional to $[EtOH]$. Using $R_{\frac{1}{2}}$ values at 60°C at $[Br_2]$ of 7.0×10^{-3}M (Table 20) gives the following rate law:

$$R_{\frac{1}{2}} \simeq \frac{k}{1 + k'[EtOH]}$$

where $k \simeq 5 \times 10^{-7}$ mole $l.^{-1}$ $sec.^{-1}$ and $k' \simeq 6.5 \times 10^{3} M^{-1}$.

Thus the reactions are insensitive to $[EtOH]$ of less than about $10^{-4}M$ and this was shown by the reactions carried out at $50^{o}C$. Ethanol inhibits chain reactions by reacting with chain propagating radicals to form unreactive species. In this reaction it appears that inhibition must be due to reaction with bromine atoms. Preirradiation by room light (Table 19) showed that ethanol can form reactive species with fragments formed by dissociation of $Mn_2(CO)_{10}$ and these would appear to be $2Mn(CO)_5$. Thus ethanol inhibits the fast propagation step:

$$B + A_2 \xrightarrow{k_4} AB + A$$

by competing for bromine atoms with $Mn_2(CO)_{10}$. This explains the relative insensity of the reaction to low $[EtOH]$ because the rate of the reaction will not be affected until R_4 is reduced to less than R_5. When this has occurred the rates become inversely proportional to $[EtOH]$.

(b) $Mn(CO)_5Br$

$[Mn(CO)_5Br]$ of $10^{-3}M$ inhibited the reaction in all the solvents used and the later work using CCl_4 indicated that autoinhibition occurred during the reaction in the absence of initial $Mn(CO)_5Br$. Discussion of the quantitative effects of $Mn(CO)_5Br$ is not meaningful considering the paucity and irreproducability of the data to date. The most obvious way in which $Mn(CO)_5Br$ can inhibit the reaction is by reversal of Step 5:

$$A + B_2 \underset{k_{-5}}{\overset{k_5}{\rightleftharpoons}} AB + B$$

(E) SUMMARY

We have shown that the $Mn_2(CO)_{10}$ reaction with Br_2 exhibits all of the features generally considered to be disgnostic of free radical chain reactions (106(a)), i.e. catalysis by light and benzoyl peroxide and inhibition by ethanol and hydroquinone. Accepting that homolytic fission of $Mn_2(CO)_{10}$ is the initiation step of the reaction leads to values of the chain lengths at the steady state of the order of 10^5. These values partially excuses our lack of success in obtaining precise data as trace impurities can have large effects on the rates of reaction by interrupting the chain. In spite of the imprecision of the results, we show, by a steady-state treatment of the probable elementary reactions, that the termination step is either $Mn(CO)_5$ radical recombination or $Mn(CO)_5$ reaction with Br and give some evidence that the former is more likely. It follows from this that bromine atoms are much more reactive towards $Mn_2(CO)_{10}$ than $Mn(CO)_5$ radicals are towards Br_2. This is probably due to (a) the greater bond strength of Br_2 (45 Kcal/mole) as compared with the value of 37 Kcal/mole obtained for $Mn_2(CO)_{10}$ and (b) the rearrangement energy of about 10 Kcal/mole which stabilises the $Mn(CO)_5$ radical.

(VI) THE THERMAL REACTIONS OF DIMANGANESE DECACARBONYL WITH BROMINE AND IODINE CATALYSED BY BENZOYL PEROXIDE

(A) INTRODUCTION

Initial studies on the thermal bromination of $Mn_2(CO)_{10}$ using CCl_4 as solvent, showed that benzoyl peroxide was a good catalyst. A concentration of 10^{-2}M increased the rate at half-reaction by a factor of about 100 at 40°C, and a parallel I.R. study showed that the only detectable product was $Mn(CO)_5Br$ which was formed in 100% yield. No evidence for the formation of $PhCOMn(CO)_5$ or $PhMn(CO)_5$, which are the only other likely products was found.

Preliminary investigations using cyclohexane and CF_2Cl . $CFCl_2$ solutions showed that in the former case benzoyl peroxide acted mainly to reduce the induction period, the subsequent rate being largely unchanged, and in the second case the rate was increased by a factor of about 10 ($[(PhCOO)_2] = 10^{-3}$M).

In view of the marked difference in effect of benzoyl peroxide on the bromination reactions in CCl_4 and cyclohexane, it was decided to attempt a systematic study of these catalysed reactions. Further study of the reaction using CF_2Cl . $CFCl_2$ solution would also be of interest but was not done here.

It was found that the reaction of $Mn_2(CO)_{10}$ with I_2 was effectively catalysed by benzoyl peroxide at room

temperature in the light. This reaction yielded 100% $Mn(CO)_5I$ over a period of about 3 hours. The catalysed reaction in the dark was much slower but was convenient to study at 80°C and the results of some initial runs are given.

Benzoyl peroxide was found to have no effect on the $Mn_2(CO)_{10}$ reaction with PPh_3.

(B) EXPERIMENTAL

Reaction solutions were contained in 1 cm, teflon stoppered, silica cells which were thermostatted in the cell compartment of a Unicam S.P. 500 spectrometer. The general techniques are described in Section II.

In these runs, a suitable quantity of benzoyl peroxide was weighed into the cell and then dissolved in 3 ml. of a solution of $Mn_2(CO)_{10}$. In the reactions with I_2, I_2 was also weighed into the cell. The addition of $Mn(CO)_5Br$ to some of the Br_2 reaction solutions was effected either by addition of a known volume of a solution or by weighing the compound into the cell containing benzoyl peroxide. Br_2 was added to the reaction solution from a micropipette after the solution had reached thermal equilibrium by being in the thermostat block for 10 minutes. Great care was exercised to exclude active light from the solutions and all operations were carried out in the light from a red lamp.

The reactions were followed by measuring the decrease of the absorbance at 340 mμ due to $Mn_2(CO)_{10}$ at suitable time

intervals. The bromine concentrations were measured spectrophotometrically from the absorbance of the peak at about 420 mμ by using known extinction coefficients (Table 3)

(C) RESULTS

(I) THE REACTION OF $Mn_2(CO)_{10}$ WITH Br_2

(a) The Reaction in Cyclohexane Solution

The effect of varying benzoyl peroxide concentration from zero to 10^{-2}M was determined at 40°C with constant initial $[Mn_2(CO)_{10}]$ and $[Br_2]$. Sigmoid curves were obtained from plots of $[Mn_2(CO)_{10}]$ versus time, and, as with the uncatalysed thermal reaction, the rate parameter was chosen as the rate at 50% reaction ($R_{\frac{1}{2}}$), and the induction period was defined as the time taken for 10% reaction. The results are given in Table 24.

The induction periods decreased with increasing benzoyl peroxide concentration and this effect is depicted in Fig 31. The $R_{\frac{1}{2}}$ values were independent of benzoyl peroxide concentration within experimental error.

No reaction of Br_2 with the solvent was detected at the completion of the reaction with $Mn_2(CO)_{10}$ in any of the runs although about 2% reaction would not be detected.

Fig. 31. $Mn_2(CO)_{10}/Br_2/(PhCOO)_2/C$-hexane.

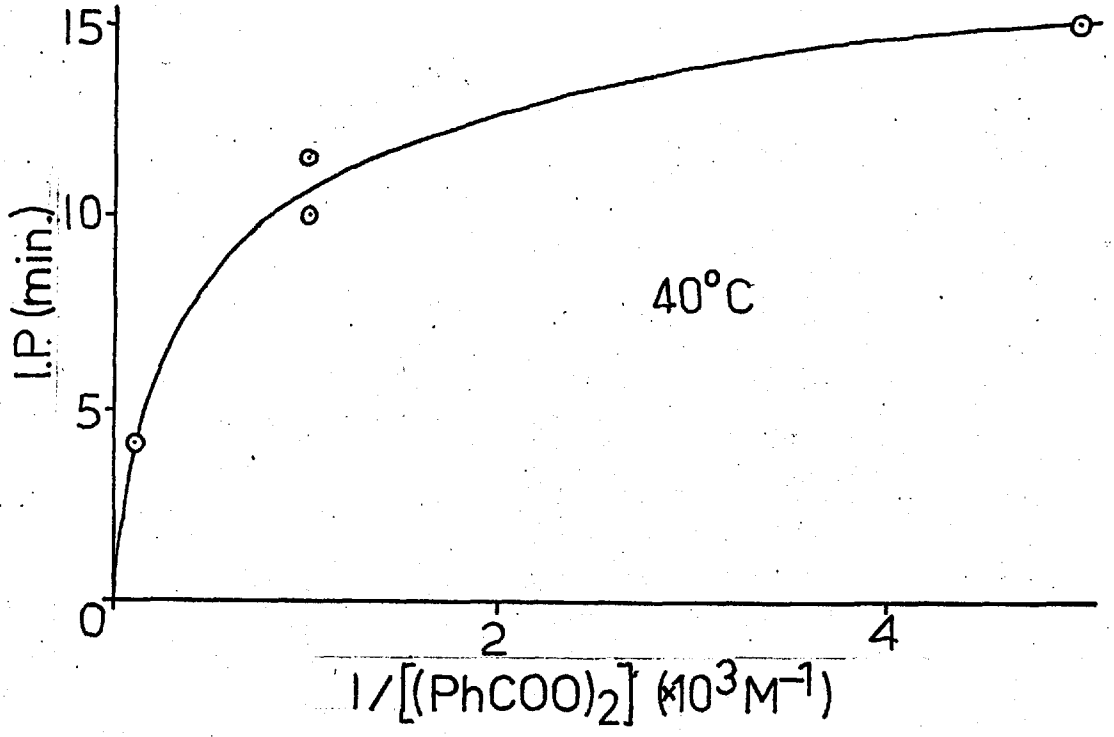

Fig. 32. $Mn_2(CO)_{10}/Br_2/(PhCOO)_2/CCl_4$.

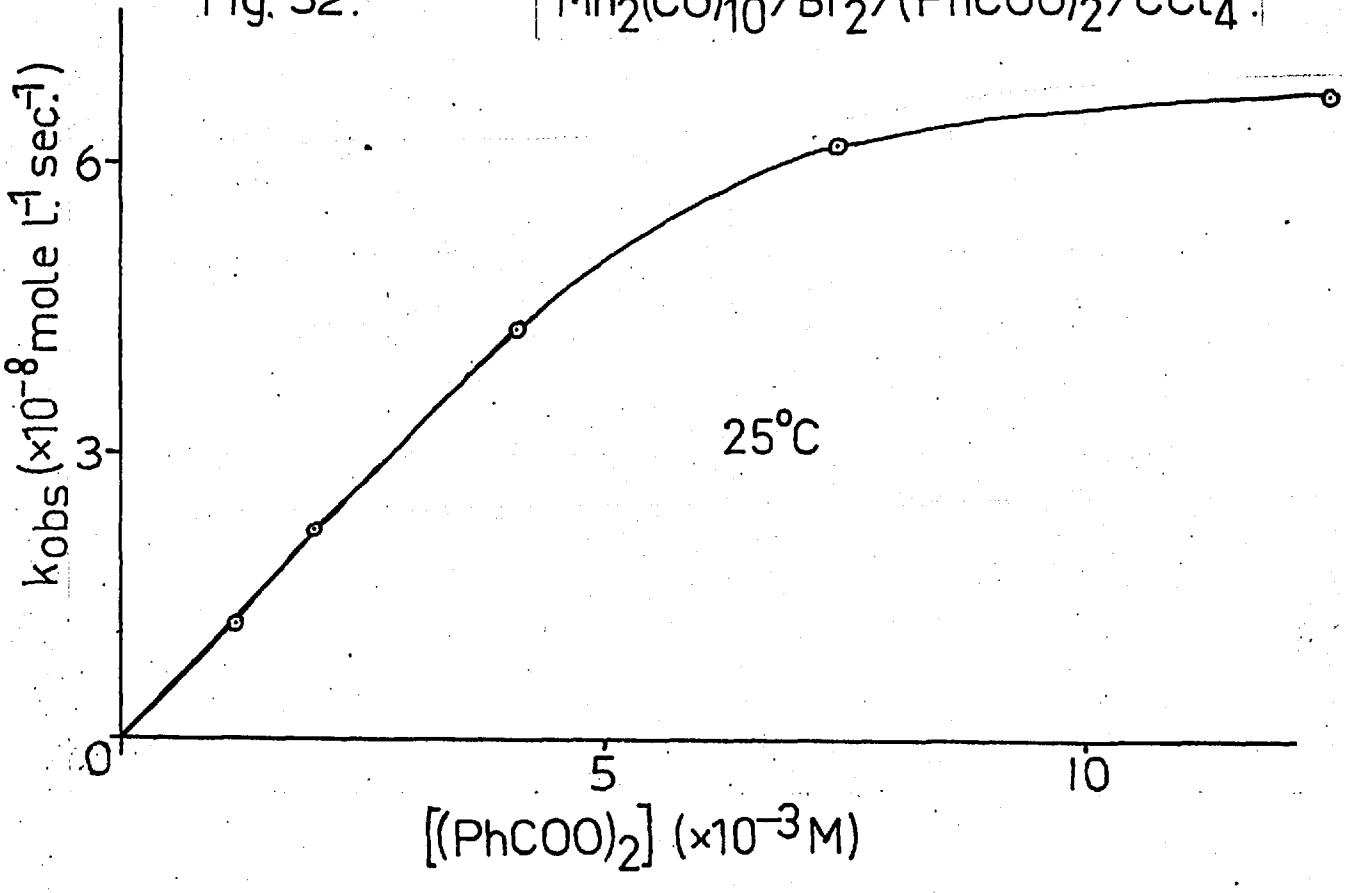

TABLE 24

THE RATES OF REACTION OF $Mn_2(CO)_{10}$ WITH Br_2 IN THE PRESENCE OF BENZOYL PEROXIDE IN CYCLOHEXANE SOLUTION

$[Mn_2(CO)_{10}] = 4.6 \times 10^{-5}M$, $[Br_2] = 6.8 \times 10^{-3}M$

Temp. = 40.0°C

$[(PhCOO)_2]$ (M)	$R_{\frac{1}{2}}$ ($\times 10^{-8}$ mole $l.^{-1}$ sec^{-1})	Induction Period (min.)
-	2.0	30
2.0×10^{-4}	2.2	15
1.0×10^{-3}	1.4	13
1.0×10^{-3}	2.0	10
1.0×10^{-2}	4.9	4

(b) The Reaction in CCl_4 Solution

Rate studies were carried out over a range of temperatures from 15 to 40°C and the dependency of the rate of reaction of $Mn_2(CO)_{10}$ on benzoyl peroxide, Br_2 and $Mn(CO)_5Br$ concentrations was determined. Sigmoid rate plots were obtained in all runs except those in which $Mn(CO)_5Br$ was present in first-order excess over the concentration of product formed, when logarithmic relationships were obtained. The sigmoid curves were essentially

linear from between 10 - 30% and up to 90% reaction and so the zero-order rate constant, k_{obs} ($k_{obs} = -d[Mn_2(CO)_{10}]/dt$) was initially used as a convenient rate parameter. The results are presented in the following sections.

(b) (i) Rate Dependence on Benzoyl Peroxide Concentration

The results are listed in Table 25 for runs carried out at constant initial $[Mn_2(CO)_{10}]$ and $[Br_2]$. The runs at 25 and 40°C show that k_{obs} is directly proportional to benzoyl peroxide concentration in the range up to 2.0×10^{-3}M, after which the increase of k_{obs} is less than first-order in benzoyl peroxide concentration (Fig 32). Thus at the lower concentrations the relationship:

$$k_{obs} = k_a[R_2] \text{ where } R_2 \equiv (PhCOO)_2 \text{ is obeyed.}$$

The runs at 25°C were used to obtain an empirical relationship of k_{obs} in terms of $[R_2]$ over the whole of the concentration range studied. It was assumed that the relationship was of the form:

$$k_{obs} = \frac{k_a[R_2]}{1 + k_b[R_2]^n}$$

where n is a half or whole integer. The values of k_{obs} from the higher concentration runs were used to calculate n which was found to be equal to 2. Theoretical curves were calculated from the expression using values of the constants given in Table 26 and well represent the data as shown in Fig 32.

TABLE 25

Rates of Reaction of $Mn_2(CO)_{10}$ with Br_2 in the Presence of Benzoyl Peroxide, using Carbon Tetrachloride as solvent.

$[Mn_2(CO)_{10}]_0 = 5.0 \times 10^{-5}$ M

Temp. (°C)	$[Br_2]$ ($\times 10^{-3}$ M)	$[(PhCOO)_2]$ ($\times 10^{-3}$ M)	I.P.* (min)	k_{obs} ($\times 10^{-8}$ moles.l.$^{-1}$ sec.$^{-1}$)
15.0	7.6	2.0	26	0.77
25.0	7.2	1.1	16	1.2
25.0	6.8	2.0	10	2.2
25.0	6.5	4.1	6	4.3
25.0	7.2	7.4	4.5	6.2
25.0	7.1	12.5	4	6.9
33.0	6.5	2.0	3	6.9
40.0	6.5	0.10		1.3
40.0	6.9	0.43		4.9
40.0	6.8	1.0		9.8
40.0	7.0	2.0		19.5
40.0	6.2	3.0		27
40.0	6.4	10.0		43

* I.P. = induction period (time taken for 10% reaction)

TABLE 26

RATE PARAMETERS USING $k_{obs} = k_a [R_2] / (1+k_b [R_2]^2)$

Temp (°C)	k_a ($X10^{-5} sec^{-1}$)	k_b ($X10^{3} M^{-2}$)
25.0	1.1	5.9
40.0	9.4	13

(b) (ii) Rate Dependence on Bromine Concentration

Runs were carried out at 25°C with constant initial $[Mn_2(CO)_{10}]$ and $[R_2]$ and various $[Br_2]$. The results are given in Table 27. $[R_2]$ of 2.0×10^{-3}M was chosen because k_{obs} is directly proportional to $[R_2]$ at this concentration.

The results are consistent with a 3/2 order in $[Br_2]$ as shown by a linear plot of k_{obs} versus $[Br_2]^{3/2}$ (Fig 33) This relationship gives an empirical rate constant of $k_c = 3.8 \times 10^{-5}$ $l.^{\frac{1}{2}}$ mole $^{-\frac{1}{2}}$ $sec.^{-1}$ from the expression:

$$k_{obs} = k_c [Br_2]^{3/2}$$

An alternative means of fitting data of order greater than 1 is by using a power series:

$k_{obs} = k' [Br_2] + k'' [Br_2]^n$ where n is a half or whole integer greater than 1. However, values of n in the range 2 to 3 were obtained and a trial and error procedure failed to yield an adequate fit of the data to the equation.

Benzoyl Peroxide Catalysis (CCl_4).

Fig. 33.

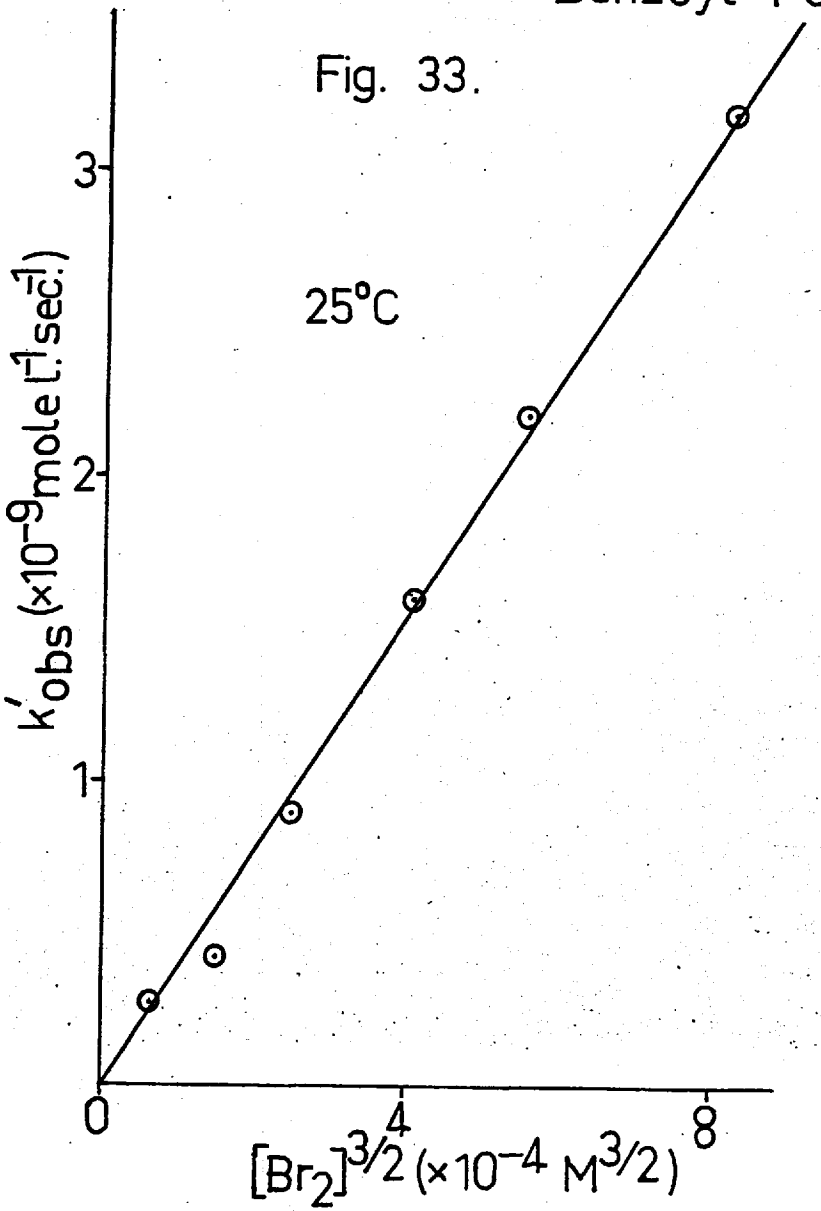

Fig. 34.

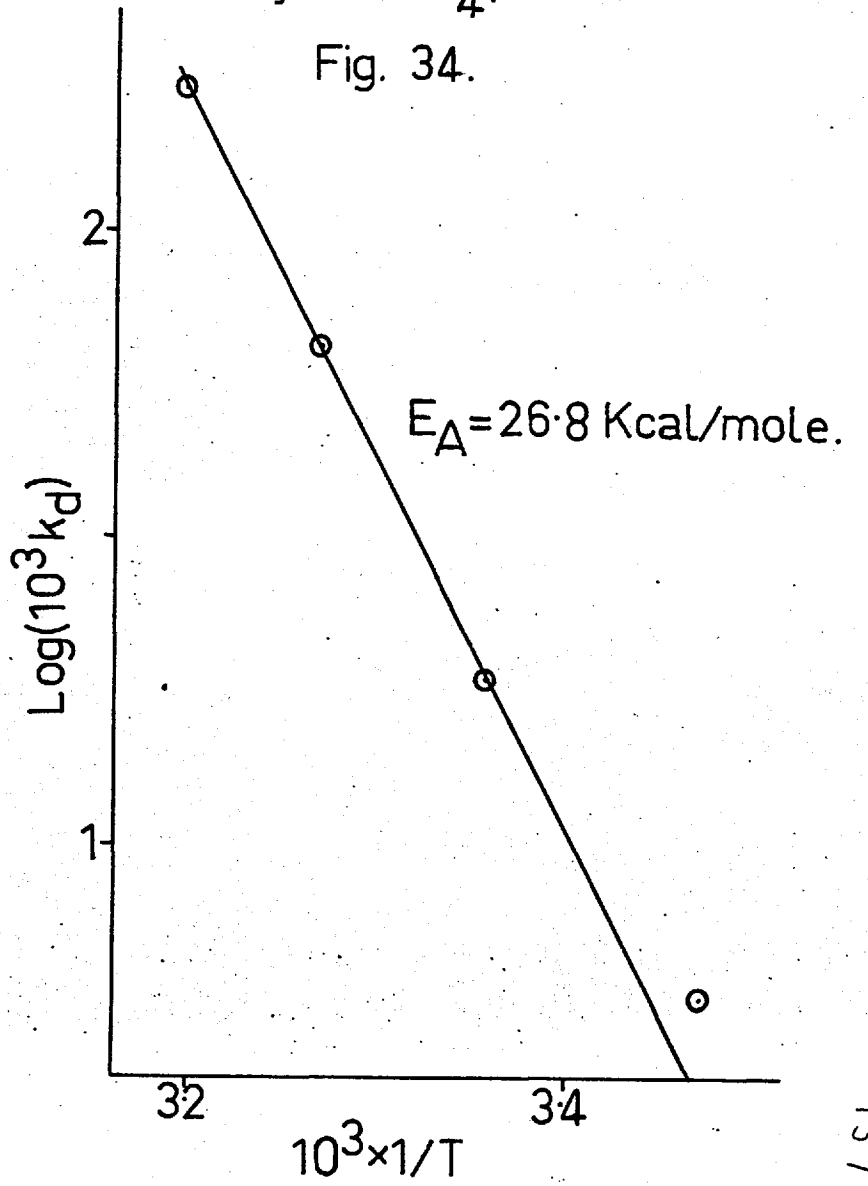

TABLE 27

The Bromine Concentration Dependence of k_{obs} from the $Mn_2(CO)_{10}$ Reaction in the Presence of Benzoyl Peroxide in CCl_4 Solution

$[Mn_2(CO)_{10}] = 5.0 \times 10^{-5}M$, $[R_2] = 2.0 \times 10^{-3}M$

Temp. = 25.0°C

$[Br_2]$ ($\times 10^{-3}M$)	k_{obs} ($\times 10^{-9}$ mole l^{-1} sec^{-1})	Induction Period* (min.)
1.6	2.7	54
2.8	4.2	30
4.0	8.9	21
5.5	16	15
6.8	22	10
8.8	32	8

* Time taken for 10% reaction

(b) (iii) Rate Dependence on Temperature

The data from runs at 25°C fits well to the empirical equation:

$$k_{obs} = \frac{k_d [R_2] [Br_2]^{3/2}}{1 + k_b [R_2]^2}$$

Thus, assuming that this relationship is valid over the temperature range 15 to 40°C, the constants given in Table 28 were calculated from the data given in Table 25.

TABLE 28

Rate Parameters Using $k_{obs} = \frac{k_d [R_2] [Br_2]^{3/2}}{1 + k_b [R_2]^2}$

Temp. (°C)	k_d ($\times 10^{-3}$ l.$^{3/2}$ sec.$^{-1}$)	k_b ($\times 10^3$ M^{-2})
15.0	5.8	
25.0	19.5	5.9
33.0	66	
40.0	170	13

Only k_d was calculated at 15 and 33°C from a single run at each temperature at $[R_2] = 2.0 \times 10^{-3}$M by assuming that $k_b [R_2]^2 \ll 1$. The values of k_d in the range 25 to 40°C excellently obey the Arrherius law (Fig 24) with an activation energy of 26.8 Kcal/mole but the value at 15°C has a deviation of 28% from the predicted value. But as k_d is probably a complex function of elementary reaction rate constants this is not surprising over this temperature range of 25°C. The values of k_b give an activation energy of about 10 Kcal/mole.

(b) (iv) Factors Influencing the Duration of the Induction Period

As stated previously, the induction period of the reaction is defined as the time taken for 10% reaction and the values are given in Tables 25 and 27. No values are given for the reactions at 40^{o} as they were all less than 1 minute.

At $25^{o}C$ the induction periods were inversely proportional to the concentrations of both benzoyl peroxide (Table 25) and bromine (Table 27) and these relationships are depicted in Figs 35 and 36 for constant $[Br_2]$ and $[R_2]$ respectively. At $[Br_2] \simeq 7 \times 10^{-3}M$ the variation of induction period (P sec) with $[R_2]$ is given by the relationship:

$$P = \frac{k_e}{[R_2]} + 160$$

where $k_e = 0.86$ mole $l.^{-1}$ sec .. Similarly at $[R_2] = 2.0 \times 10^{-3}M$ the following expression is obeyed:

$$P = \frac{k_f}{[Br_2]}$$

where $k_f = 4.9$ mole $l.^{-1}$ sec.

The variation of induction period with temperature is such that, at constant $[Br_2]$ ($\simeq 7 \times 10^{-3}M$) and $[R_2]$ ($2.0 \times 10^{-3}M$) a plot of log (I/P) versus I/T (Fig 37) over the temperature

Induction Period ($(PhCOO)_2/CCl_4$).

Fig. 35.

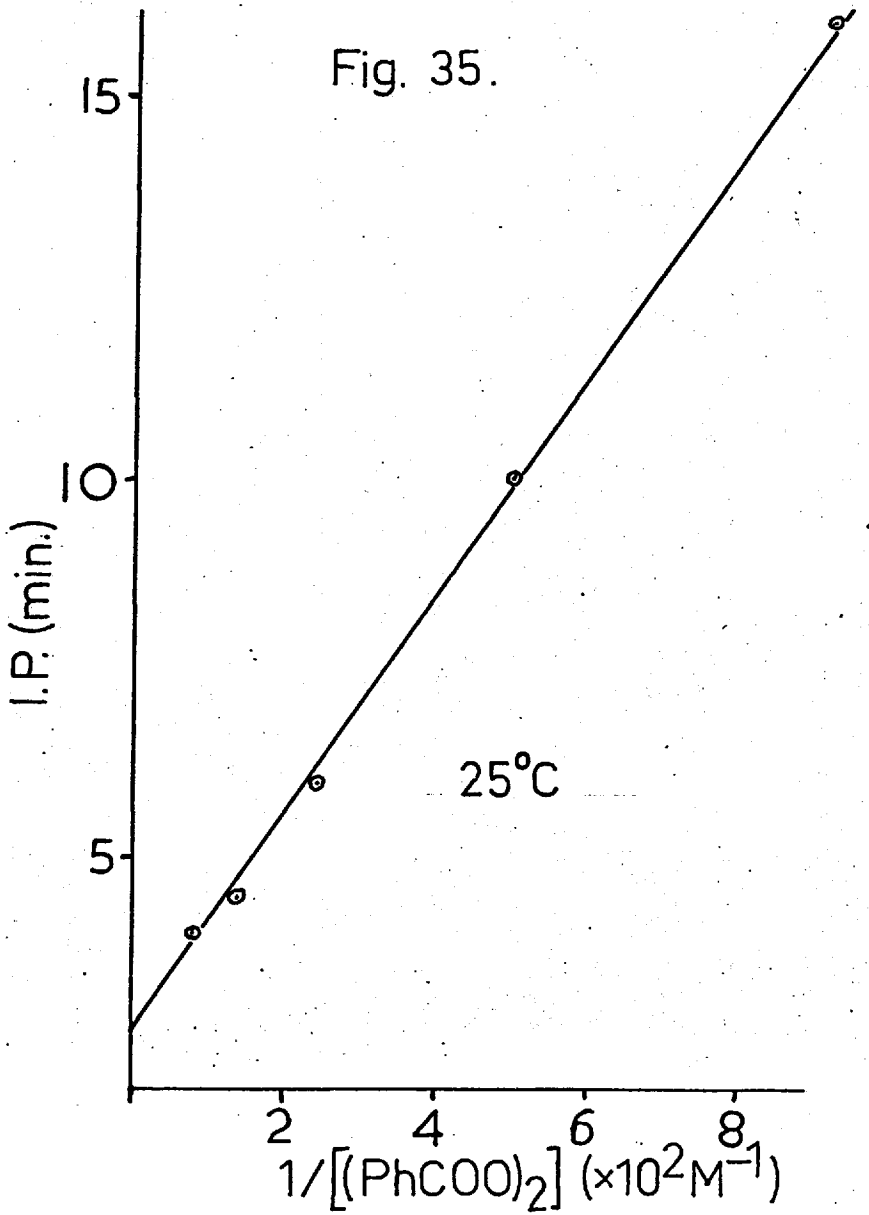

Fig. 36.

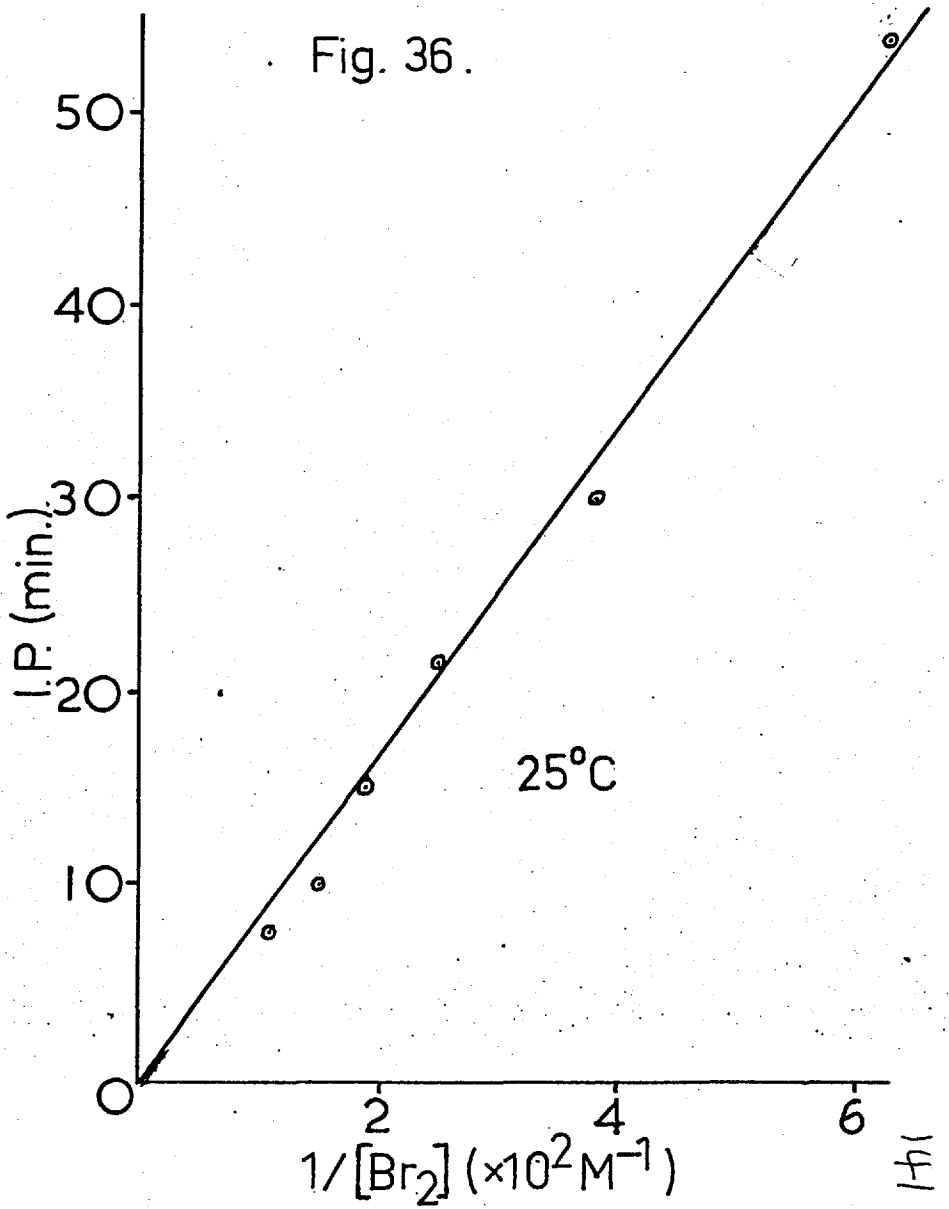

$Mn_2(CO)_{10}/Br_2/(PhCOO)_2/CCl_4$.

Fig. 37.

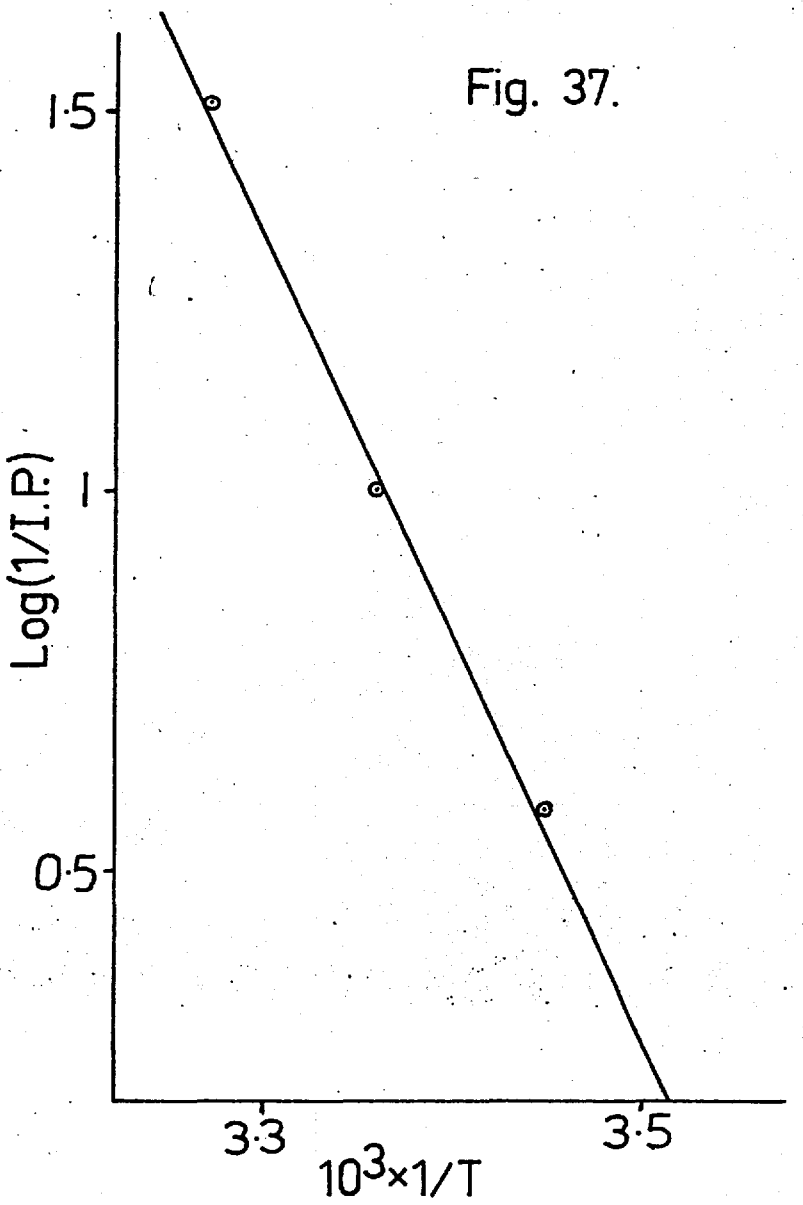

Fig. 38.

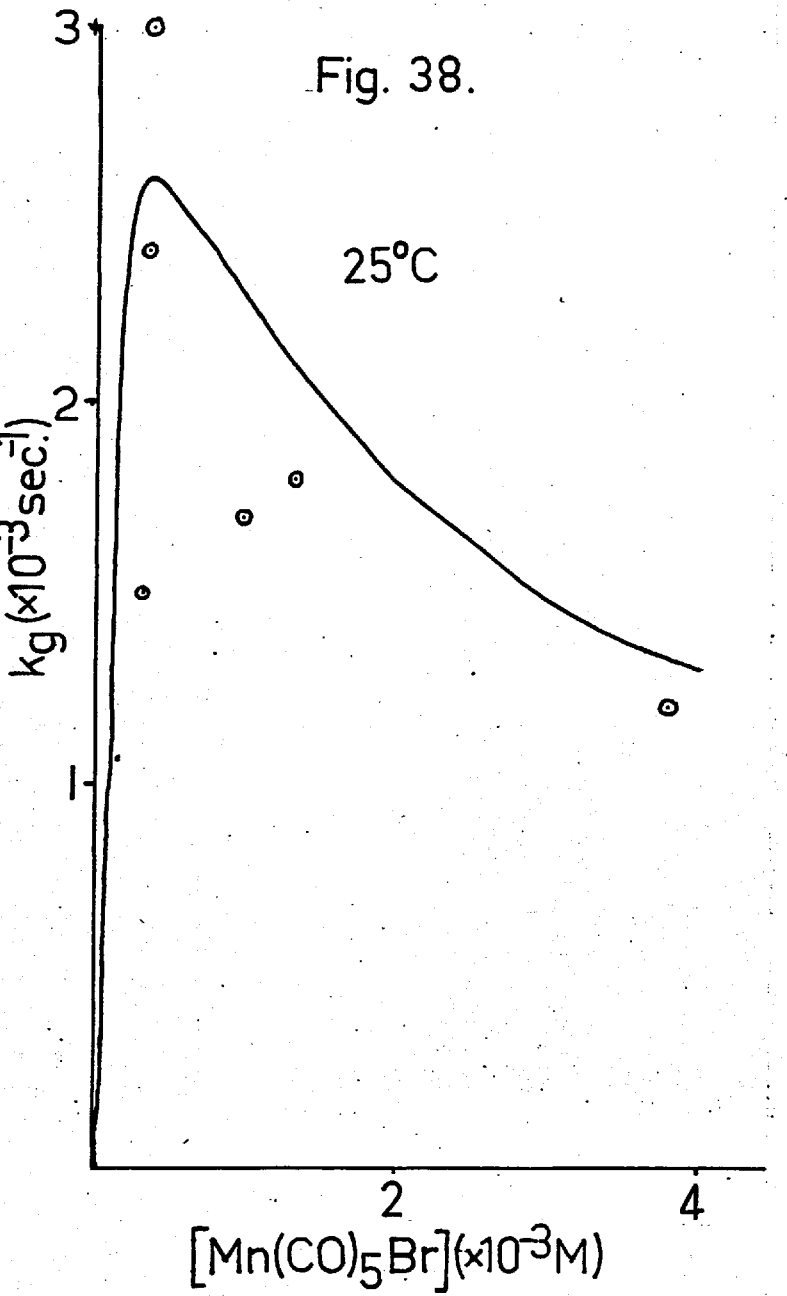

range 15 to 33°C is approximately linear giving an apparent activation energy of about 20 Kcal/mole.

(b) (v) Rate Dependence on $Mn(CO)_5Br$ Concentration

Since the previous rate plots were sigmoid the effect of added product was investigated at 25°C. Addition of $Mn(CO)_5Br$ immediately changed the rate plots to logarithmic ones, i.e. the reaction becomes first-order in $[Mn_2(CO)_{10}]$.

Some reactions carried out using a standard solution of $Mn(CO)_5Br$ showed a pronounced effect due to the age of the solution such that the first-order rate constant decreased with increasing age of the solution (1 to 12 hours) all other variables being constant. Thus the rate parameters recorded in Table 29 were determined by using reaction solutions in which the $Mn(CO)_5Br$ was dissolved in the $Mn_2(CO)_{10}$ solution 10 minutes prior to the start of the reaction.

The runs gave good linear plots of $\log [Mn_2(CO)_{10}]$ versus time except for the case in which $[Mn(CO)_5Br]$ was only in 2.8 times excess over the amount formed in the reaction. The slope of this reaction plot increased during the course of the reaction and values of the first-order rate constant (k_g) calculated from the slopes at various values of total $[Mn(CO)_5Br]$ are given in Table 29.

TABLE 29

Rate Dependence on $Mn(CO)_5Br$ Concentration

$[Mn_2(CO)_{10}] = 5.0 \times 10^{-5}M$, $[R_2] = 2.0 \times 10^{-3}M$

Temp. = 25.0°C

$[Br_2]$ ($\times 10^{-3}M$)	$[Mn(CO)_5Br]$ ($\times 10^{-4}M$) Initial	Total	k_g ($\times 10^{-3} sec^{-1}$)
		3.1	1.5
6.8	2.8	3.5	2.3
		3.8	3.0
6.5	9.7		1.7
6.5	13		1.8
6.8	38		1.2

The variation of k_g with $[Mn(CO)_5Br]$ is depicted in Fig 38 which shows that the role of $Mn(CO)_5Br$ in the reaction is complex. Evidently the compound can act both as a catalyst and an inhibitor, with the former effect being predominant at concentrations below about $4 \times 10^{-4}M$. Thus at the $[Mn(CO)_5Br]$ of $10^{-4}M$ formed during a run, it is likely that the inhibitory effect is negligible. The logarithmic plots of $[Mn_2(CO)_{10}]$ in the reactions in the presence of excess $Mn(CO)_5Br$ show that the autocatalytic reaction is first-order in $[Mn_2(CO)_{10}]$. The sigmoid rate plots from the runs at 25°C were analysed by assuming that

in the presence of excess $[Br_2]$ and $[R_2]$ the following rate law is obeyed:

$$-d[Mn_2(CO)_{10}]/dt = k_h[Mn_2(CO)_{10}][Mn(CO)_5Br]$$

The integrated form of this equation is:

$$k_h t = \frac{1}{2A_o + B_o} \ln \left\{ \frac{A_o}{B_o} \cdot \frac{(2A_o + B_o - 2A)}{A} \right\}$$

where $A = [Mn_2(CO)_{10}]$, $B = [Mn(CO)_5Br]$, and the subscript o refers to initial concentrations. (The integration is given in Appendix II). B_o is the trace amount of product initially present which is necessary for the autocatalytic reaction to occur and this obviously can be formed by the mechanism operating in the absence of benzoyl peroxide.

Rearranging the above equation gives the expression:

$$\log \frac{(2A_o + B_o - 2A)}{A} = \frac{k_h(2A_o + B_o)}{2.303} t - \log \frac{A_o}{B_o}$$

Plots of $\log (2(A_o - A)/A)$ versus time (B_o ignored as much less than A_o) were linear from about 15 to 95% of reaction and values of k_h were calculated from the gradients which are equal to $2k_hA_o/2.303$ (B_o ignored). The values of k_h together with values of B_o, calculated from the intercepts at $t = 0$ which are equal to $-\log A_o/B_o$, are recorded in Table 30 for the runs at 25°C. Also recorded in Table 30 is the ratio k_h/k_{obs} (k_{obs} from Table 25) which is constant at $8.1 \times 10^8 M^{-2}$ ($\sigma = \pm 2\%$) Thus values of k_h can be calculated for any of the runs from the slope of the straight portion of the sigmoid curves.

TABLE 30

Parameters from a Second-Order Autocatalytic Treatment of the Benzoyl Peroxide Runs in CCl_4 at 25°C

$[Mn_2(CO)_{10}] = 5.0 \times 10^{-5}M$, $[Br_2] \simeq 7 \times 10^{-3}M$

$[R_2]$ ($\times 10^{-3}M$)	k_h ($l.mole^{-1}sec^{-1}$)	B_o ($\times 10^{-6}M$)	k_h/k_{obs} ($\times 10^{8}M^{-2}$)
1.1	10	5.0	8.3
2.0	17	6.0	7.7
4.1	34	3.0	7.9
7.4	52	2.5	8.5
12.5	57	2.5	8.3

This linearity is due to the relative insensitivity of the product of $[Mn_2(CO)_{10}] \times [Mn(CO)_5Br]$ during the course of a reaction (from 20 to 80% reaction, $\delta = \pm$ 10%). At 50% reaction the theoretical value of $k_h/k_{obs} = 1/([Mn_2(CO)_{10}][Mn(CO)_5Br]) = 8.0 \times 10^{8}M^{-2}$ which compares very well with the experimental value.

Thus the runs in the absence of initial $Mn(CO)_5Br$ obey a rate law:

$$\frac{-d[Mn_2(CO)_{10}]}{dt} = \frac{k_i[Mn_2(CO)_{10}][Mn(CO)_5Br][R_2][Br_2]^{3/2}}{1 + k_b[R_2]^2}$$

with values of k_i as given in Table 31

TABLE 31

Values of k_i

Temp. (°C) :	15	25	33	40
k_i ($\times 10^6$ l.$^{7/2}$ mole$^{-7/2}$ sec^{-1}) :	4.6	16	53	135

It is now possible to calculate an expression to correct the equation for inhibition by $Mn(CO)_5Br$ at concentrations greater than about 4×10^{-4}M. For the runs given in Table 29, the above equation predicts that:

$$k_g = k_i [R_2] [Br_2]^{3/2} [Mn(CO)_5Br] \text{ sec}^{-1}$$

$$= 17 [Mn(CO)_5Br] \text{ sec}^{-1}$$

At $[Mn(CO)_5Br] = 9.7 \times 10^{-4}$M, $k_g = 1.7 \times 10^{-3}$ sec^{-1} which is a factor of 10 slower than that predicted for $Mn(CO)_5Br$ acting only as a catalyst. Accordingly an empirical expression of:

$$k_g = \frac{17 [Mn(CO)_5 Br]}{1 + k_j [Mn(CO)_5Br]^n}$$

where n is a half or whole integer greater than 1 is used to correlate the date. The only value of n which is reasonably satisfactory is 3/2 and a theoretical curve is shown in Fig 38 which was calculated using a value of k_j of 2×10^5M$^{-3/2}$. This relationship is however only qualitatively successful.

(b) (vi) Conclusion

All the data recorded here for the $Mn_2(CO)_{10}$ reaction with Br_2 in the presence of benzoyl peroxide using CCl_4 as solvent fit the empirical rate law:

$$\frac{-d\left[Mn_2(CO)_{10}\right]}{dt} = \frac{k_i \left[Mn_2(CO)_{10}\right]\left[Mn(CO)_5Br\right]\left[R_2\right]\left[Br_2\right]^{3/2}}{(1 + k_j\left[Mn(CO)_5Br\right]^{3/2})(1 + k_b\left[R_2\right]^2)}$$

Further tests of this equation under a variety of different conditions are required and it is at present regarded as only tentative

(2) THE REACTION OF $Mn_2(CO)_{10}$ WITH I_2

The results of a brief initial study are reported. The reactions were done at 80°C using decalin as solvent.

Three runs with $\left[Mn_2(CO)_{10}\right] = 5.0 \times 10^{-5}$ M, $\left[R_2\right] = 2.2 \times 10^{-3}$ M, and $\left[I_2\right] = 1.2$, 1.3 and 1.8×10^{-3} M showed logarithmic decreases of $\left[Mn_2(CO)_{10}\right]$, all giving first-order rate constants of about 6×10^{-5} sec.$^{-1}$. However these reactions only went to between 70 and 80% completion due to loss of I_2 by a competing reaction.

Accordingly two runs were carried out in the absence of $Mn_2(CO)_{10}$ with an identical $\left[R_2\right]$ as previously and with $\left[I_2\right]$ of 1.2 and 1.5×10^{-3} M. A logarithmic decrease of $\left[I_2\right]$ was observed with the first-order rate constants of 3.1 and 3.3×10^{-5} sec.$^{-1}$ respectively.

(D) DISCUSSION

Benzoyl peroxide is a very well known initiator of free radical reactions in solution and both this effect of the compound and its mode of decomposition have been the subject of exhaustive study over the past 30 years. The field has been reviewed by Walling (106(b)) and this review will be used as a basis for some remarks on the subject as it affects the reactions reported here.

The decomposition of benzoyl peroxide follows a first-order law at concentrations below about 0.01M but at higher concentrations the order increases due to induced decomposition by a chain mechanism of some sort. This leads to kinetic rate laws of simultaneous first- and second-order in others. The rate of first-order decomposition varies somewhat with solvent but the activation energy of 30 Kcal/mole is independent of solvent.

The initiation of radical reactions can be either due to benzoyloxy or phenyl radicals, the latter formed by CO_2 dissociation from the former:

$$(PhCOO)_2 \longrightarrow 2PhCOO$$

$$PhCOO \longrightarrow Ph + CO_2$$

Benzoyl peroxide reacts with I_2 to give benzoyl hypoiodite and iodine atoms, the former subsequently decomposing to iodobenzene:

$$PhCOO + I_2 \longrightarrow PhCOOI + I$$

$$PhCOOI \longrightarrow PhI + CO_2$$

(1) THE $Mn_2(CO)_{10}$ REACTION WITH I_2

The first-order rate constant of 3.2×10^{-5} sec.$^{-1}$ determined from the rate of reaction of I_2 in the absence of $Mn_2(CO)_{10}$, is in very good agreement with reported values determined from the rate of decomposition of benzoyl peroxide in CCl_4 (3.0×10^{-5} sec.$^{-1}$) and cyclohexane (3.4×10^{-5} sec.$^{-1}$) (109) These reactions were carried out in the presence of various inhibitors to suppress the induced decomposition. I_2 was used as an inhibitor because of the unreactivity of the iodine atoms formed. Thus the mechanism must be:

$$R_2 \xrightarrow{k_1} 2R$$

$$R + I_2 \xrightarrow{\text{fast}} RI + I$$ with the possible

radical combination steps:

$$R + I \longrightarrow RI \quad \text{and} \quad 2I \longrightarrow I_2$$

This mechanism gives a rate law:

$$-d[I_2]/dt = k_1[R_2] \simeq k_1[I_2] \text{ since } [R_2] \simeq [I_2]$$

which is in agreement with the data.

However in the presence of $Mn_2(CO)_{10}$, with $[I_2]$ in about fifty-fold excess over $[Mn_2(CO)_{10}]$, the rate of reaction of I_2 was approximately doubled but its reaction

with $Mn_2(CO)_{10}$ did not go to completion. Thus iodine atom reaction with $Mn_2(CO)_{10}$ is an unfavourable process compared with bromine atom reaction. Nevertheless the rate constant for $Mn_2(CO)_{10}$ reaction, of about 6 X 10^{-5} sec.$^{-1}$, is about 10 times faster than that observed for the uncatalysed reaction (Table 9). Now as benzoyl peroxide has no effect on the $Mn_2(CO)_{10}/PPh_3$ reaction, this degree of catalysis is most likely due to iodine atom attack on $Mn_2(CO)_{10}$:

$$I + Mn_2(CO)_{10} \longrightarrow Mn(CO)_5I + Mn(CO)_5$$

but only about 2% of the iodine atoms formed react in this way. This reaction is followed by the step:

$$Mn(CO)_5 + I_2 \longrightarrow Mn(CO)_5I + I$$

which we have previously shown to be favourable (Section IV).

(2) THE $Mn_2(CO)_{10}$ REACTION WITH Br_2

By analogy with the known reaction with I_2 we propose a similar reaction with Br_2:

$$R + Br_2 \longrightarrow RBr + Br$$

(a) Cyclohexane Solution

The only effect of benzoyl peroxide was to decrease the induction period leaving the subsequent rate of reaction of $Mn_2(CO)_{10}$ unchanged. Thus the rate of attainment of the steady-state is increased but the stationary concentration of

bromine atoms is unchanged. This result is very surprising considering the marked difference of effect of benzoyl peroxide on the reaction in CCl_4 solution.

(b) CCl_4 Solution

The overall rate law obtained for this reaction is very complex and it has not proved possible to infer any simple mechanism from it by steady-state treatments of possible elementary steps. Nevertheless some interesting conclusions can be drawn from the data.

An estimate of the catalytic efficiency of benzoyl peroxide can be made by comparing the values of $R_{\frac{1}{2}}$ obtained for the uncatalysed reaction (Table 21) with k_{obs} (Table 32), at 40°C and $[Br_2] \simeq 7 \times 10^{-3}$M. At $[R_2] \leqslant 2.0 \times 10^{-3}$M, $k_{obs} = 9.4 \times 10^{-5} [R_2]$ mole $l.^{-1}$ $sec.^{-1}$ and $R_{\frac{1}{2}} \simeq 4 \times 10^{-9}$ mole $l.^{-1} sec.^{-1}$

$$k_{obs}/R_{\frac{1}{2}} \simeq 2 \times 10^4 [R_2]$$

The apparent activation energy of the reaction of 27 Kcal/mole (Fig 34) is very similar to the value of 30 Kcal/mole obtained from the dissociation of benzoyl peroxide (106(b)). Using the latter value with the known rate constant, for dissociation at 80°C, of 3.0×10^{-5} $sec.^{-1}$ (109) gives a rate constant of 1.2×10^{-7} $sec.^{-1}$ at 40°C. Thus the chain length (L) of the reaction is:

$$L = \frac{-d[Mn_2(CO)_{10}]/dt}{-2d[R_2]/dt} \simeq \frac{9.4 \times 10^{-5}}{2 \times 1.2 \times 10^{-7}}$$

$$\simeq 400$$

This short chain length explains the excellent reproducibility obtained in this system as compared with the uncatalysed reaction where the chain lengths were longer by a factor of about 10^3 (Table 23). This reaction is therefore much less sensitive to trace impurities which can act as chain breakers.

At low $[Mn(CO)_5Br]$ the reaction is catalysed by $Mn(CO)_5Br$ which is the opposite of its effect as an inhibitor on the thermal bromination of $Mn_2(CO)_{10}$. The catalytic effect is similar to the catalysis by $Mn(CO)_5Br$ of the thermal bromination of cyclohexane. A further study of this reaction by Haines (110) showed that at high $[Mn(CO)_5Br]$ the compound acts as an inhibitor which parallels the dual role of $Mn(CO)_5Br$ found here. The dependence on $[Br_2]^{3/2}$ is also found in the bromination of cyclohexane (Fig 28), this reaction having been followed after the completion of the thermal bromination of $Mn_2(CO)_{10}$. The $([Mn(CO)_5Br][Br_2]\ 3/2)/(1 + k_j [Mn(CO)_5Br]^{3/2})$ term of the rate law therefore seems to occur in the catalysed bromination of both cyclohexane and $Mn_2(CO)_{10}$ and this may provide a clue in the future understanding of the mechanism. The $[R_2]/(1 + k_b [R_2]^2)$ part of the rate expression has not been observed in any other system and so at present arguments by analogy of this sort are not open to us.

The regular relationships observed for the variation of the induction period with $[R_2]$ and $[Br_2]$ (Fig 35 and 36)

indicate that the initial reaction of $Mn_2(CO)_{10}$ obeys a rate law:

$$-d\left[Mn_2(CO)_{10}\right]/dt = k\left[R_2\right]\left[Br_2\right]$$

When sufficient $Mn(CO)_5Br$ has been produced (B_o in the integrated autocatalytic rate equation) the autocatalytic behaviour is observed.

Extension of this type of study to other systems such as $Re_2(CO)_{10}/Br_2$ may help to elucidate the complex behaviour observed in this reaction.

VII SOME OBSERVATIONS ON THE PHOTOCHEMICAL REACTIONS OF DIMANGANESE DECACARBONYL WITH BROMINE

(A) INTRODUCTION

Preliminary studies of the thermal reactions of $Mn_2(CO)_{10}$ ($\simeq 5 \times 10^{-5}$M) with Br_2 ($\simeq 7 \times 10^{-3}$M) showed that the reaction was strongly catalysed by room light in all of the solvents used, i.e. cyclohexane, CCl_4, and $CF_2Cl.CFCl_2$. The light, from fluorescent tubes, had a bandwidth which cut off at about 340 mμ at the high energy end of the spectrum.

Previous workers reported that $Mn_2(CO)_{10}$ reacts with CCl_4 at room temperature to give $Mn(CO)_5Cl$ but did not specify the conditions (69). We have found that this reaction is not detectable in the absence of light over a period of more than two weeks but that it occurs readily in the light. In view of this complication the photochemical reactions were studied in cyclohexane and $CF_2Cl.CFCl$, the latter solvent being relatively stable to radical attack.

(B) EXPERIMENTAL

The reaction solutions were contained in 1 cm. stoppered silica cells in the cell compartment of a Perkin-Elmer 137 U.V. spectrometer. The manipulations of reactants were as described in Section V for the thermal bromination reactions. The reaction cell, at a temperature of $23 \pm 1^{\circ}C$,

was placed in a fixed position in the cell mount and irradiated by room light by opening the cell compartment lid for measured periods of time. The spectrum of the solution was taken after each irradiation in the range 290 to 400 mμ to record the $Mn_2(CO)_{10}$ peak at 340 mμ and also occasionally in the range 350 to 600 mμ to record the absorbance of the Br_2 peak at 420 mμ.

It was assumed that the intensity of light incident on a cell was constant during a series of runs.

(C) RESULTS

(1) THE $Mn_2(CO)_{10}$ REACTION WITH Br_2 IN $CF_2Cl.CFCl_2$

The majority of the runs (14 out of 17) gave quite good logarithmic decreases, with respect to irradiation times, of the absorbance at 340 mμ due to $Mn_2(CO)_{10}$. The first-order rate constants (k_{obs}) are presented in Table 32 together with the same parameter calculated from the initial rate of reaction of runs which deviated from this simple behaviour. The data are plotted as k_{obs} versus $[Br_2]$ in Fig 39 which shows that the reaction obeys the rate law:

$$-d[Mn_2(CO)_{10}]/dt = k_a [Mn_2(CO)_{10}][Br_2]$$

to within the limits of accuracy of the data. The value of k_a is 0.28 ± 0.04 l. mole.$^{-1}$ sec.$^{-1}$.

TABLE 32

The Photochemical Rates of Reaction of $Mn_2(CO)_{10}$ with Br_2 using $CF_2Cl.CFCl_2$ as solvent.

$[Mn_2(CO)_{10}]_0$ ($\times 10^{-5}$ M)	$[Br_2]_0$ ($\times 10^{-3}$ M)	Rate Constant. ($\times 10^{-3}$ sec^{-1})
2.7	1.6	0.75
4.8	2.0	0.95
3.7	2.5	1.16
3.1	2.9	1.03
6.0	3.4	1.03
5.5	3.5	1.6
4.8	4.2	1.65
2.7	4.4	2.30
2.8	5.5	1.96
6.0	5.8	2.03
2.0	6.5	2.52
3.6	6.5	2.26
5.5	6.5	2.24
5.5	12	2.7
5.8	12	2.7
5.8	18	4.02
5.8	24	5.9

$Mn_2(CO)_{10}/Br_2$ Photochemical Reactions.

Fig. 39. $CF_2Cl.CFCl_2$.

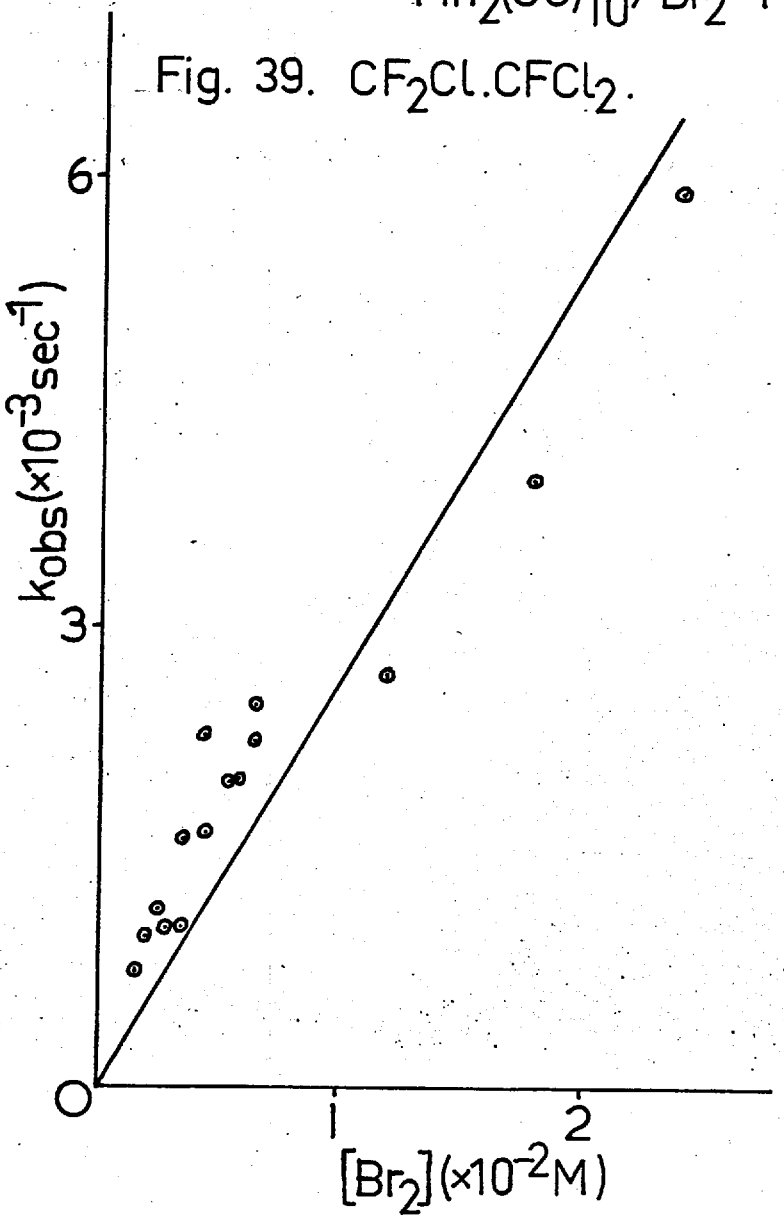

Fig. 40. Cyclohexane.

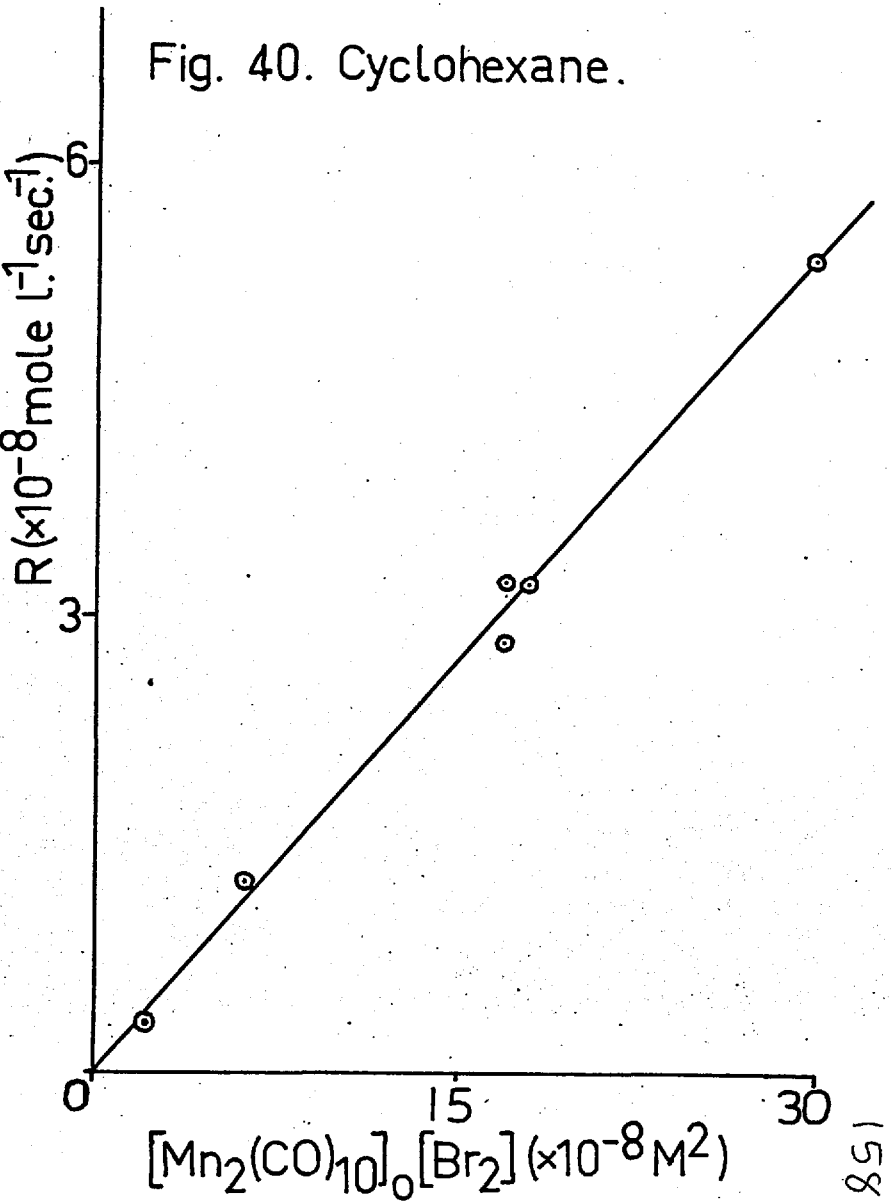

At the temperature of the reaction (23 ± 1°C) the thermal reaction was not detectable on the time scales used and no residual reaction was detected on the cessation of the light.

(2) THE $Mn_2(CO)_{10}$ REACTION WITH Br_2 IN CYCLOHEXANE

Very shallow sigmoid curves were obtained when the absorbance at 340 mμ was plotted against time of irradiation, the plots being linear over 20 to 90% of reaction. These slopes were used to obtain values of the zero-order rate constants ($R = -d[Mn_2(CO)_{10}]/dt$) and these are given in Table 33.

TABLE 33

The Photochemical Rates of Reaction of $Mn_2(CO)_{10}$ with Br_2 using Cyclohexane as solvent

$[Mn_2(CO)_{10}]_o$ ($\times 10^{-5}$M)	$[Br_2]$ ($\times 10^{-3}$M)	$[Mn_2(CO)_{10}]_o [Br_2]$ ($\times 10^{-8}$M^2)	R^* ($\times 10^{-9}$ mole l.$^{-1}$ sec.$^{-1}$)
2.1	1.0	2.1	3.3
2.3	2.7	6.2	12.5
2.3	7.2	17	32.0
2.5	7.1	18	32.0
4.7	3.6	17	28.2
4.6	6.5	30	53.5
4.7	6.5	30	53.5

*R = $-d[Mn_2(CO)_{10}]/dt$ between 20 and 90% reaction

A plot of R versus $[Mn_2(CO)_{10}]_o[Br_2]$ (Fig 40) shows the reaction obeys the relationship:

$$R = k_b [Mn_2(CO)_{10}]_o [Br_2]$$

with $k_b = 0.18$ l. mole.$^{-1}$ sec.$^{-1}$

A parallel I.R. study at $[Mn_2(CO)_{10}]$ of 5×10^{-4}M and $[Br_2]$ of 5×10^{-3}M showed that $Mn(CO)_5Br$ was formed in 100% yield.

No reaction of Br_2 with the solvent was detected at the completion of the $Mn_2(CO)_{10}$ reaction.

Two runs carried out in the presence of 10^{-4}M concentrations of triphenylene and of pyrene, which have triplet state energies of 66.6 and 48.7 Kcal/mole respectively (111), showed no effects either of sensitisation or retardation of the reaction.

(D) DISCUSSION

These runs were carried out with a two-fold purpose (a) to estimate solvent effects on the light catalysed reaction as compared with the thermal bromination and (b) to obtain some data prior to a quantitative photochemical study.

There are two possible photoinitiators, $Mn_2(CO)_{10}$ and Br_2, in the systems studied. A study of the photoinitiation of vinyl polymerisation (112) shows that photolysis of $Mn_2(CO)_{10}$ occurs at 436mμ and also the reaction of $Mn_2(CO)_{10}$ with CCl_4 shows that room light in an effective catalyst.

Br_2 photodissociates with light of wavelength less than 511 mμ (94(a)). Thus the question of the initiation step of the reaction must await detailed photochemical investigation using monochromatic light at several wavelengths.

However since it was thought possible that the photochemical excitation of $Mn_2(CO)_{10}$ involves the formation of a triplet intermediate prior to fission, the reaction was followed in the presence of triphenylene or pyrene. These compounds can sensitise or retard the formation of triplet species depending on the excitation energy of the species (111). If either effect had been observed it would have established the importance of photoinitiation by $Mn_2(CO)_{10}$ because a Br_2 molecule is promoted directly into a dissociative excited state on absorption of a quantum of light. In the event no effects were observed and thus no information concerning the initiation process can be inferred.

Similar rates of reaction of $Mn_2(CO)_{10}$ were observed in cyclohexane and $CF_2Cl.CFCl_2$ although the form of the rate curves was quite different. The rate law obtained in the former solvent implies that the reaction may be autocatalytic with a rate expression:

$$R = k_b \left[Mn_2(CO)_{10}\right] \left[\text{Product}\right] \left[Br_2\right]$$

thus explaining the fact that pseudo first-order plots were not obtained despite the form of the rate law and the behaviour in $CF_2Cl.CFCl_2$. If this is so then the rate constants, k_a and k_b, can be directly compared: $k_a = 1.5k_b$.

This is readily explained if bromine atom formation is the rate controlling step of the reaction because in cyclohexane competion will exist between $Mn_2(CO)_{10}$ and the solvent for bromine atoms whereas this effect would be absent in $CF_2Cl.CFCl_2$. However this is very speculative reasoning at present because no catalytic product has been yet looked for but precedents exist in the autocatalytic behaviour found in the catalysis of the $Mn_2(CO)_{10}/Br$ reaction in CCl_4 by benzoyl peroxide and the thermal bromination of cyclohexane in the presence of $Mn(CO)_5Br$.

In any case the effects of the two solvents are quite different in the thermal and photochemical bromination of $Mn_2(CO)_{10}$.

A very surprising feature of the reaction in $CF_2Cl.CFCl_2$, which was noted previously (Section V), is that $[Mn(CO)_5Br]$ of $10^{-3}M$ completely inhibited the reaction in the light, but no such effect was observed in CCl_4 under the same conditions. The former effect is completely inexplicable at present.

In conclusion, we have shown that reproducible behaviour occurs in the photochemical reactions and that they are suitable for a detailed study.

REFERENCES

(1) J. Chatt, P.L. Pauson, and L.M. Venanzi, in "Organometallic Chemistry", ed. H. Zeiss, Reinhold, New York, 1960, p. 468, and references cited therein.

(2) E.W. Abel, Quart. Rev., 1963, 17, 133, and references cited therein.

(3) W. Hieber, W. Beck, and G. Braun, Angew . Chem., 1960, 72, 795, and references cited therein.

(4) F.G.A. Stone, Plenary Lecture, VIII th Internat. Conf. Coord. Chem., Vienna, 1964, Butterworths, London, 1965, p. 37.

(5) R.B. King, Advan. Organomet. Chem., 1964, 2, 157, and references cited therein.

(6) T.A. Manuel, Advan. Organomet. Chem., 1965, 3, 181, and references cited therein.

(7) J. Birmingham, Advan. Organomet. Chem., 1964, 2, 365, and references cited therein.

(8) M.A. Bennett, Chem. Rev., 1962, 62, 611.

(9) R.G. Guy and B.L. Shaw, Advan. Inorg. Chem. Radiochem.,

1962, 4, 78, and references cited therein.

(10) H. Zeiss, in "Organometallic Chemistry", ed. H. Zeiss, Reinhold, New York, 1960, p. 380.

(11) R. Pettit and G.F. Emerson, Advan. Organomet. Chem., 1964, 1, 1.

(12) P.M. Treichel and F.G.A. Stone, Advan. Organomet. Chem., 1964, 1, 143.

(13) M.L.H. Green and P.L.I. Nagy, Advan. Organomet. Chem., 1964, 2, 325.

(14) J. Lewis, Plenary Lecture, VIII th Internat. Conf. Coord. Chem., Vienna, 1964, Butterworths, London, 1965, p. 11, and references cited therein.

(15) O.S. Mills, Acta Cryst., 1958, 11, 620.

(16) E.R. Corey, L.F. Dahl, and W. Beck, J. Am. Chem. Soc., 1963, 85, 1202.

(17) L. Pauling, "The Nature of the Chemical Bond", Third Edit., Oxford Univ. Press, London, 1960.

(18) L.F. Dahl, E. Ishishi, and R.E. Rundle, J. Chem. Phys., 1957, 26, 1750; L.F. Dahl and R.E. Rundle, Acta Cryst., 1963, 16, 419.

(19) M.F. Bailey and L.F. Dahl, Inorg. Chem., 1965, 4, 1140.

(20) R.B. King and M.B. Bisnette, Inorg. Chem., 1964, 3, 785.

(21) A.N. Nesmeyanov, K.N. Anisimov, N.E. Kobolova, and V.N. Khandozhko, Doklady. Akad. Nauk. S.S.S.R., 1964, 156, 383.

(22) T. Kruck and M. Höfler, Angew, Chem., Int. Ed., 1964, 3, 701.

(23) E.H. Schubert and R.K. Sheline, Z. Naturforsch., 1965, 20b, 1306.

(24) Interatomic Distances, "Special Publication No. 18", The Chemical Society, London, 1965.

(25) F.A. Cotton and R.R. Monchamp, J. Chem. Soc., 1960, 533.

(26) C.E. Coffey, J. Lewis, and R.S. Nyholm, J. Chem. Soc., 1964, 1741.

(27) E.R. Corey and L.F. Dahl, J. Am. Chem. Soc., 1961, 83, 2203.

(28) E.R. Corey and L.F. Dahl., Inorg. Chem., 1962, 1, 521.

(29) R.S. Nyholm, Proc. Chem. Soc., 1961, 273, and references cited therein.

(30) C - H. Wei and L.F. Dahl, J. Am. Chem. Soc., 1966, 88, 1821.

(31) H.M. Powell and R.V.G. Ewans, J. Chem. Soc., 1939, 286.

(32) A.F. Wells, "Structural Inorganic Chemistry", Third Edit., Clarendon Press, Oxford, 1962, p. 748.

(33) V. Anders and W.A.G. Graham, Chem. Comm., 1966, 291.

(34) L.F. Dahl and J.F. Blout, Inorg. Chem., 1965, 4, 1373.

(35) G. Gardner-Sumner, H.P. Klug, and L.E. Alexander, Acta Cryst., 1964, 17, 732.

(36) K. Noack, Spect. Acta, 1963, 19, 1925.

(37) E.O. Fischer, H. Schuster-Woldan, and K. Bittler, Z. Naturforsch., 1963, 18b, 429.

(38) L.F. Dahl and C - H. Wei, Acta Cryst., 1963, 16, 611.

(39) L.F. Dahl, C. Martell, and D.L. Wampler, J. Am. Chem. Soc., 1961, 83, 1761.

(40) L.F. Dahl and C - H. Wei, Inorg. Chem., 1963, 2, 328.

(41) C - H. Wei and L.F. Dahl, Inorg. Chem., 1965, 4, 1.

(42) L.F. Dahl and P.W. Sutton, Inorg. Chem., 1963, 2, 1067.

(43) J.F. Blout, L.F. Dahl, C. Hoogzand, and W. Hübel, J. Am. Chem. Soc., 1966, 88, 292.

(44) R.P. Dodge and V. Schomaker, J. Organometal. Chem., 1965, 3, 274.

(45) W.G. Sly, J. Am. Chem. Soc., 1959, 81, 18.

(46) N.A. Bailey, M.R. Churchill, R. Hunt, R. Mason, and G. Wilkinson, Proc. Chem. Soc., 1964, 401.

(47) L.F. Dahl and D.L. Smith, J. Am. Chem. Soc., 1962, 84, 2450.

(48) O.S. Mills and G. Robinson, Proc. Chem. Soc., 1959, 156.

(49) A.A. Hock and O.S. Mills, Acta Cryst., 1961, 14, 139.

(50) G.S.D. King, Acta Cryst, 1962, 15, 243.

(51) R.P. Dodge, O.S. Mills, and V. Schomaker, Proc. Chem. Soc., 1963, 380.

(52) R. Markby, I. Wender, R.A. Friedel, F.A. Cotton, and H.W. Sternberg, J. Am. Chem. Soc., 1958, 86, 6529; U. Krüerke and W. Hübel, Chem. Ind., 1960, 1264.

(53) W.T. Dent, L.A. Duncanson, R.G. Guy, H.W.B. Reed, and B.L. Shaw, Proc. Chem. Soc., 1961, 169.

(54) L. Marko, G. Bor, and E. Klumpp, Chem. Ind., 1961, 1491.

(55) S.A. Khattab, L. Marko, G. Bor, and B. Marko, J. Organometal. Chem., 1964, 1, 373.

(56) F. Calderazzo, R. Cini, and R. Ercoli, Chem. Ind., 1960, 934 and references cited therein.

(57) R.B. King, J. Am. Chem. Soc., 1966, 88, 2075 and references cited therein.

(58) W. Hieber and E. Winter, Chem. Ber., 1964, 97, 1037.

(59) R. Burton, L. Pratt, and G. Wilkinson, J. Chem. Soc., 1960, 4290.

(60) U. Anders and W.A.G. Graham, Chem. Comm., 1965, 499.

(61) L.B. Handy, P.M. Treichel, L.F. Dahl, and R.G. Hayter, J. Am. Chem. Soc., 1966, 88, 366.

(62) E.W. Abel, A. Singh, and G. Wilkinson, J. Chem. Soc., 1960, 1321.

(63) A. Davison, W. Mcfarlane, L. Pratt, and G. Wilkinson, J. Chem. Soc., 1962, 3653.

(64) E.O. Fischer, O. Beckert, W. Hafner, and H.O. Stahl, Z. Naturforsch., 1955, 10b, 598.

(66) N. Flitcroft, D.K. Huggins, and H.D. Kaesz, Inorg. Chem., 1964, 3, 1123.

(67) J. Lewis, A.R. Manning, J.R. Miller, M.J. Ware, and F. Nyman, Nature, 1965, 207, 142; F.A. Cotton and R.M. Wing, Inorg. Chem., 1965, 4, 1328.

(68) R.E. Winters and R.W. Kiser, J. Phys. Chem., 1965, 69, 1618.

(69) J.C. Hileman, D.K. Huggins, and H.D. Kaesz, Inorg. Chem., 1962, 1, 933, and references cited therein.

(70) D.K.Kaesz, W. Fellmann, J.M. Smith, and H.D. Kaesz J. Am. Chem. Soc., 1964, 86, 4841.

(71) E.W. Abel and G. Wilkinson, J. Chem. Soc., 1959, 1501.

(72) E.W. Abeland I.S. Butler, J. Chem. Soc., 1964, 434.

(73) A.G. Osbourne and M.H.B. Stiddard, J. Chem. Soc., 1964 634.

(74) D.J. Parker and M.H.B. Stiddard, J. Chem. Soc. (A), 1966, 695, and references cited therein.

(75) W. Hieber and W. Freyer, Chem. Ber., 1959, 92, 1765.

(76) H. Wawersik and F. Basolo, Chem. Comm., 1966, 366.

(77) M.L. Ziegler, H. Hass, and R.K. Shelime, Chem. Ber., 1965,

98, 2454.

(78) F. Nyman, Chem. Ind., 1965, 604.

(79) P.W. Jolly and F.G.A. Stone, J. Chem. Soc., 1965, 5259.

(80) M.H. Chisholm, A.G. Massey, and N.R. Thompson, Nature, 1966, 211, 67.

(81) G.R. Dobson and R.K. Sheline, Inorg. Chem., 1963, 2, 1313.

(82) B.F.G. Johnson, J. Lewis, I.G. Williams, and J. Wilson, Chem. Comm., 1966, 391.

(83) H.J. Keller and H Wawersik, Z. Naturforsch., 1965, 20b, 938.

(84) F. Basolo and A. Wojcicki, J. Am. Chem. Soc., 1961, 83, 520.

(85) M.R. Tirpak, J.H. Wotiz, and C.A. Hollingsworth, J. Am. Chem. Soc., 1958, 80, 4265.

(86) W. Hieber and J. Ellerman, Z. Naturforsch., 1963, 18b, 595, and references cited therein.

(87) E.O. Fischer and C. Palm, Chem. Ber., 1958, 91, 1725.

(88) H.D. Kaesz and D.K. Huggins, Canad. J. Chem., 1963 41, 1250

(89) A.G. Osborne and M.H.B. Stiddard, J. Organomet. Chem., 1965, 3, 340.

(90) W. Hieber and H. Fuchs, Z. Anorg. Chem., 1941, 248, 256.

(91) R.S. Nyholm and D.V. Ramana Rao, Proc. Chem. Soc., 1959, 130.

(92) E.O. Brimm, M.A. Lynch, and W.J. Sesny, J.Am. Chem.Soc., 1954, 76, 3831.

(93) C.C. Addison, M. Kilner, and A. Wojcicki, J. Chem. Soc., 1961, 4839.

(94) (a) "Mellor's Inorganic and Theoretical Chemistry", Vol. II, Supplement I, "The Halogens", Longmans, London, 1956, p. 778-784.
(b) ibid, p. 924
(c) ibid, p. 707

(95) R.J. Angelici and F. Basolo, J. Am, Chem. Soc., 1962, 84, 2495

(96) N.M. Atherton, H.W. Melville, and D.H. Wiffen, Trans. Farad. Soc., 1958, 54, 1300.

(97) S.J. Wyard, J. Sci. Inst., 1965, 42, 769.

(98) J.F. Gibson, personal communication.

(99) A.M. North, "The Collision Theory of Chemical Reactions in Liquids", Methuen, London, 1964.

(100) F. Basolo and H. Wawersik, personal communication.

(101) A.A. Frost and R.G. Pearson, "Kinetics and Mechanism" 2nd Edit., Wiley, London, 1961, p. 166-171.

(102) (a) W.F. Seyer and J.D. Leslie, J. Am. Chem. Soc., (1942), 64, 1912.
(b) J. Timmermans, "Physico-Chemical Constants of Pure Organic Compounds", Elsevier, Amsterdam, Vol, II, 1965, p. 170-173.

(103) A. Seidell, "Solubilities of Inorganic and Metal Organic Compounds", 3rd Edit., Van Nostrand, New York, 1940, p. 1358.

(104) C.H. Bamford and R. Denyer, Trans, Farad. Soc., 1966, 62, 1567.

(105) D.R. Bidinosti and N.S. McIntyre, Chem. Comm., 1966, 555.

(106) C. Walling, "Free Radicals in Solution", Wiley, New York, 1957, (a) p. 35, (b) p. 474-491, and (c) p. 376-378.

(107) E.W.R. Steacie, "Atomic and Free Radical Reactions", 2nd Edit., Reinhold, New York, 1954, (a) Vol. II, p.718
(b) Vol. I., p. 71

(108) C.H. Bamford and C.A. Finch, Proc. Roy. Soc. A, 1962 268, 553.

(109) C.G. Swain, W.H. Stockmeyer and J.T. Clark, J. Am. Chem. Soc., 1950, 72, 5426.

(110) L.I.B. Haines, personal communication.

(111) W.G. Herkstroeter, A.A. Lamola, and G.S. Hammond, 1964, 86, 4537.

(112) C.H. Bamford, P.A. Crowe, and R.P. Wayne, Proc. Roy. Soc. A, 1965, 284, 455.

A P P E N D I X

(I) STEADY-STATE TREATMENT OF THE $Mn_2(CO)_{10}$ REACTION WITH Br_2 (SECTION V)

The following symbols are used:

$$A \equiv Mn(CO)_5, \qquad B \equiv Br.$$

Concentrations are given in lower case e.g.

$$[Mn_2(CO)_{10}] \equiv [A_2] \equiv a_2$$

The following elementary reactions are treated according to the steady-state approximation i.e. the radical concentrations are assumed to be constant:

Initiation:

$$A_2 \xrightarrow{k_1} (2A)$$

$$(2A) + B_2 \xrightarrow{k_2} AB + A + B$$

Propagation:

$$B + A_2 \xrightarrow{k_4} AB + A$$

$$A + B_2 \xrightarrow{k_5} AB + B$$

Termination:

(a) $A + A \xrightarrow{k_6} A_2$

(b) $A + B \xrightarrow{k_7} AB$

(c) $B + B \xrightarrow{k_8} B_2$

The rate of reaction of $Mn_2(CO)_{10}$:

$$-da_2/dt = k_4 a_2 b$$

k_1 and k_6 are ignored as the chain lengths are long (Table 23).

Rate laws are calculated for each termination step with the initiation and propagation steps:

(1) Termination (a)

$$d(2a)/dt = 0 = k_1 a_2 - k_2(2a) b_2 \quad \ldots\ldots\ldots\ldots (1)$$

$$da/dt = 0 = k_2(2a)b_2 + k_4 a_2 b - k_5 a b_2 - 2k_6 a^2 \quad \ldots\ldots\ldots (2)$$

$$db/dt = 0 = k_2(2a)b_2 - k_4 a_2 b + k_5 a b_2 \quad \ldots\ldots\ldots\ldots (3)$$

$$(1) + (3): \; k_1 a_2 - k_4 a_2 b + k_5 a b_2 = 0 \quad \ldots\ldots\ldots\ldots (4)$$

$$(2) - (3): \; k_4 a_2 b - k_5 a b_2 - k_6 a^2 = 0 \quad \ldots\ldots\ldots\ldots (5)$$

$$(4) + (5): \; k_1 a_2 - k_6 a^2 = 0$$

$$\therefore \; a = (k_1/k_6)^{\frac{1}{2}} a_2^{\frac{1}{2}} \quad \ldots\ldots\ldots\ldots\ldots\ldots (6)$$

Substituting (6) into (4):

$$k_1 a_2 - k_4 a_2 b + k_5 (k_1/k_6)^{\frac{1}{2}} a_2^{\frac{1}{2}} b_2 = 0$$

$$\therefore \; b = (k_5/k_4)(k_1/k_6)^{\frac{1}{2}} (b_2/a_2^{\frac{1}{2}}) \quad \text{(ignoring } k_1 a_2\text{)}$$

$\therefore$ The rate law is:

$$-da_2/dt = k_4 a_2 b$$

$$= k_5 (k_1/k_6)^{\frac{1}{2}} a_2^{\frac{1}{2}} b_2$$

(2) Termination (b)

$d(2a)/dt = 0 = k_1a_2 - k_2(2a)b_2$ .....(1)

$da/dt = 0 = k_2(2a)b_2 + k_4a_2b - k_5ab_2 - k_7ab$ .....(2)

$db/dt = 0 = k_2(2a)b_2 - k_4a_2b + k_5ab_2 - k_7ab$ .....(3)

(1) + (2): $k_1a_2 + k_4a_2b - k_5ab_2 - k_7ab = 0$ .....(4)

(2) - (3): $k_4a_2b - k_5ab_2 = 0$ .....(5)

(4) - (5): $k_1a_2 - k_7ab = 0$

$\therefore \quad a = k_1a_2/k_7b$ .....(6)

Substituting (6) into (5) and rearranging:

$$b = (k_1k_5/k_4k_7)^{\frac{1}{2}}b_2^{\frac{1}{2}}$$

$\therefore$ The rate law is:

$$-da_2/dt = k_4a_2b = (k_1k_4k_5/k_7)^{\frac{1}{2}}\, a_2b_2^{\frac{1}{2}}$$

(3) Termination (c)

$d(2a)/dt = 0 = k_1a_2 - k_2(2a)b_2$ .....(1)

$da/dt = 0 = k_2(2a)b_2 + k_4a_2b - k_5ab_2$ .....(2)

$db/dt = 0 = k_2(2a)b_2 - k_4a_2b + k_5ab_2 - 2k_8b^2$ .....(3)

(2) + (3): $k_2(2a)b_2 - k_8b^2 = 0$ .....(4)

(1) + (4): $k_1a_2 - k_8b^2 = 0$

$\therefore \quad b = (k_1/k_8)^{\frac{1}{2}}\, a_2^{\frac{1}{2}}$ .....(5)

$\therefore$ The rate law is:

$$-da_2/dt = k_4a_2b = k_4(k_1/k_8)^{\frac{1}{2}}\, a_2^{3/2}$$

(II) INTEGRATION OF AUTOCATALYTIC RATE LAW (SECTION VI)

The rate law to be integrated is:

$$-\,d\left[Mn_2(CO)_{10}\right]/dt = k\left[Mn_2(CO)_{10}\right]\left[Mn(CO)_5Br\right]$$

Let $\left[Mn_2(CO)_{10}\right] \equiv A$ and $\left[Mn(CO)_5Br\right] \equiv B$ with a subscript o indicating the initial concentrations.

The stoichiometric equation is:

$$A \longrightarrow 2\,B$$

$2(A_o - A) = B - B_o$ (B_o is the trace of product initially present which is necessary for the reaction to occur)

$$B = 2A_o + B_o - 2A$$

$$-dA/dt = kAB$$

$$= kA(2A_o + B_o - 2A)$$

$$-\int \frac{dA}{A(2A_o + B_o - 2A)} = k\int dt = kt$$

This equation is solved using the standard integral:

$$\int \frac{dx}{x(a + bx)} = -\frac{1}{a}\ln\frac{(a + bx)}{x}$$

$$kt = \frac{1}{(2A_o + B_o)}\ln\frac{(2A_o + B_o - 2A)}{A} + I$$

At $t = 0$:

$$I = -\frac{1}{(2A_o + B_o)}\ln\frac{B_o}{A_o}$$

$$kt = \frac{1}{(2A_o + B_o)}\ln\frac{A_o}{B_o}\,\frac{(2A_o + B_o - 2A)}{A}$$